



*Development of an Innovative Insulation Fire Resistant Façade
from the Construction and Demolition Waste*

**Development of an Innovative Insulation Fire Resistant Façade
from the Construction and Demolition Waste**

DEFEAT

INTEGRATED/0918/0052

DELIVERABLE D4.1

**FULL CHARACTERISATION OF THE SEPARATED WASTE CONCRETE
AND CERAMICS**



The Project DEFEAT (INTEGRATED/0918/0052) has been co-funded by the European Regional Development Fund (ERDF) and the Cyprus Government, through the RESTART 2016-20 framework program of the Cyprus Research & Innovation Foundation

Table of Contents

SUMMARY	10
1. LASER PARTICLE ANALYSIS RESULTS	12
1.1. Background	12
1.2. Sample preparation	13
1.3. Results	14
1.4. Discussion	18
2. X-RAY FLUORESCENCE (XRF) ANALYSIS	19
2.1. Background	19
2.2. Sample preparation	21
2.3. Results	22
2.4. Discussion	28
3. X-RAY DIFFRACTION (XRD) ANALYSIS	30
3.1. Background	30
3.2. Sample preparation	33
3.3. Results	33
3.4. Discussion	38
4. DENSITY MEASUREMENTS	40
4.1. Background	40
4.2. Separation and grinding of the raw materials	40
4.3. Particle size distribution of the finely ground raw materials	43
4.4. Density determination of the finely ground raw materials	44
5. DISSOLUTION TESTS	50
5.1. Results and Discussion	50
6. CONCLUSIONS	54
REFERENCES	57
Acknowledgements	58

APPENDIX 1.....	59
Particle Size Analysis For All CDW Samples	59
APPENDIX 2.....	81
XRF Analysis For All CDW Samples.....	81
APPENDIX 3.....	102
XRD Analysis For All CDW Samples.....	102

LIST OF FIGURES

Figure 1. Basic operation of a LALLS device (Renliang, 2001).....	13
Figure 2. Average particle size analysis for the CWD brick material.....	15
Figure 3. Average particle size analysis for CWD concrete material.....	16
Figure 4. Average particle size analysis for CDW ceramic tile material.	17
Figure 5. Summary of elemental and oxide analysis for CDW brick.....	23
Figure 6. Summary of elemental and oxide analysis for CDW concrete.	24
Figure 7. Summary of elemental and oxide analysis for CDW ceramic tile.	25
Figure 8. The SIEMENS D5000 X-ray diffractometer used in the experiment.	31
Figure 9. XRD analysis summary for CDW brick.	35
Figure 10. XRD analysis summary for CDW concrete.	36
Figure 11. XRD analysis summary for CDW ceramic tile.....	37
Figure 12. The raw materials as received from CDW (waste brick).....	41
Figure 13. The raw materials as received from CDW (waste tiles).....	41
Figure 14. The raw materials as received from CDW (waste concrete).....	42
Figure 15. The Los Angeles abrasion machine.	42
Figure 16. The stainless balls inside the Los Angeles abrasion machine.....	43
Figure 17. Particle size distribution of the raw materials.	44
Figure 18. The ground raw materials from CDW.....	46
Figure 19. Weighing and immersion of samples.....	47
Figure 20. Measurement of pycnometer filled with water to a calibration mark.	47
Figure 21. The sample tested in a saturated surface dry condition (right picture).	48
Figure 22. Summary of density determinations and water absorption values of CDW.	50
Figure 23. Particle size analysis for Sample 1 (Brick) measurement 1.....	59

Figure 24. Particle size analysis for Sample 1 (Brick) measurement 2.	60
Figure 25. Particle size analysis for Sample 1 (Brick) measurement 3.	60
Figure 26. Particle size analysis for Sample 1 (Brick) measurement 4.	61
Figure 27. Particle size analysis for Sample 1 (Brick) measurement 5.	61
Figure 28. Particle size analysis for Sample 1 (Brick) measurement 8.	63
Figure 29. Particle size analysis for Sample 1 (Brick) measurement 9.	63
Figure 30. Particle size analysis for Sample 1 (Brick) measurement 10.	64
Figure 31. Particle size analysis for Sample 1 (Brick) measurement 11.	65
Figure 32. Particle size analysis for Sample 1 (Brick) measurement 12.	65
Figure 33. Particle size analysis for Sample 1 (Brick) measurement 13.	66
Figure 34. Particle size analysis for Sample 2 (Concrete) measurement 1.	67
Figure 35. Particle size analysis for Sample 2 (Concrete) measurement 2.	67
Figure 36. Particle size analysis for Sample 2 (Concrete) measurement 5.	69
Figure 37. Particle size analysis for Sample 2 (Concrete) measurement 6.	69
Figure 38. Particle size analysis for Sample 2 (Concrete) measurement 7.	70
Figure 39. Particle size analysis for Sample 2 (Concrete) measurement 8.	70
Figure 40. Particle size analysis for Sample 2 (Concrete) measurement 9.	71
Figure 41. Particle size analysis for Sample 2 (Concrete) measurement 10.	71
Figure 42. Particle size analysis for Sample 2 (Concrete) measurement 11.	72
Figure 43. Particle size analysis for Sample 2 (Concrete) measurement 12.	72
Figure 44. Particle size analysis for Sample 3 (Ceramic tile) measurement 2.	74
Figure 45. Particle size analysis for Sample 3 (Ceramic tile) measurement 3.	75
Figure 46. Particle size analysis for Sample 3 (Ceramic tile) measurement 4.	75
Figure 47. Particle size analysis for Sample 3 (Ceramic tile) measurement 5.	76

Figure 48. Particle size analysis for Sample 3 (Ceramic tile) measurement 6.	76
Figure 49. Particle size analysis for Sample 3 (Ceramic tile) measurement 7.	77
Figure 50. Particle size analysis for Sample 3 (Ceramic tile) measurement 8.	77
Figure 51. Particle size analysis for Sample 3 (Ceramic tile) measurement 9.	78
Figure 52. Particle size analysis for Sample 3 (Ceramic tile) measurement 12.	79
Figure 53. Particle size analysis for Sample 3 (Ceramic tile) measurement 13.	80
Figure 54. Particle size analysis for Sample 1 (Brick) measurement 1.	103
Figure 55. Particle size analysis for Sample 1 (Brick) measurement 2.	103
Figure 56. Particle size analysis for Sample 1 (Brick) measurement 3.	104
Figure 57. Particle size analysis for Sample 1 (Brick) measurement 4.	104
Figure 58. Particle size analysis for Sample 1 (Brick) measurement 5.	105
Figure 59. Particle size analysis for Sample 1 (Brick) measurement 6.	105
Figure 60. Particle size analysis for Sample 1 (Brick) measurement 7.	106
Figure 61. Particle size analysis for Sample 1 (Brick) measurement 8.	106
Figure 62. Particle size analysis for Sample 1 (Brick) measurement 9.	107
Figure 63. Particle size analysis for Sample 1 (Brick) measurement 10.	107
Figure 64. Particle size analysis for Sample 1 (Brick) measurement 11.	108
Figure 65. Particle size analysis for Sample 1 (Brick) measurement 12.	108
Figure 66. Particle size analysis for Sample 1 (Brick) measurement 13.	109
Figure 67. Particle size analysis for Sample 2 (Concrete) measurement 1.	110
Figure 68. Particle size analysis for Sample 2 (Concrete) measurement 2.	111
Figure 69. Particle size analysis for Sample 2 (Concrete) measurement 3.	111
Figure 70. Particle size analysis for Sample 2 (Concrete) measurement 4.	112
Figure 71. Particle size analysis for Sample 2 (Concrete) measurement 5.	112

Figure 72. Particle size analysis for Sample 2 (Concrete) measurement 6.	113
Figure 73. Particle size analysis for Sample 2 (Concrete) measurement 7.	113
Figure 74. Particle size analysis for Sample 2 (Concrete) measurement 8.	114
Figure 75. Particle size analysis for Sample 2 (Concrete) measurement 9.	114
Figure 76. Particle size analysis for Sample 2 (Concrete) measurement 10.	115
Figure 77. Particle size analysis for Sample 2 (Concrete) measurement 11.	115
Figure 78. Particle size analysis for Sample 2 (Concrete) measurement 12.	116
Figure 79. Particle size analysis for Sample 2 (Concrete) measurement 13.	116
Figure 80. Particle size analysis for Sample 3 (Ceramic tile) measurement 1.	117
Figure 81. Particle size analysis for Sample 3 (Ceramic tile) measurement 2.	118
Figure 82. Particle size analysis for Sample 3 (Ceramic tile) measurement 3.	118
Figure 83. Particle size analysis for Sample 3 (Ceramic tile) measurement 4.	119
Figure 84. Particle size analysis for Sample 3 (Ceramic tile) measurement 5.	119
Figure 85. Particle size analysis for Sample 3 (Ceramic tile) measurement 6.	120
Figure 86. Particle size analysis for Sample 3 (Ceramic tile) measurement 7.	120
Figure 87. Particle size analysis for Sample 3 (Ceramic tile) measurement 8.	121
Figure 88. Particle size analysis for Sample 3 (Ceramic tile) measurement 9.	121
Figure 89. Particle size analysis for Sample 3 (Ceramic tile) measurement 10.	122
Figure 90. Particle size analysis for Sample 3 (Ceramic tile) measurement 11.	122
Figure 91. Particle size analysis for Sample 3 (Ceramic tile) measurement 12.	123
Figure 92. Particle size analysis for Sample 3 (Ceramic tile) measurement 13.	123

LIST OF TABLES

Table 1. Summary of elemental and oxide content analysis for the 3 CDW materials	25
Table 2. Description of the test procedures as per ASTM 128-88.	45
Table 3. Densities and water absorption values of the raw materials.....	49
Table 4. XRF analysis results for Sample 1 (Brick) Run 1.	81
Table 5. XRF analysis results for Sample 1 (Brick) Run 2.	82
Table 6. XRF analysis results for Sample 1 (Brick) Run 3.	82
Table 7. XRF analysis results for Sample 1 (Brick) Run 4.	83
Table 8. XRF analysis results for Sample 1 (Brick) Run 5.	83
Table 9. XRF analysis results for Sample 1 (Brick) Run 6.	84
Table 10. XRF analysis results for Sample 1 (Brick) Run 7.	84
Table 11. XRF analysis results for Sample 1 (Brick) Run 8.	85
Table 12. XRF analysis results for Sample 1 (Brick) Run 9.	85
Table 13. XRF analysis results for Sample 1 (Brick) Run 10.	86
Table 14. XRF analysis results for Sample 1 (Brick) Run 11.	86
Table 15. XRF analysis results for Sample 1 (Brick) Run 12.	87
Table 16. XRF analysis results for Sample 1 (Brick) Run 13.	87
Table 17. XRF analysis results for Sample 2 (Concrete) Run 1.....	88
Table 18. XRF analysis results for Sample 2 (Concrete) Run 2.....	88
Table 19. XRF analysis results for Sample 2 (Concrete) Run 3.....	89
Table 20. XRF analysis results for Sample 2 (Concrete) Run 4.....	89
Table 21. XRF analysis results for Sample 2 (Concrete) Run 5.....	90
Table 22. XRF analysis results for Sample 2 (Concrete) Run 6.....	90
Table 23. XRF analysis results for Sample 2 (Concrete) Run 7.....	91

Table 24. XRF analysis results for Sample 2 (Concrete) Run 8.....	91
Table 25. XRF analysis results for Sample 2 (Concrete) Run 9.....	92
Table 26. XRF analysis results for Sample 2 (Concrete) Run 10.....	92
Table 27. XRF analysis results for Sample 2 (Concrete) Run 11.....	93
Table 28. XRF analysis results for Sample 2 (Concrete) Run 12.....	93
Table 29. XRF analysis results for Sample 2 (Concrete) Run 13.....	94
Table 30. XRF analysis results for Sample 3 (Ceramic tile) Run 1.	95
Table 31. XRF analysis results for Sample 3 (Ceramic tile) Run 2.	95
Table 32. XRF analysis results for Sample 3 (Ceramic tile) Run 3.	96
Table 33. XRF analysis results for Sample 3 (Ceramic tile) Run 4.	96
Table 34. XRF analysis results for Sample 3 (Ceramic tile) Run 5.	97
Table 35. XRF analysis results for Sample 3 (Ceramic tile) Run 6.	97
Table 36. XRF analysis results for Sample 3 (Ceramic tile) Run 7.	98
Table 37. XRF analysis results for Sample 3 (Ceramic tile) Run 8.	98
Table 38. XRF analysis results for Sample 3 (Ceramic tile) Run 9.	99
Table 39XRF analysis results for Sample 3 (Ceramic tile) Run 10.	99
Table 40. XRF analysis results for Sample 3 (Ceramic tile) Run 11.	100
Table 41. XRF analysis results for Sample 3 (Ceramic tile) Run 12.	100
Table 42. XRF analysis results for Sample 3 (Ceramic tile) Run 13.	101

SUMMARY

The general objective of the DEFEAT project is the strategic separation and transformation of Construction and Demolition Wastes (CDW) into an innovative insulation fire resistant façade. The management of CDW in Cyprus faces several challenges and appears to be underperforming, despite the fact that a comprehensive legislative framework concerning the management of CDW is in place since 2011.

Work Package 4 (WP4) of this research programme is led by the University of Cyprus (UCY) who is the strategic partner responsible for the management, timely execution, completion and delivery of the required outputs. The WP4 targets a comprehensive set of generic characterization techniques conducted on as-received samples of CDW from different sources in order to investigate their full chemical and mineralogical composition which is a crucial step towards the development of the end product.

The UCY leads the overall tasks included in WP4 and ensures a robust output of the deliverables. Two technical reports have been prepared, namely a full characterization report (D4.1) and a CDW material data sheet (D4.2).

The present report (D4.1) includes results from a set of analytical techniques, namely:

- X-Ray Diffraction (XRD);
- X-Ray Fluorescence (XRF);
- Particle Size Analysis;
- Density Measurements; and
- Dissolution Tests

on thirteen samples of each of the following three as-received CDW materials:

- Brick (waste ceramic), thereon noted as **Sample 1** and included in the relevant Appendices;
- Concrete (waste concrete) thereon noted as **Sample 2** and included in the relevant Appendices;
- Tiles (waste ceramic) thereon noted as **Sample 3** and included in the relevant Appendices.

This report provides a comprehensive understanding of the physio-chemical and mineralogical properties of the examined materials, based on parameters and variables (such as source) which were not ascertained.

The characterization of the above, as received materials, involves utilizing both qualitative and quantitative approaches when analysing the samples. Both approaches are essential for full and accurate output of results and for a valid discussion on the values obtained.

Each analytical technique is presented in the next sections of this report along with the relevant background, the sample preparation procedure and the output results.

Along with the present report, a data sheet (D4.2) has been prepared by the research team in line with the outputs and deliverables of WP4.

1. LASER PARTICLE ANALYSIS RESULTS

1.1. Background

The laser diffraction method or more specifically, the Low Angle Laser Light Scattering (LALLS) method, is an optical method of measuring particle size distribution based on the technique scattering of light into particles. Its use has been growingly expanded within the manufacturing, chemistry and construction industries for its effectiveness in obtaining mean distribution diameters of particles.

When a ray of light emits on a particle, a partial amount of light is absorbed, part of it is refracted, part of it is diffracted and a partial amount is emitted. As a result, interference phenomena occur leading to the formation of traces (imprints) of dispersion with maximum and minimum intensity characteristics. In order to fully describe the dispersion trace using a LALLS device, it is necessary to assume that the particles are optically homogeneous and spherical and that they are randomly located within the sample (Renliang, 2001).

The scattering trace is attributed to the unknown particle size distribution according to the Fraunhofer model and Mie theory (Syvitski, 1991; Storti and Balsamo, 2010). The model suggests that if the particle size of a particle is known – provided that additional information about the structure of the particle is also known- then the scatter distribution characteristics of the emitted beam light may be accurately predicted. Laser particle analysis relies on the above concept for the determination of particle size. The exact light scattering imprint of the aligned laser beam collected in the focal area of one of the collection lens within the LALLS device translates to specific particle size - as each particle size has its own characteristic dispersion footprint. By utilizing this method a particle size distribution of a material can be calculated and depicted (Renliang, 2001).

A basic LALLS device consists of an analyser with a lens setup device installed, a low power visible wavelength laser beam (He-Ne, $\lambda = 0.63\text{m}$), as well as a series of photodetectors (approximately 16-32 photodetectors) as shown in Figure 1. The initial stage prior to sample analysis involves the pump, stirrer, and ultrasonic nozzle. The procedure involves the transmission of a laser beam onto the sample and collection of the relevant refractory signal by a receiver and an amplifier (analogue to digital inverter) connected to a computer and a monitor. An illustration of the technique used is shown in Figure 1.

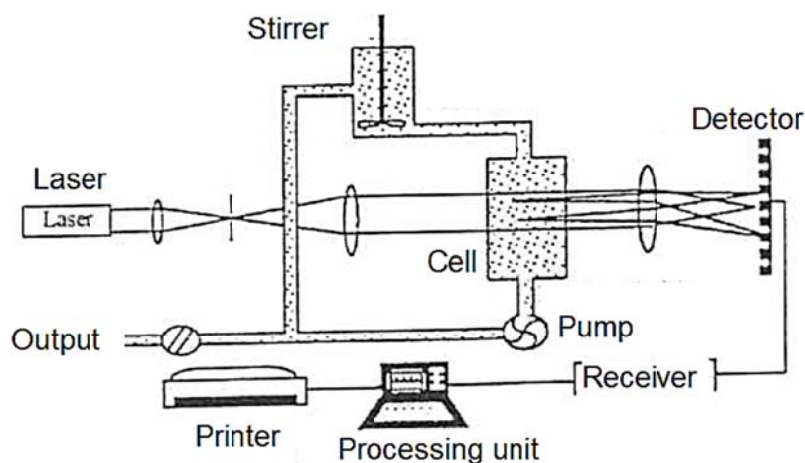


Figure 1. Basic operation of a LALLS device (Renliang, 2001).

1.2. Sample preparation

Preparation of the three as-received CDW materials involved pulverization of thirteen samples for each CDW material followed by sieving to 125µm sieve and collecting the finely ground sieved powder. A total of approximately 500g for each of the three CDW materials was obtained upon sieving, to allow for sufficient amounts to be used for the analytical techniques and the necessary quantities were utilized accordingly for all analyses described in this report as per the deliverables. All samples were maintained at $20 \pm 2^\circ\text{C}$, 65% RH until the specified day of analysis. The samples were carefully placed within the cell of the LALLS device where the laser beam was subsequently transmitted to the sample as per the configuration in Figure 1. The refractory signal was then received by the receiver compartment which was connected to the computer to output the relevant results. Thirteen samples were analysed for each of the 3 CDW materials to give a total of 39 sets of results.

1.3. Results

Figures 2 to 4 show the average particle size analysis runs for all samples, and Appendix 1 shows the individual runs per each of the 13 samples for each of the 3 CDW materials. The x-axis in graphs represents the particle size in microns whereas the y-axis represents the volume (%).

[In Appendix 1: Sample 1= CDW brick; Sample 2= CDW concrete; Sample 3= CDW ceramic tile]

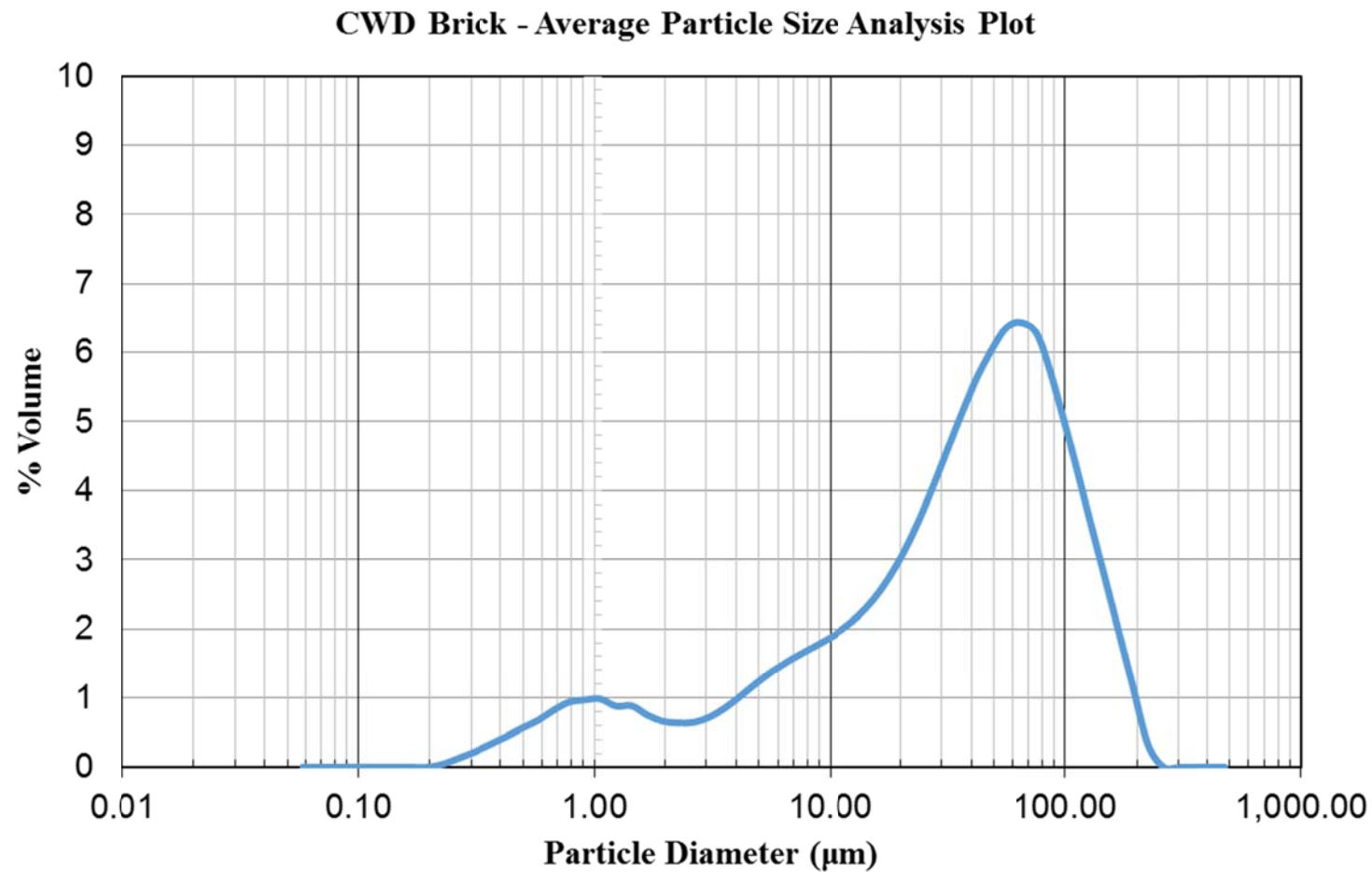


Figure 2. Average particle size analysis for the CWD brick material.

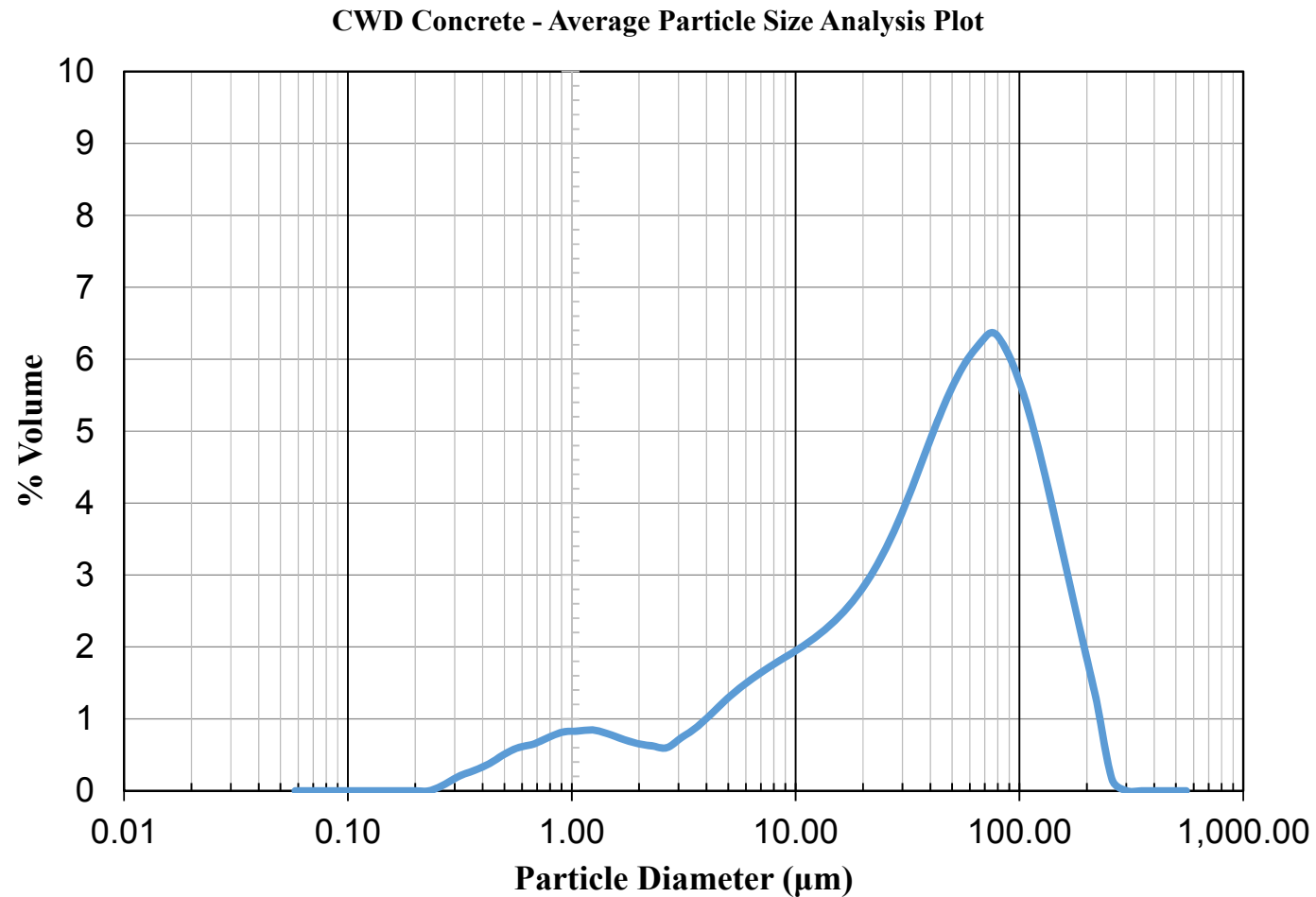


Figure 3. Average particle size analysis for CWD concrete material.

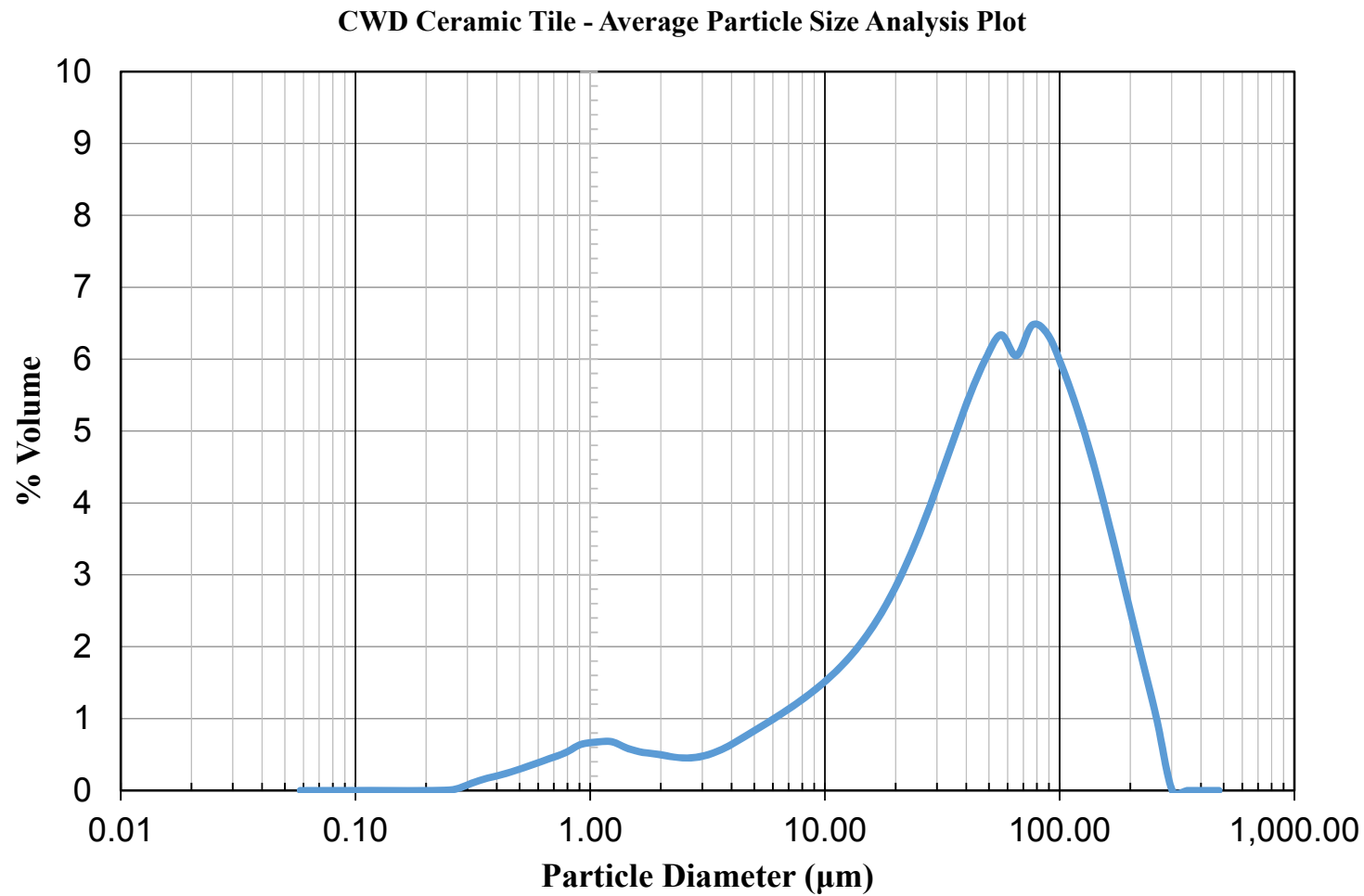


Figure 4. Average particle size analysis for CDW ceramic tile material.

1.4. Discussion

Figures 2 to 4 show the particle size analyses and distributions for the three investigated CDW materials. In the predominant measurement runs, it was observed that the percentage volume of the samples reached its peak value approximately within the range of 60-80 microns. A slight increase of volume at 1 micron size occurred followed by a 0.5% volume reduction at the regime between 2 and 3 microns. Past the peak, the volume fraction was thereon decreased in the samples reaching zero at around 200-300 microns. The particular pattern was evident in almost all investigated CDW samples i.e. brick, concrete and ceramic tiles. This was due to the consistent and identical sieving technique that was applied to all samples, which was utilised for the purposes of reproducibility, consistency, repeatability and validity in the sample examinations. It should be noted that the specific particle size analysis technique provides useful regimes of volume distributions across a range of diameters for the as-received samples, however, it is not possible to ascertain any information on the physio/chemical and mineralogical composition of the materials through the specific analysis.

2. X-RAY FLUORESCENCE (XRF) ANALYSIS

2.1. Background

The XRF (X-Ray Fluorescence) method provides qualitative and quantitative measurements of the elemental composition of solid materials. The XRF analysis can be used to determine the concentration of all elements with atomic weight greater than that of aluminium. The technique is relatively fast and reliable, and it is suitable for measurements on standard samples of known mineralogical/phase compositions. The minimum quantity sample required is 5-10g.

Typical applications of the method involve the determination of the composition of metal alloys, thin films with technological applications, trace elements in environmental samples (soil, aerosols deposited in filters), as well as non-destructive analysis of archaeological objects.

The analysis of major and trace elements in various materials by X-ray fluorescence is conducted as these interact with radiation. When materials are excited with short wavelength high-energy radiation (e.g., X-rays), then they can become ionized. Should the radiation energy become sufficient to dislodge an inner electron, then the atom becomes unstable and the missing inner electron is replaced by an outer electron. Energy is then released due to the decreased binding energy of the inner electron orbital compared with an outer one. The emitted radiation is associated with lower energy than the primary incident X-rays, which is termed fluorescent radiation. The resulting fluorescent X-rays can be used to detect the abundances of elements present in the sample because the energy of the emitted photon is characteristic of a transition between specific electron orbitals in a particular element (Jenkins, 1999).

When this primary X-ray beam illuminates the sample, excitation occurs. The excited sample in turn emits X-rays along a spectrum of wavelengths which essentially reflects a footprint of the types of atoms that are present in the sample. The atoms in the sample absorb X-ray energy by the process of ionization, ejecting electrons from the lower (usually K and L) energy levels. The ejected electrons are replaced by electrons from an outer, higher energy orbital. When this happens, energy is released (in the form of emission of characteristic X-rays indicating the type of atom present) due to the decreased binding energy of the inner electron orbital compared with an outer one. In most minerals and rocks where numerous elements are present, the emitted X-ray spectrum is quite complex and it is separated into characteristic wavelengths for each element present with the use of a Wavelength Dispersive

Spectrometer. The intensity of the emitted beam is measured using various types of detectors (gas flow proportional and scintillation). The flow counter is commonly utilized for measuring long-wavelength (>0.15 nm) X-rays that are typical of K spectra from elements lighter than Zn. The scintillation detector is commonly used to analyze shorter wavelengths in the X-ray spectrum (K spectra of an element from Nb to I; L spectra of Th and U). X-rays of intermediate wavelength (K spectra produced from Zn to Zr and L spectra from Ba and the rare earth elements) are generally measured by using both detectors in tandem. The abundance of the element in the sample is identified by the intensity of the energy measured by these detectors proportionally. The exact value of this proportionality for each element is derived by comparison to mineral or rock standards whose composition is known from prior analyses by other techniques (Fitton, 1997; Beckhoff et al, 2006).

XRF analysis is growingly used in a wide range of applications (Beckhoff et al, 2006), including:

- soil surveys
- research in igneous, sedimentary, and metamorphic petrology
- cement production
- ceramic and glass manufacturing
- environmental studies (e.g., analyses of particulate matter on air filters)
- metallurgy (e.g., quality control)
- mining (e.g., measuring the grade of ore)
- petroleum industry (e.g., sulfur content of crude oils and petroleum products)

The particular analysis is also well-suited for investigations that involve (Rollinson, 1993; Beckhoff et al, 2006):

- bulk chemical analyses of trace elements (in abundances >1 ppm; Ba, Ce, Co, Cr, Cu, Ga, La, Nb, Ni, Rb, Sc, Sr, Rh, U, V, Y, Zr, Zn) in rock and sediment.
- bulk chemical analyses of major elements (Si, Ti, Al, Fe, Mn, Mg, Ca, Na, K, P) in rock and sediment

X-ray fluorescence is, however, limited (Jenkins, 1999; Beckhoff et al, 2006) to the analysis of:

- materials containing high abundances of elements for which absorption and fluorescence effects are only reasonably well understood and researched
- materials that can be prepared in powder form and homogenized effectively
- relatively large samples, typically > 1 gram
- materials for which compositionally similar, well-characterized standards are available

In order to prepare the samples for analysis, grinding to a fine powder initially takes place. At this point, it may be analyzed directly, typically for trace element analysis. Nevertheless, the wide range in abundances of various elements as well as the wide range of sizes of grains in a powdered sample, makes the proportionality comparison to the standards particularly rigorous and time consuming. For this reason, it is usually implemented a mixing of the powdered sample with a chemical flux and use a furnace to melt the powdered sample, in order to create a homogenous glass for efficient analysis (Beckhoff et al, 2006).

2.2. Sample preparation

Preparation of the three as-received CDW materials involved pulverization of thirteen samples for each CDW material followed by sieving to 125µm sieve and collecting the finely ground sieved powder. A total of approximately 500g for each of the three CDW materials was obtained upon sieving, to allow for sufficient amounts to be used for the analytical techniques and the necessary quantities were utilized accordingly for all analyses described in this report as per the deliverables. All samples were maintained at 20±2°C, 65% RH until the specified day of analysis.

To determine the chemical composition of the samples using X-ray fluorescence, a combination of energy dispersion XRF analysis using Spectro Xepos coupled with a fusion method involving dissolution of the sample in HNO₃ was adopted. According to the latter, each sample was melted at 1000° C with a mixture of fusion materials (Li₂B₄O₇ and KNO₃ in a ratio of 15:1 by weight) and the resulting melt was then dissolved in densely concentrated HNO₃ solution at a ratio of 1:10 by volume. Thirteen samples were analysed for each of the 3 CDW materials for a total of 39 sets of results.

2.3. Results

Summaries of elemental and oxide analyses for each of the three CDW materials investigated are shown in Figures 5 to 7 and in Table 1, whereas the individual XRF results for CDW material, for which 13 runs were conducted for each, are shown in Appendix 2.

[In Appendix 2: Sample 1= CDW brick; Sample 2= CDW concrete; Sample 3= CDW ceramic tile]

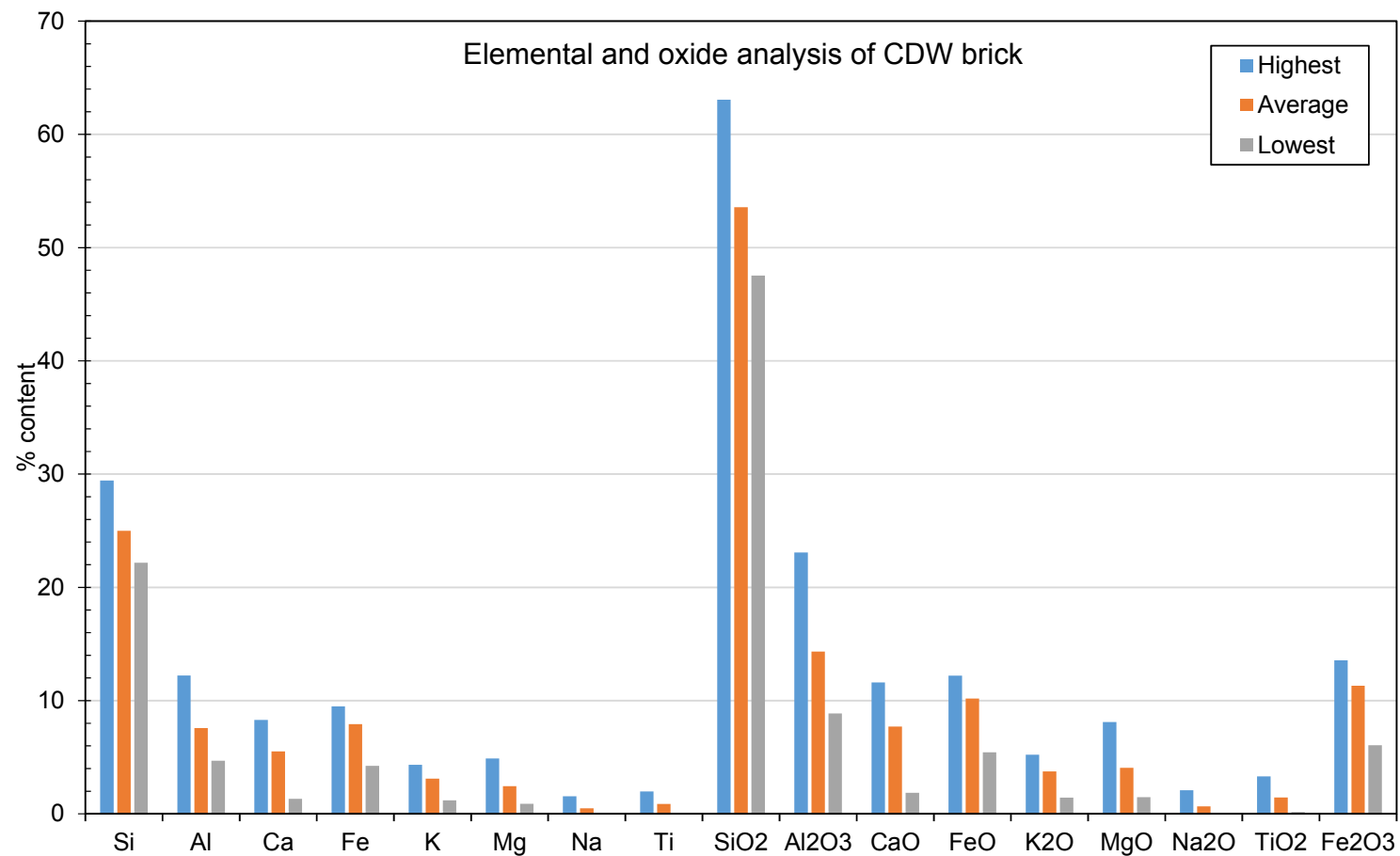


Figure 5. Summary of elemental and oxide analysis for CDW brick

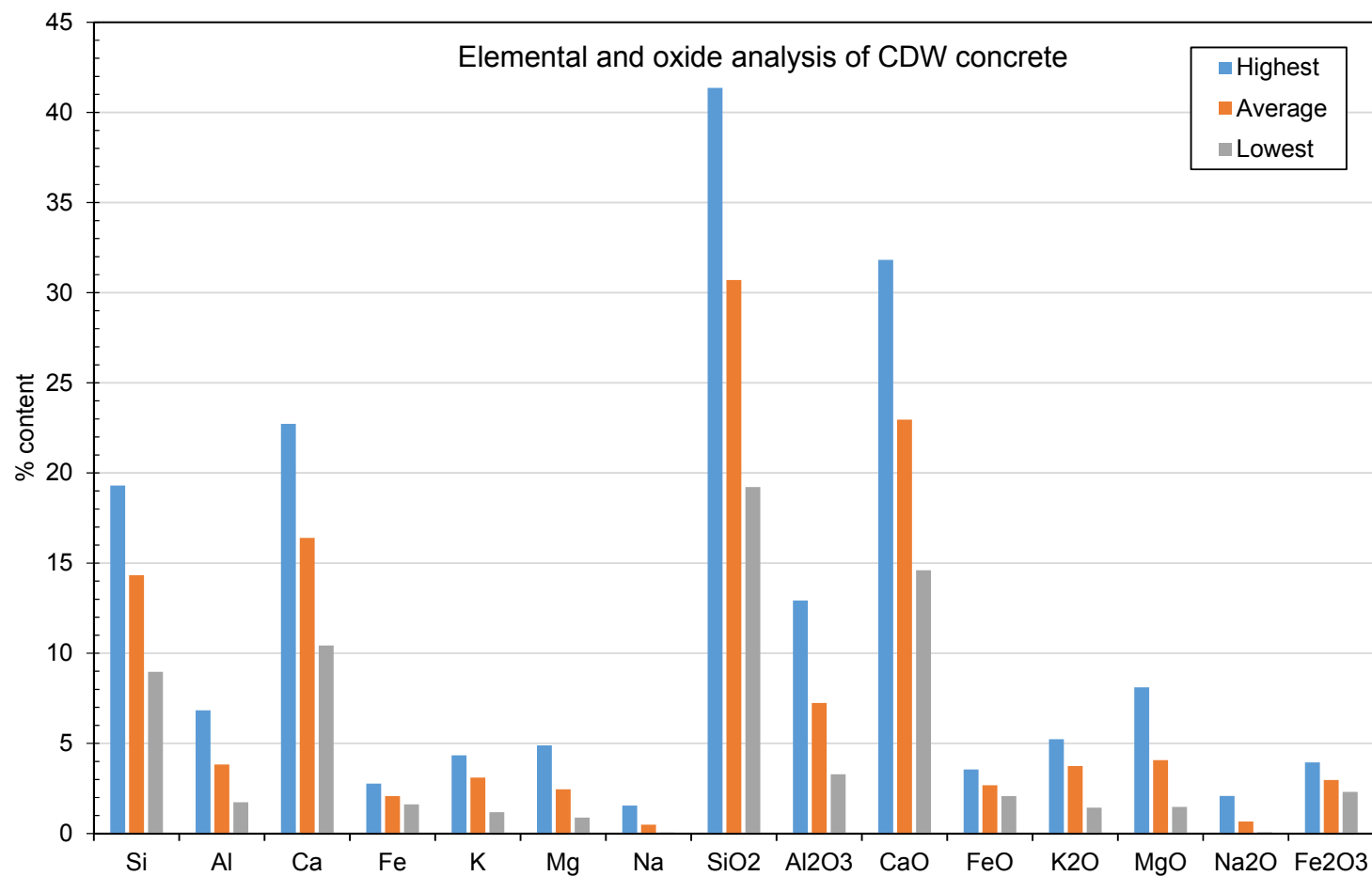


Figure 6. Summary of elemental and oxide analysis for CDW concrete.

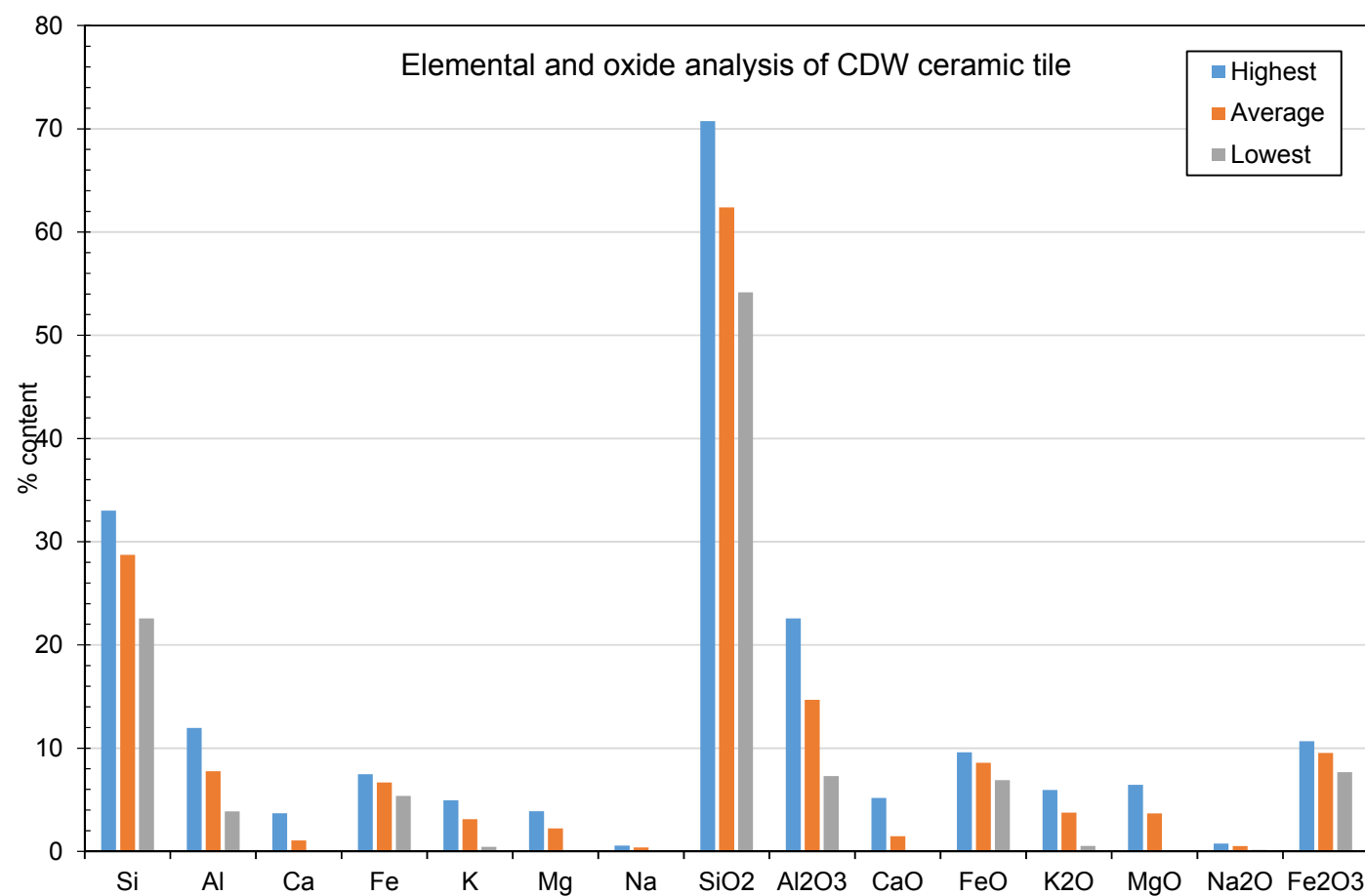


Figure 7. Summary of elemental and oxide analysis for CDW ceramic tile.

Table 1. Summary of elemental and oxide content analysis for the 3 CDW materials

	BRICK				CONCRETE				CERAMIC TILE			
	Highest %	Lowest %	δ max %	Average %	Highest %	Lowest %	δ max %	Average %	Highest %	Lowest %	δ max %	Average %
Si	29.43	22.18	7.25	25.00	19.30	8.97	10.33	14.33	33.01	22.57	10.44	28.73
Al	12.21	4.69	7.52	7.59	6.84	1.74	5.10	3.83	11.95	3.87	8.08	7.77
Ca	8.29	1.32	6.97	5.51	22.73	10.43	12.30	16.40	3.70	0.04	3.66	1.05
Fe	9.49	4.23	5.26	7.92	2.77	1.62	1.15	2.08	7.47	5.37	2.10	6.68
K	4.34	1.19	3.15	3.10	4.34	1.19	3.15	3.10	4.94	0.44	4.50	3.12
Mg	4.89	0.89	4.00	2.45	4.89	0.89	4.00	2.45	3.89	0.02	3.87	2.22
Na	1.55	0.06	1.49	0.49	1.55	0.06	1.49	0.49	0.56	0.11	0.45	0.39
Ti	1.98	0.09	1.89	0.87	-	-	-	-	-	-	-	-
SiO₂	63.06	47.53	15.53	53.57	41.36	19.22	22.14	30.71	70.74	54.16	16.58	62.40
Al₂O₃	23.07	8.86	14.21	14.33	12.92	3.29	9.63	7.24	22.57	7.30	15.27	14.68
CaO	11.60	1.85	9.75	7.71	31.82	14.60	17.22	22.96	5.18	0.06	5.12	1.48
FeO	12.20	5.44	6.76	10.19	3.56	2.08	1.48	2.68	9.60	6.90	2.70	8.58
K₂O	5.23	1.43	3.80	3.74	5.23	1.43	3.80	3.74	5.95	0.53	5.42	3.76
MgO	8.11	1.48	6.63	4.07	8.11	1.48	6.63	4.07	6.45	0.03	6.42	3.68
Na₂O	2.09	0.08	2.01	0.66	2.09	0.08	2.01	0.66	0.75	0.15	0.60	0.52

TiO₂	3.30	0.16	3.14	1.46	-	-	-	-	-	-	-	-
Fe₂O₃	13.55	6.05	7.50	11.32	3.95	2.31	1.64	2.98	10.67	7.67	3.00	9.54

2.4. Discussion

Elemental and oxide analysis results for all three CDW materials are shown in Figures 5 to 7 and in Table 1. Summary of elemental and oxide content analysis for the 3 CDW materials Individual XRF analysis results for all materials are shown in Appendix 2.

Measurements for CDW brick and CDW ceramic tile expectedly showed predominant amounts of aluminosilicates within their chemical composition. The highest amounts of silica reached almost 30.00% for the brick samples and 33.01% for the ceramic tiles whereas their corresponding lowest reached 22.18% and 25.27% respectively. Similar variations in aluminium contents were observed, with the highest contents for Sample 1 and Sample 3 reaching an interesting 12.21 % and 11.95% respectively. It was observed, however, that such high Al contents occurred only in isolated runs for both samples, whereas the predominance of analysis results was indicating towards the range of approximately 9-9.5% contents for the samples.

The CDW concrete sample was expectedly characterised by mainly calcium silicates (up to 22.73% for calcium in some samples and 19.3% for silicon). A notable variability was also observed in silicon contents with the lowest content being 11% and the highest being 19%. Lower amounts of potassium magnesium and sodium were detected in all samples which were less varied across the 13 analysis runs. An interesting point was the significant variations that occurred in the CaO contents, with the highest oxide concentration reaching up to 31% and the lowest being down to 15% in specific samples. This oxide content provides indirect information on the degree of carbonation that the material suffered from during its design life. In samples with low CaO contents, it is possible that the as-received examined materials were either taken from locations near a surface exposed to atmospheric CO₂, (e.g. column edges, external wall demolished piece, etc.) that was most probably carbonated, i.e. Ca(OH)₂ reacted with CO₂ in the presence of moisture to yield CaCO₃ products. However, because the source and any other compositional information regarding the materials are unknown, it is unlikely to ascertain any accurate or valid explanations of any possible mechanisms stated above.

Based on the results, it is evident that source is a major factor affecting the main mineralogical phases in the materials and particularly the calcium, silicon and aluminium contents, and to a lesser extent the

potassium, sodium and magnesium contents. A number of factors contribute to the variability shown in the results of concrete samples and these are non-exhaustively listed below:

- Difference in mix proportions within each concrete sample for achieving different design strengths in the demolished structures (such as different aggregate contents, cement contents, w/c ratios)
- Performance requirements, design life and intended purpose of concrete used in the demolished structures yielding different microstructural characteristics
- Portland cement type/class used in different demolished structures i.e. 42.5/52.5 N/R/ SR
- Existence of admixtures in several mixtures used in the structures
- Quality of each constituent used in the mixture, i.e. aggregate absorption/density/porosity values, particle size distribution, sand quality, texture surface roughness, angularity/sphericity and surface area
- Difference in ambient conditions (temperature, humidity and weather) that vary from source to source

For the ceramic samples investigated in this deliverable, the following factors underpin the high variabilities observed in the mineralogical compositions:

- Different manufacturing processes of the products prior to being utilized in the demolished structure (temperatures in kilns, duration of heating, constituent proportions during production)
- Quality of the raw materials utilized in the plant for the manufacturing process led to elemental variations during the final formation
- Different performance based specifications, design life, intended purpose microstructural characteristics

3. X-RAY DIFFRACTION (XRD) ANALYSIS

3.1. Background

X-ray powder diffraction (XRD) is a rapid analytical technique predominantly used for phase identification of crystalline materials. It has the capability of providing information on unit cell dimensions of a finely ground, homogenized material to determine its average bulk composition.

X-ray diffraction is based on constructive interference of monochromatic X-rays and a crystalline sample. If the sample is amorphous, the analysis is not possible due to the noise generated. These X-rays are generated by a cathode ray tube and filtered to produce monochromatic radiation, collimated to concentrate, and directed towards the sample. The interaction of the sample with the incident rays produces constructive interference (and a diffracted ray) when conditions satisfy Bragg's Law ($n\lambda = 2d \sin \theta$). This law relates the wavelength of electromagnetic radiation to the diffraction angle and the lattice spacing in a crystalline sample. These diffracted X-rays are then detected, processed and counted. By scanning the sample through a range of 2θ angles, all possible diffraction directions of the lattice should be attained due to the random orientation of the powdered material. Conversion of the diffraction peaks to d-spacings allows identification of the mineral because each mineral has a set of unique d-spacings. Typically, this is achieved by comparison of d-spacings with standard reference patterns (Klug and Alexander, 1974; Moore and Reynolds, 1997). All diffraction methods are based on the generation of X-rays within an X-ray tube. These X-rays are directed at the sample, and the diffracted rays are collected. A key component of all diffraction is the angle between the incident and diffracted rays.

X-ray diffractometers, such as the SIEMENS D5000 used in this research programme (Figure 8) consist of three basic elements: an X-ray tube, a sample holder, and an X-ray detector. X-rays are generated in a cathode ray tube. A filament is heated to produce electrons, accelerating these towards a target by applying a voltage, and fusing the target material with electrons. When electrons have sufficient energy to dislodge inner shell electrons of the target material, characteristic X-ray spectra are produced and they consist of several components, the most common being $K\alpha$ and $K\beta$. The former is constituted by $K\alpha_1$ and $K\alpha_2$ where $K\alpha_1$ has a slightly shorter wavelength and twice the intensity as $K\alpha_2$. The specific wavelengths are characteristic of the target material (Cu, Fe, Mo, Cr). $K\alpha_1$ and $K\alpha_2$

are, however, sufficiently close in wavelength such that a weighted average of the two is used. In single-crystal diffraction, copper is the most common target material. These X-rays are collimated and targeted onto the sample. As the sample and detector are rotated, the intensity and characteristics of the reflected X-rays are recorded. When the geometry of the incident X-rays injecting the sample coheres with the Bragg Equation, constructive interference occurs and a peak in intensity is outputted. This X-ray signal is recorded and processed by a mechanical detector which converts the signal to a count rate that is extracted to a device such as a printer or a computer monitor. (Waseda et al, 2011; Klug and Alexander, 1974; Moore and Reynolds, 1997).

The geometry of an X-ray diffractometer allows the sample to rotate at an angle θ while the X-ray detector is mounted on an arm to collect the diffracted X-rays and rotates at an angle of 2θ . The instrument used to maintain the angle and rotate the sample is termed a goniometer. For typical powder patterns, data is collected at 2θ from $\sim 5^\circ$ to 70° .



Figure 8. The SIEMENS D5000 X-ray diffractometer used in the experiment.

X-ray powder diffraction is most widely used for the identification of unknown crystalline materials (e.g. minerals, inorganic compounds). Determination of unknown solids is critical to studies in geology, environmental science, material science, engineering and biology.

Other applications (Waseda et al, 2011) include:

- characterization of crystalline materials (amorphous materials are difficult to detect)
- identification of fine-grained minerals such as clays that are difficult to determine optically
- measurement of the purity of a random sample
- determine, quantitatively, crystal structures using Rietveld refinement
- determining the thickness, roughness and density of films using glancing incidence X-ray reflectivity measurements
- determine of modal amounts of numerous minerals (quantitative analysis)
- determining dislocation density and quality of such films by rocking curve measurements
- measuring superlattices within multilayered epitaxial structures

XRD analysis offers the following advantages (Waseda et al, 2011):

- Fast and effective (< 20 min) technique for identification of an unknown mineral and its composition
- Wide availability of XRD instrumentation
- In most cases, it provides an unambiguous mineral determination
- Sample preparation is minimal and quick
- Data interpretation, given a database, is relatively simple and straightforward

Whereas, there are certain limitations to be considered (Waseda et al, 2011) when utilizing XRD analysis:

- The analysis requires tenths of a gram of material which must be rigorously ground into a powder
- Preferably, a homogeneous and single-phase material is best for identifying structures
- Peak overlay or overlapping may occur and it exacerbates for high angle 'reflections'

- Access is needed to a database or to a standard reference file of inorganic compounds (d-spacings, hkl's)

3.2. Sample preparation

Preparation of the three as-received CDW materials involved pulverization of thirteen samples for each CDW material followed by sieving to 125 μ m sieve and collecting the finely ground sieved powder. A total of approximately 500g for each of the three CDW materials was obtained upon sieving, to allow for sufficient amounts to be used for the analytical techniques and the necessary quantities were utilized accordingly for all analyses described in this report as per the deliverables. All samples were maintained at 20 \pm 2°C, 65% RH until the specified day of analysis.

To determine the chemical composition of the samples using X-ray diffraction, a SIEMENS D5000 Diffractometer was used with Cu K α 1 (Ni filtered radiation) set for a 2-theta angle range of 2° – 60° and with a 0.02°/sec step interval. Thirteen samples were analysed for each of the 3 CDW materials to give a total of 39 sets of results. The intensity of diffracted X-rays was continuously recorded as the sample and detector rotate through their respective angles. A peak in intensity occurs when the mineral contains lattice planes with d-spacings appropriate to diffract X-rays at that value of θ . Although each peak consists of two separate reflections (K α 1 and K α 2), at small values of 2θ the peak locations overlap with K α 2 appearing as a hump on the side of K α 1. Greater separation occurs at higher values of θ . These combined peaks were treated as one. The 2λ position of the diffraction peak was measured as the centre of the peak at 80% peak height. Results are presented as peak positions at 2θ and X-ray counts (intensity) in the form of plots. Intensity (I) was reported as peak height intensity. The relative intensity was recorded as the ratio of the peak intensity to that of the most intense peak (relative intensity = $I/I_1 \times 100$). The d-spacing of each peak was then obtained by solution of the Bragg equation for the appropriate value of λ .

3.3. Results

The XRD results for each of the 3 CDW materials are shown in Figures 9 to 11 below. Detailed individual XRD runs for each material are shown in Appendix 3.

[In Appendix 3: Sample 1= CDW brick; Sample 2= CDW concrete; Sample 3= CDW ceramic tile]

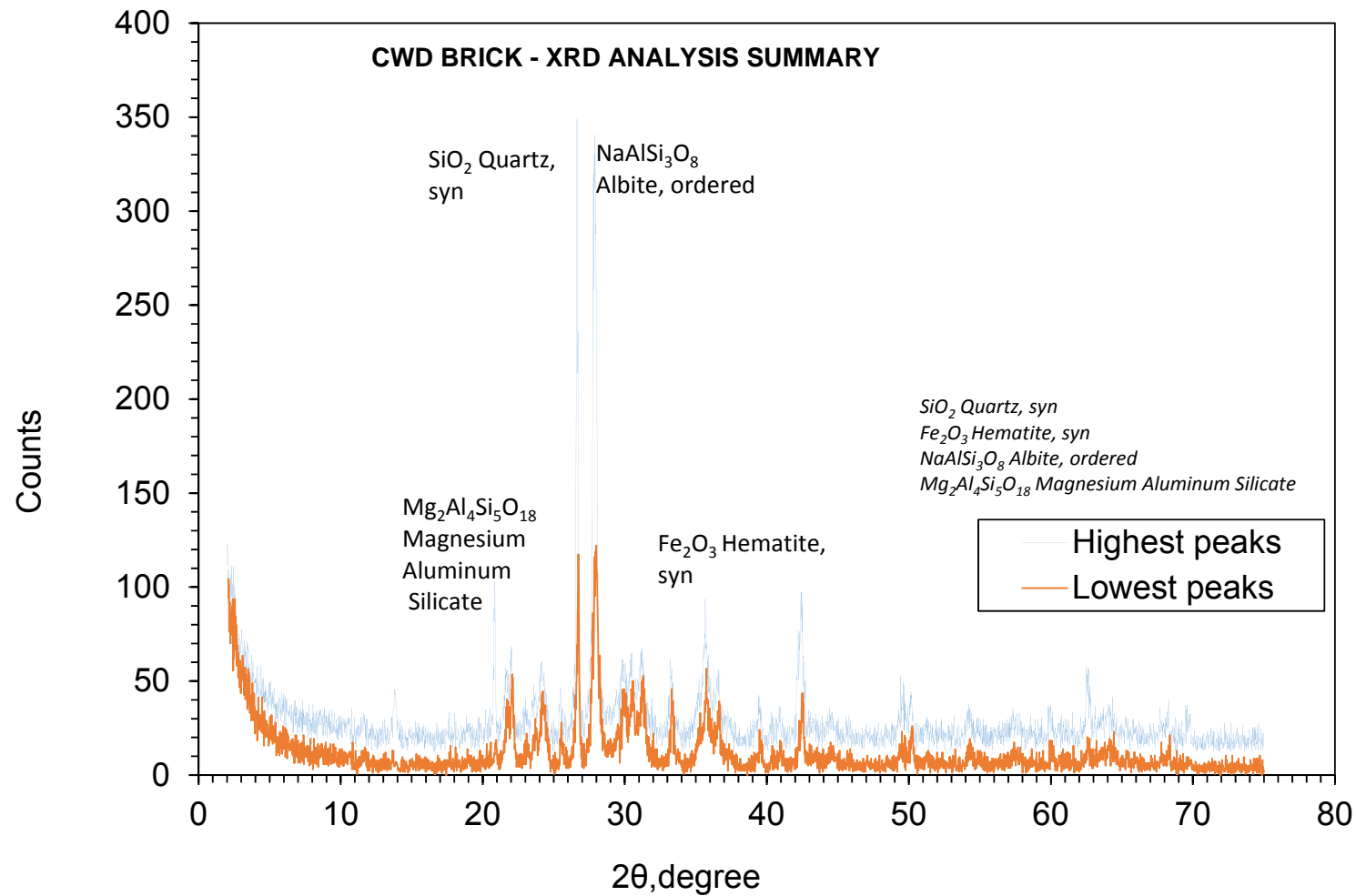


Figure 9. XRD analysis summary for CDW brick.

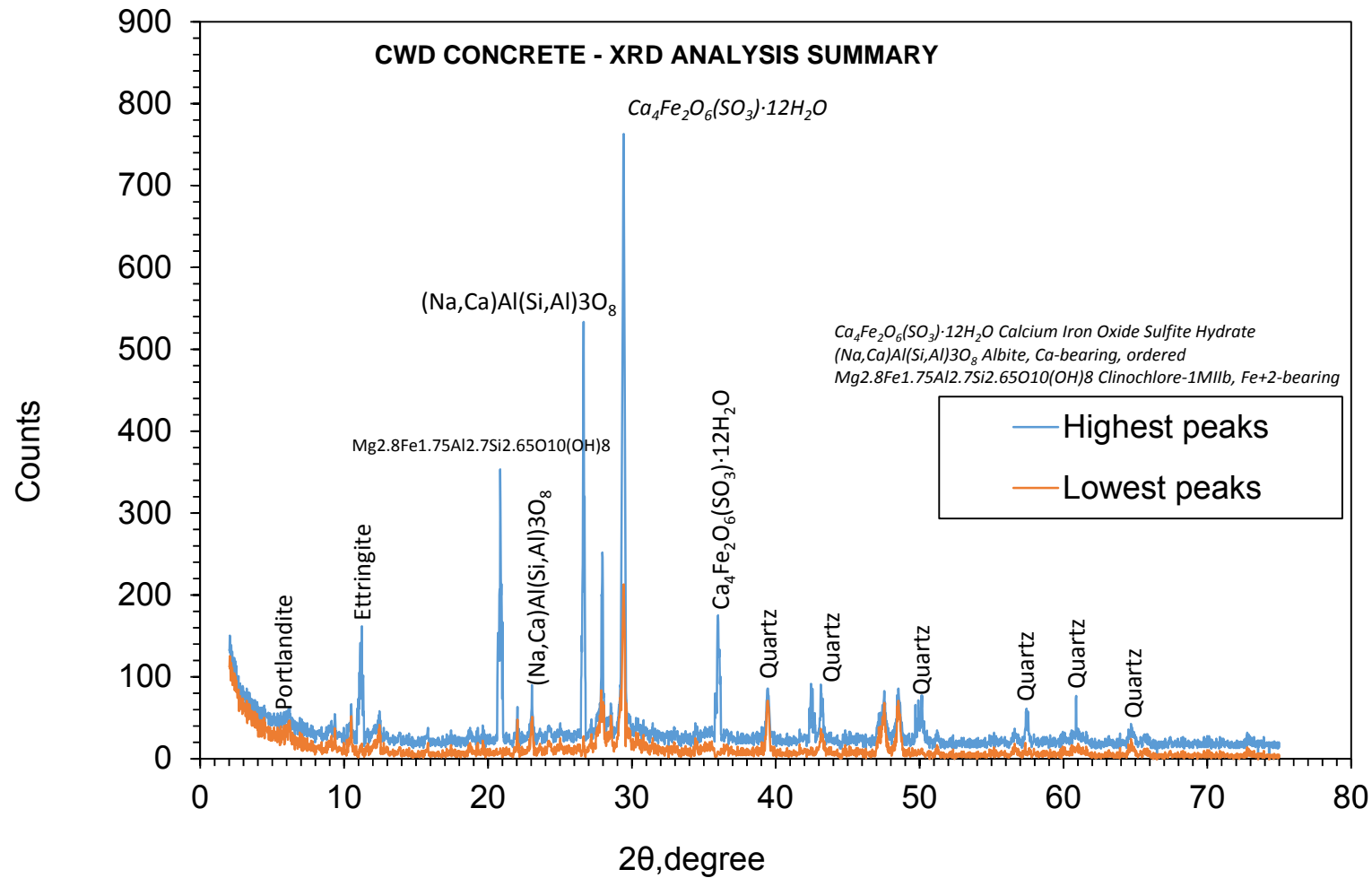


Figure 10. XRD analysis summary for CDW concrete.

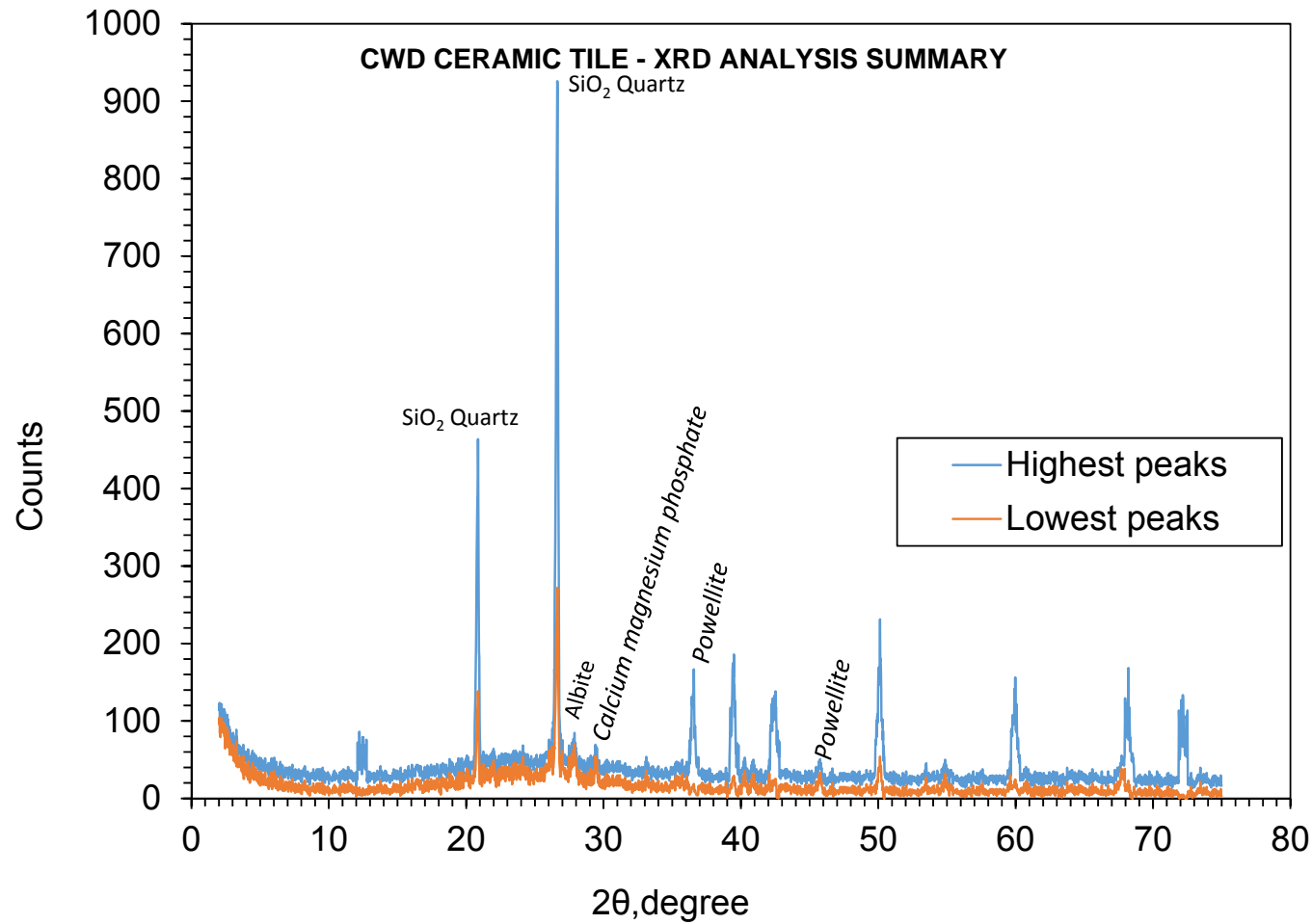


Figure 11. XRD analysis summary for CDW ceramic tile.

3.4. Discussion

Figures 9 to 11 show the summary of XRD diffractograms for the three as received CDW materials. Detailed individual XRD runs for each material are shown in Appendix 3.

In both samples 1 and 3 (bricks and ceramic tiles) there was, expectedly, a strong presence of SiO_2 peaks detected at a 2 theta of approximately 26.5° , with some brick samples exhibiting albite peaks at 27.5° of similar intensity or even higher than that of quartz. In both materials, relatively strong peaks of magnesium aluminium silicates were detected at approximately 20.5° , however, these seemed to appear weaker in ceramic tile samples (approximately 100 counts lower than those detected in brick samples). Generally, in both samples, there was a presence of aluminosilicate based phases as expected, albeit these phases were additionally embodying certain salts or minerals, e.g. Na (in the form of albite) or Mg.

The high intensity of albite peaks in some brick samples may indicate a slightly stronger presence of sodium minerals bound in aluminosilicate-based phases. This indication may be attributed to a number of possible causes, such as the location of the CDW structure being close to the sea. In such a scenario, possible air transportation of sodium-based minerals on the former CDW structure may have increased the content of sodium in the existing elements of the structure to reflect such amounts by means of a more intense peak.

Other peaks commonly detected in both ceramic tile and brick samples were those reflecting ferrite-based phases, such as hematite (Fe_2O_3). The intensity of the particular phase was varying in both samples and at different 2-theta angles (higher than 40°), denoting the different ambient conditions of the formerly CDW structures and the different locations of the sources.

Slightly more complicated crystalline phases were detected in concrete samples, with the predominant ones being calcium sulfoferrites, calcium carbonates and to a lesser intensity calcium hydroxide, ettringite, calcium silicates (possibly anhydrous) and calcium aluminosilicates. As hydrated C-S-H are associated with an amorphous microstructure, it would not be possible to evidence their presence in the diffractograms.

Most of the concrete samples exhibited low intensity of the calcium hydroxide peaks, which most probably indicates the depletion of the phase due to carbonation and the formation of calcium carbonate which was reflected in the plots. Some samples, in addition, exhibited weak peaks of ettringite whereas in other samples the particular peak was almost non-existent. This is possibly attributed to the disintegration of the ettringite in high temperatures as ettringite is known to be a thermodynamically unstable crystalline phase.

4. DENSITY MEASUREMENTS

4.1. Background

The DEFEAT project is the innovative separation and transformation of construction demolition wastes (CDW) into innovative thermal insulation, acoustic insulation, fire-resistant façade and recycled aggregate (RA). This project comprises of four (4) main work packages as follows: (1) Construction and demolition waste separation (2) Raw material characterization, (3) Design and development of composite materials (4) Materials and properties engineering. Density and absorption determinations as well as dissolution tests have been carried out by Frederick Research Center.

4.2. Separation and grinding of the raw materials

The construction demolition waste was obtained from a local construction and demolition waste recycling company, Resource Recovery Cyprus (RRC), i.e. PA2 of the consortium. Masonry-like materials were separated by hand and temporarily packed each in its own transparent plastic bag as shown in Figures 12 to 14. The raw materials were grinded at the laboratory of Latomia Pharmakas (PA1 of the consortium), by using a Los Angeles Abrasion machine. The machine contained 12 stainless steel balls, each of which ball weighs 439g, as shown in Figure 15 and Figure 16. The waste concrete, ceramic and red clay bricks were separately allowed to grind at 2000 rotations for 1.5 hours to increase its fineness and specific surface area.



Figure 12. The raw materials as received from CDW (waste brick).



Figure 13. The raw materials as received from CDW (waste tiles).



Figure 14. The raw materials as received from CDW (waste concrete).

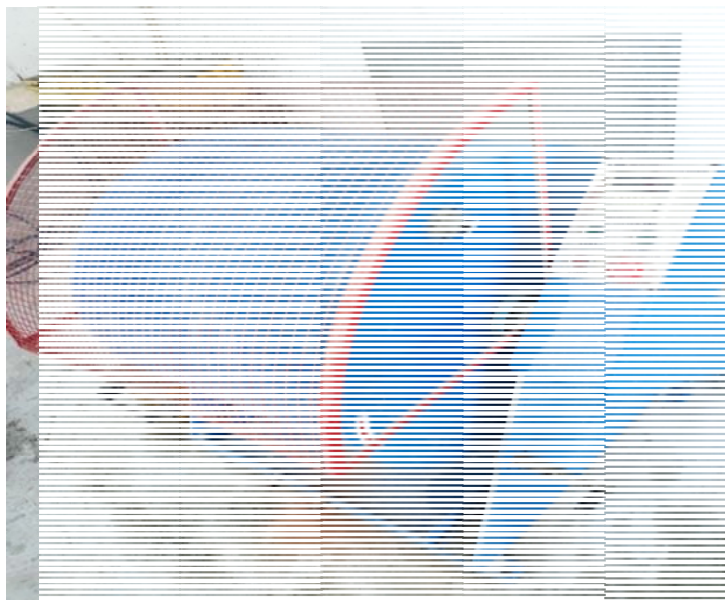


Figure 15. The Los Angeles abrasion machine.



Figure 16. The stainless balls inside the Los Angeles abrasion machine.

4.3. Particle size distribution of the finely ground raw materials

The ground waste bricks, waste tiles and waste concrete were separately sieved, as per CYS EN993-2:2020 and CYS EN 12948-2010. The analysis showed that brick has a high percentage of fines compared to tiles and concrete. Figure 17 shows the particle size distribution of the raw materials.

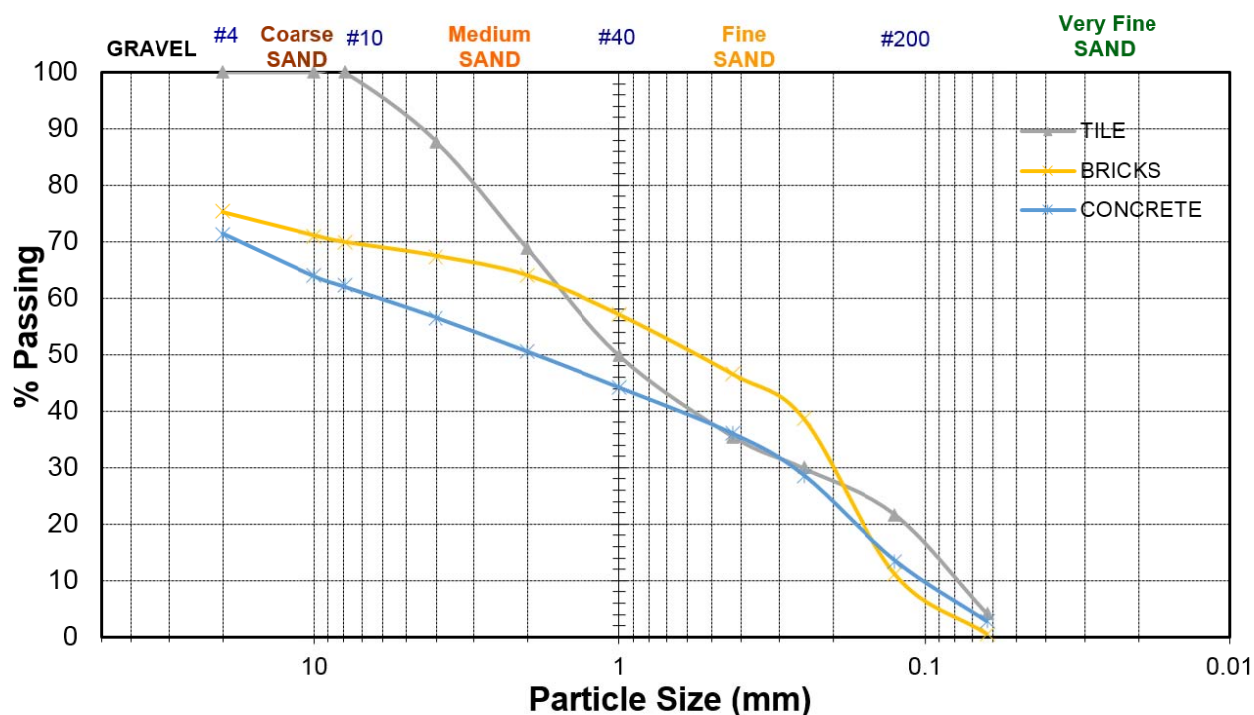


Figure 17. Particle size distribution of the raw materials.

4.4. Density determination of the finely ground raw materials

The determination of the densities and water absorption of the ground raw materials (waste ceramic, bricks and concrete) from construction demolition waste was conducted as per ASTM C128, where densities are expressed as bulk specific gravity and apparent specific gravity, in saturated surface dry condition. Table 2. Description of the test procedures as per ASTM 128-88 are shown in Table 2. The density test was conducted at Frederick Research Center laboratory by using the Pycnometer method.

Table 2. Description of the test procedures as per ASTM 128-88.

TEST #:	Densities and water absorption of CDW (ceramic, bricks and concrete)	
TEST METHOD:	AS per ASTM 128-88	
	Apparatus	Role
1	Los Angeles abrasion machine	For grinding the CDW
2	Pycnometer 500ml	Density determination
3	Balance with accuracy 0.1g	For weighing the sample
4	Water with a constant temperature $25^{\circ}\text{C} \pm 0.1^{\circ}\text{C}$	For moistening the sample to the desired moisture content
5	Heating oven which can maintain $110^{\circ}\text{C} \pm 5^{\circ}\text{C}$	For drying sample
6	Distilled water	
7	Metal mould in the form of a frustrum of a cone with dimensions as follows $40 \pm 3\text{mm}$ inside diameter at the top, $90 \pm 3\text{mm}$ inside diameter at the bottom and $75 \pm 3\text{mm}$ height and the metal having a minimum thickness of 0.8mm	For determination of saturated surface dry condition
8	Metal tamper $340 \pm 15\text{g}$ and having a flat circular tamping face of $25 \pm 3\text{mm}$ in diameter	For determination of saturated surface dry condition

The waste tile, waste red clay brick and waste concrete were ground into a fine powder and sieved to obtain the desired particle size as per ASTM C128, as shown in Figure 18. The ground raw materials from CDW.



Figure 18. The ground raw materials from CDW.

The samples of the ground i.e. waste bricks, waste tiles and waste concrete were prepared as specified by ASTM and sieved separately by using a 4 mm sieve. The materials passing on 4 mm sieve for each sample were used for this test. 2 kg of each sample was measured by using a balance with an accuracy of 0.1g and then the samples were allowed to dry in a suitable pan to a constant weight at a temperature of 120⁰C for 24 hours. Thereafter these were cooled for 1 hr, then immersed in water for 24 hrs as illustrated in Figure 19.



Figure 19. Weighing and immersion of samples.

The weight of the 500ml pycnometer filled with water was measured and recorded as B, shown in Figure 20.



Figure 20. Measurement of pycnometer filled with water to a calibration mark.

The samples were spread on a flat stainless pan and exposed to gently warm air and stirred frequently to cause homogeneous drying for achieving saturated surface dry condition. The process continued until tall specimens approached a free-flowing condition. A portion of the partially dried powder of the raw materials was placed loosely in the mold and lightly compacted with 25 light drops of the rod. Each compaction started about 5mm above the top of the surface of the specimen and allowed the tamper to drop freely under gravitational force on each drop.

The loose sand was removed from the base and the mold was lifted vertically. In case the surface moisture was still present, the specimen was allowable to dry again until the specimen slump slightly indicating that it has reached a saturated surface dry condition (Figure 21).



Figure 21. The sample tested in a saturated surface dry condition (right picture).

500g of each specimen of SSD sample was measured and the weight was recorded as weight, B. The pycnometer was initially filled partially with water and with 500g of the SSD sample, which was then rolled, inverted and agitated to remove air bubbles. Following this, the pycnometer was then fully filled with additional water and with the aid of a small paper which was dipped into the pycnometer, bubbles were removed. The total weight of the pycnometer filled with SSD and water to a calibration mark was measured and recorded as weight, C. All the sample was thoroughly poured into a drying pan and placed in a 120⁰C oven for 24hrs until it dries to constant weight and then, the dry sample was weighed and record as weight, A.

Calculation Procedure

Mass of oven dry sample(g), A

Mass of saturated surface dry sample + pycnometer (g) , B

Mass of saturated surface dry sample + pycnometer + water (g) , B

Volume of pycnometer (cm³), D

Mass of clean pycnometer (g), E

$$\text{Bulk density, } \rho_{bd} = \frac{A}{D - (C - B)/0.997}$$

$$\text{Apparent Density, } \rho_{ad} = \frac{A}{D - (C - A - E)/0.997}$$

$$\text{Water Absorption, } W_{abs} = \frac{(B - A - E)}{A} \times 100\%$$

The density values of waste tiles, waste bricks and waste concrete were 1.82, 1.63 and 1.87 g/cm³ as shown in Table 3 and Figure 22.

Table 3. Densities and water absorption values of the raw materials.

Categories	Raw Material		
	Tiles	Bricks	Concrete
Bulk density in g/cm ³	1.82	1.63	1.87
Apparent density in g/cm ³	2.56	2.81	2.68
Water absorption in %	15.77	25.57	15.98

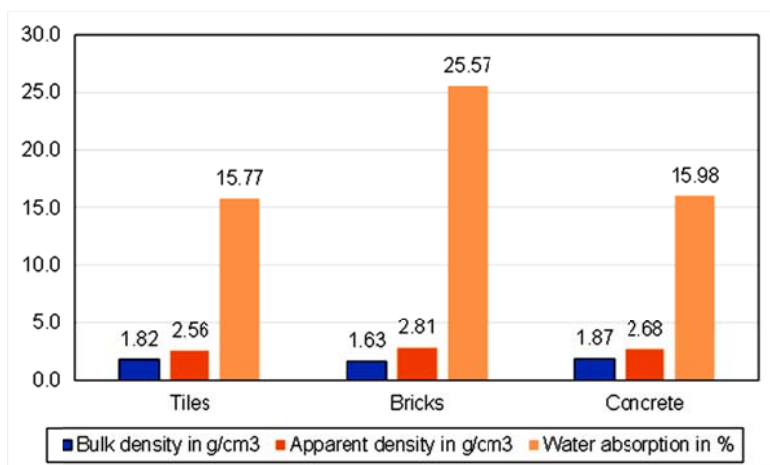


Figure 22. Summary of density determinations and water absorption values of CDW.

5. DISSOLUTION TESTS

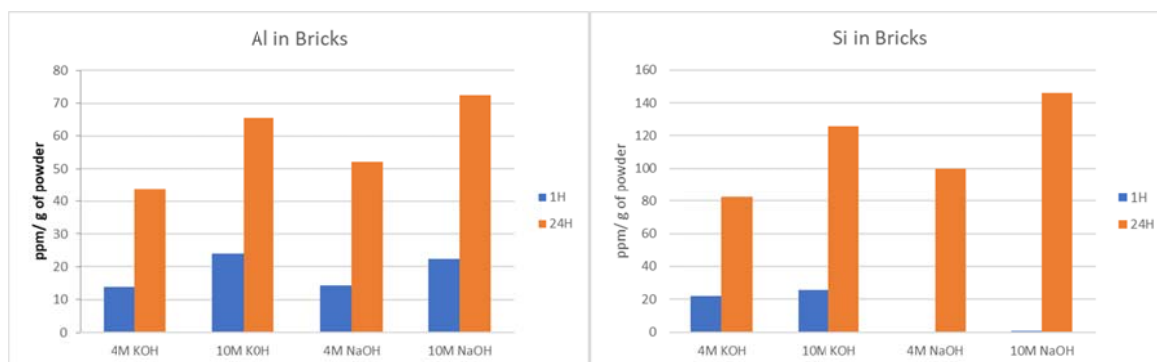
5.1. Results and Discussion

Dissolution of the two powders, tiles and bricks, presented a similar trend, Fig. 23. They dissolved significantly more of both Si and Al as the experiment lasted longer and as the molarity of the solution

Page 50 of 123

increased. Regarding the solution molarity, this showed to affect equally the initial dissolution as well as the dissolution after 24 hours for Al, while for Si, the initial dissolution seemed not to be affected significantly, if at all. Overall, the dissolution was being developed between the first 24 hours of reaction as the amount of Al increased about 3 times for bricks- and about 4 times for tiles- samples, while higher increase were always observed for NaOH based solutions. Regarding Si amounts, here, the relationships seemed to be more complex, as the type of alkali ion played a significant role. While in both powders, at least some Si was determined after 1h, when activated with KOH solutions, no or only very limited amount of Si was dissolved after 1h, when NaOH based solutions were used, regardless its molarity. Interestingly, higher Si values were determined after 24h in NaOH solutions. Overall, the dissolution of SI and Al initiated faster in KOH solutions but after 24h was more pronounced in NaOH solutions.

Rather different behavior was observed in case of Sulphur, where rather high amounts were determined already after 1h reaction. The S amounts varied between 78 and 230 ppm/g of powder for tiles, depending on type and molarity of the solution. In case of bricks samples, the S content stayed relatively constant ~170 ppm/g of powder. In both materials, it was observed that when 10M NaOH solution was used, the amount of S decreased over time, which could indicate a precipitation of some S-containing phases. The decreasing amount of S over time was observed in bricks sample also for the 10M KOH solution.



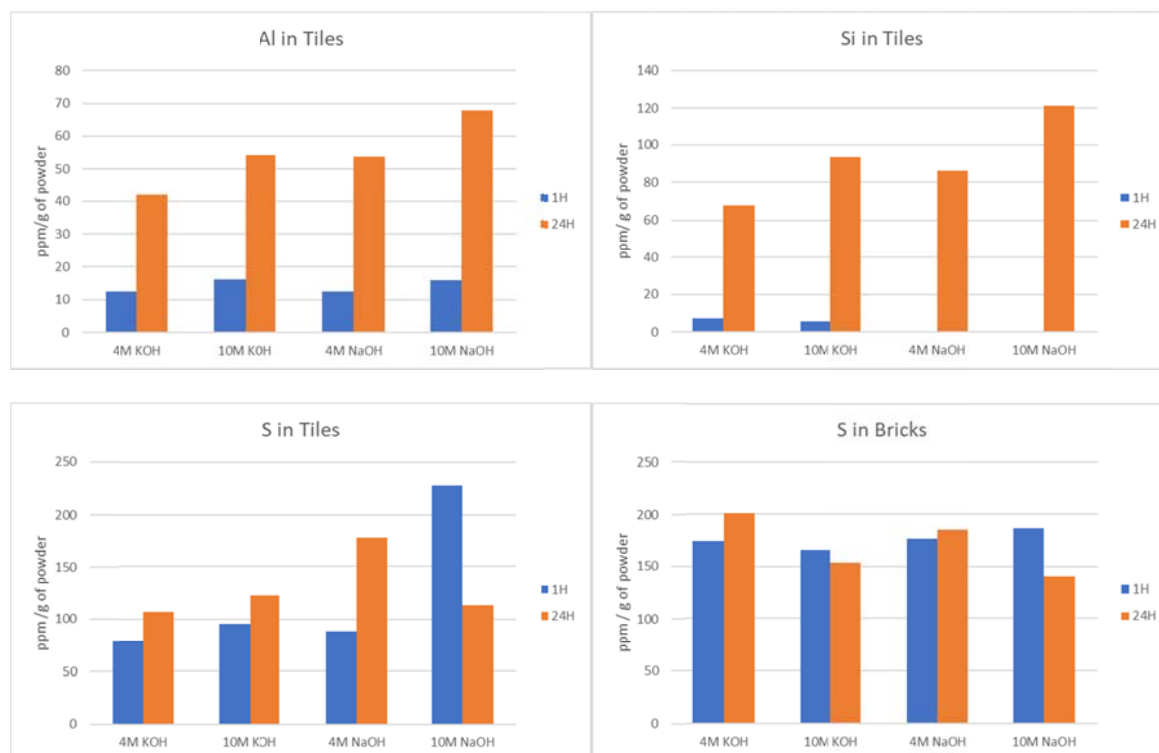


Figure 23: Dissolution of Al, Si and S from tiles and bricks in NaOH and KOH based solutions.

Isothermal calorimetry curves, Fig. 24, show low heat release of tiles and bricks powder when mixed with both water (top) and alkali solution (bottom). Regarding the water samples, here a small hump is observed between 5-30 hours for tiles sample, no hump is observed in bricks sample during the whole period. Nevertheless, in both samples a small amount of heat is generated over the time, however this is very low and the overall heat release does only reach 5 J/g and 1 J/g after 90 hours of reaction for tiles and bricks, respectively.

Samples activated with 1.6KS65 activating solution showed a peak within the first 20 hours. The heat release gradually decreases up to 60 – 80 h of reaction. The cumulative heat release curves, demonstrate that the heat release is more pronounced in the bricks sample, however after 110 h it seems to be equal for both materials and extrapolating the results beyond the measured period indicates that the tiles remain releasing more heat. Assuming that the heat release is associated to the binder

formation reaction the above points to the fact that although the bricks are reacting faster, the overall activation potential of tiles seems to be higher.

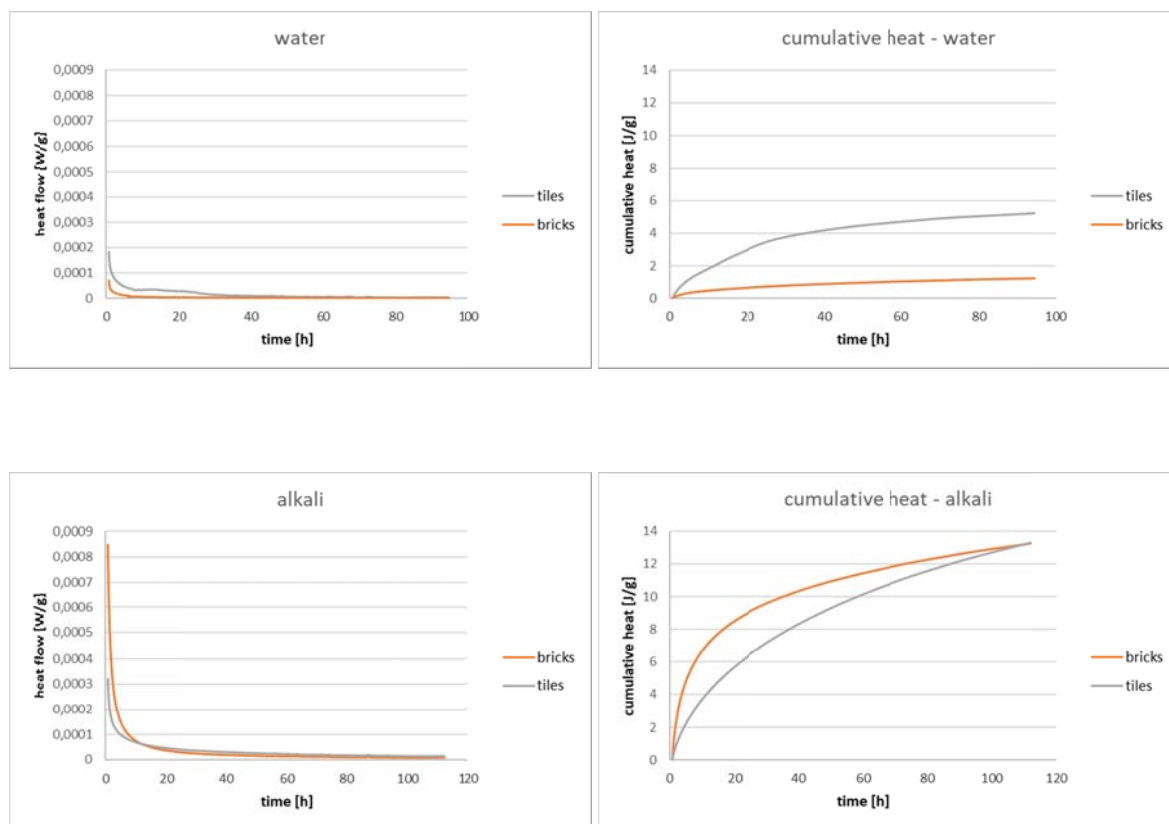


Figure 24: Isothermal calorimetry curves for material mixed with water (top) and with alkali solution (bottom).

6. CONCLUSIONS

Work Package 4 (WP4) of the DEFEAT research programme is led by the University of Cyprus (UCY) who is the strategic partner responsible for the management, timely execution, completion and delivery of the required outputs. WP4 targets a comprehensive set of generic characterization techniques conducted on as-received samples of CDW from different sources in order to investigate their full chemical and mineralogical composition which is a crucial step towards the development of the end product.

The present report (D4.1) includes results from a set of analytical techniques, namely X-Ray diffraction (XRD) X-Ray Fluorescence (XRF); particle size analysis and density determinations on thirteen samples of each of the following three as-received CDW materials:

- Brick (waste ceramic), noted as **Sample 1**;
- Concrete (waste concrete) noted as **Sample 2**;
- Tiles (waste ceramic) noted as **Sample 3**.

The characterization of the above as received materials involved utilizing both qualitative and quantitative approaches. These were essential for full and accurate output of results as well as for a valid discussion on the values obtained.

The materials were collected from variable sources, and the source was found to be a crucial parameter affecting the variability of mineralogical and oxide compositions. Quantitative results from XRF analysis provided numerical sets of information related to the oxide contents of the materials, whereas a qualitative set of data in XRD analysis gave relative sets of peak intensities of existing crystals within the samples. Particle size analysis provided distributions of particle volumes across a range of different diameters.

As the source of each of the as-received CDW materials was unknown, it was expected that significant variations in the mineralogical compositions would occur between the runs. It is concluded that the source is the largest determinant of the main mineralogical phases in the CDW materials. Particularly in concrete samples the calcium, silicon and aluminium contents have been significantly varying, whereas the potassium, sodium and magnesium contents were altered to a lesser extent. A number of factors have been found to affect the differences in mineralogical compositions:

- Difference in mix proportions within each concrete sample for achieving different design strengths in the demolished structures (such as different aggregate contents, cement contents, w/c ratios)
- Performance requirements, design life and intended purpose of concrete used in the demolished structures yielding different microstructural characteristics
- Portland cement type/class used in different demolished structures i.e. 42.5/52.5 N/R/ SR
- Existence of admixtures in several mixtures used in the structures
- Quality of each constituent used in the mixture, i.e. aggregate absorption/density/porosity values, particle size distribution, sand quality, texture surface roughness, angularity/sphericity and surface area

- Difference in ambient conditions and geographical location (temperature, humidity and weather) that vary from source to source leading to different degrees of mechanisms occurring (such as carbonation)

For the ceramic samples investigated in this deliverable, the following factors are underpinning the high variabilities observed in the mineralogical compositions:

- Different manufacturing processes of the products procured for usage in the demolished structure (temperatures in kilns, duration of heating, constituent proportions during production)
- Quality of the raw materials utilized in the plant for the manufacturing process led to elemental variations during the final formation
- Different performance-based specifications, design life, intended purpose microstructural characteristics.

REFERENCES

- Beckhoff, B., Kanngießer, B., Langhoff, N., Wedell R., and Wolff, H., 2006. Handbook of Practical X-Ray Fluorescence Analysis. 2nd ed. New York: Springer.
- F. Storti and F. Balsamo, 2010. Particle size distributions by laser diffraction: sensitivity of granular matter strength to analytical operating procedures. Solid Earth, 1, pp. 25–48.
- Fitton, G., 1997. X-Ray fluorescence spectrometry, in: Gill, R. (ed.), Modern Analytical Geochemistry: An Introduction to Quantitative Chemical Analysis for Earth, Environmental and Material Scientists: Addison Wesley Longman, UK.
- Jenkins, R., 1999. X-Ray Fluorescence Spectrometry. 2nd ed. New Jersey: John Wiley & Sons.
- Klug, H. P., and L. E. Alexander. 1974. X-ray diffraction procedures for polycrystalline and amorphous materials. 2nd ed. New Jersey: Wiley & Sons.
- Moore, D. M. and R. C. Reynolds, Jr. 1997. X-Ray diffraction and the identification and analysis of clay minerals. 2nd ed. New York: Oxford University Press.
- Potts, P.J., 1987. A Handbook of Silicate Rock Analysis: Chapman and Hall.
- Renliang X., 2001. Particle Characterization: Light Scattering Methods. New York: Springer.
- Rollinson, H., 1993. Using Geochemical Data: Evaluation, Presentation, Interpretation: John Wiley, NY.
- Syvitski, J. 1991. Principles, Methods and Application of Particle Size Analysis. Cambridge: Cambridge University Press.
- Waseda, Y., Matsubara, E., and Shinoda, K. 2011. X-Ray Diffraction Crystallography: Introduction, Examples and Solved Problems. 2nd ed. New York: Springer.

Acknowledgements

The authors would like to express their sincere gratitude to the Republic of Cyprus, the Cyprus Research & Innovation Foundation (RIF) and the European Regional Development Fund, for funding the research project entitled “Development of an Innovative Insulation Fire Resistant Façade from the Construction and Demolition Wastes” (Contract Number: INTEGRATED/0918/0052).

APPENDIX 1

Particle Size Analysis For All CDW Samples

[SAMPLE 1= BRICK; SAMPLE 2= CONCRETE; SAMPLE 3= CERAMIC TILE]

[each sample was analysed in 13 runs]

SAMPLE 1

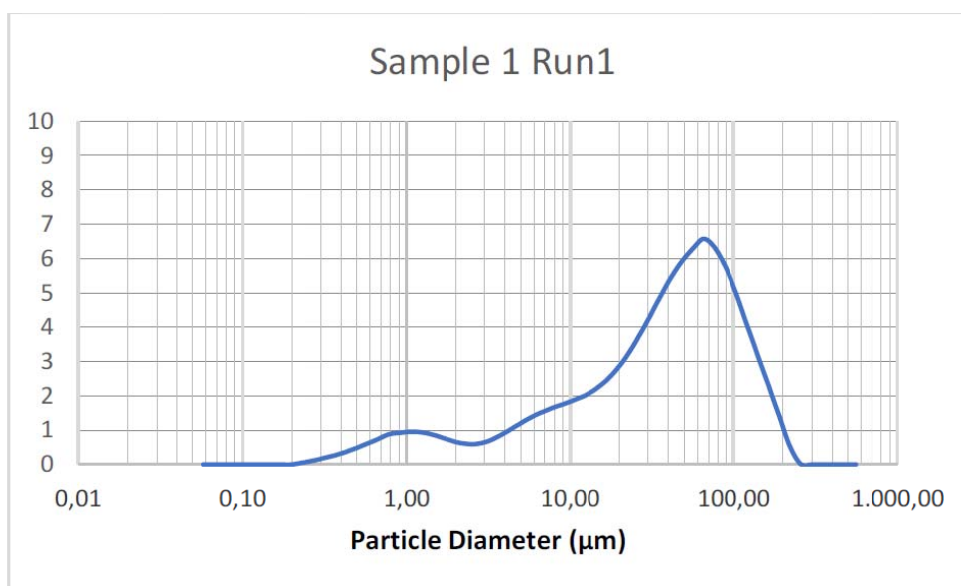


Figure 23. Particle size analysis for Sample 1 (Brick) measurement 1.

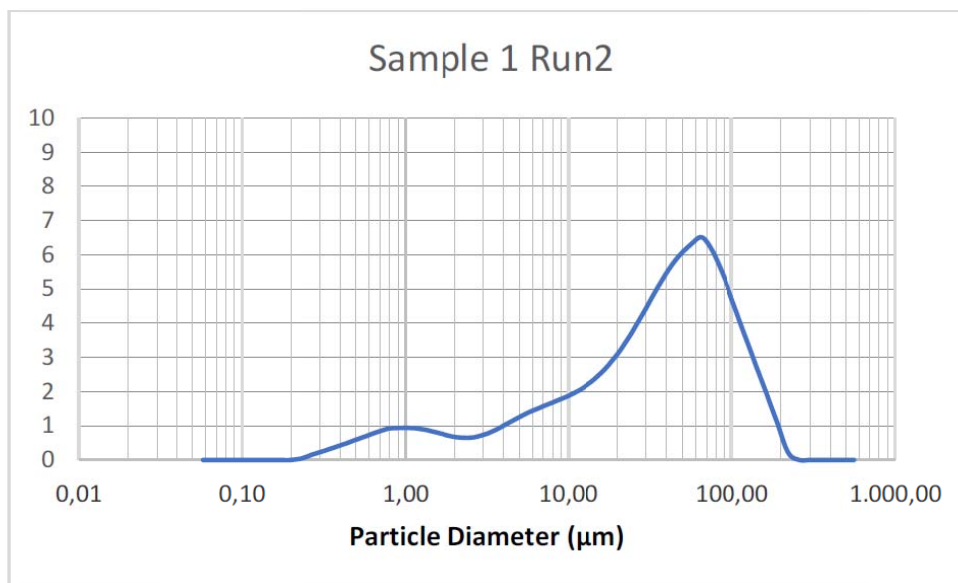


Figure 24. Particle size analysis for Sample 1 (Brick) measurement 2.

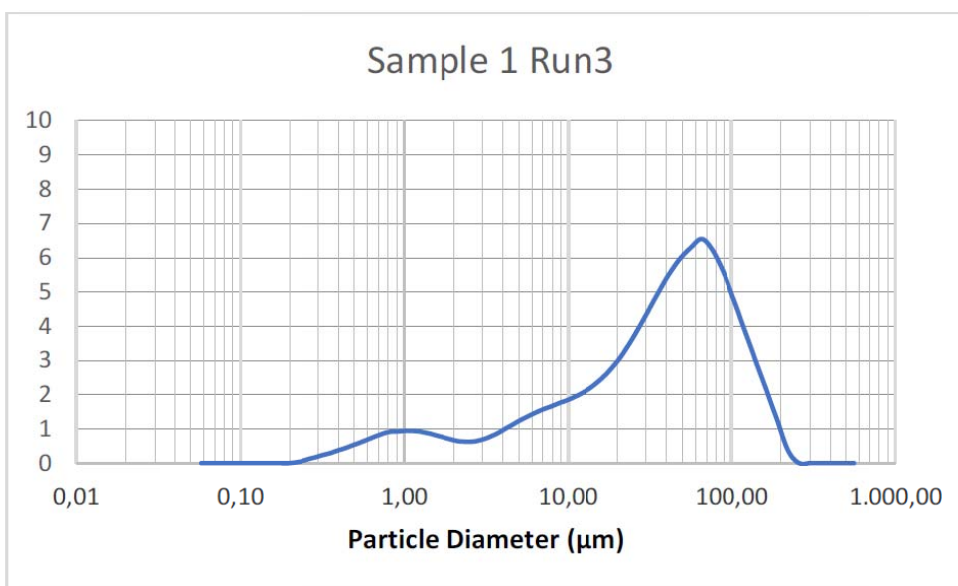


Figure 25. Particle size analysis for Sample 1 (Brick) measurement 3.

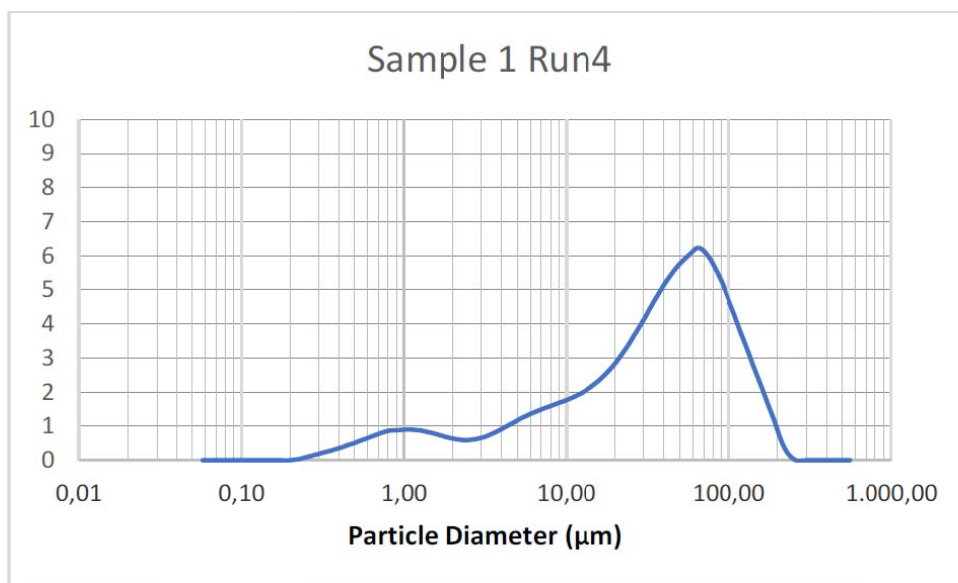


Figure 26. Particle size analysis for Sample 1 (Brick) measurement 4.

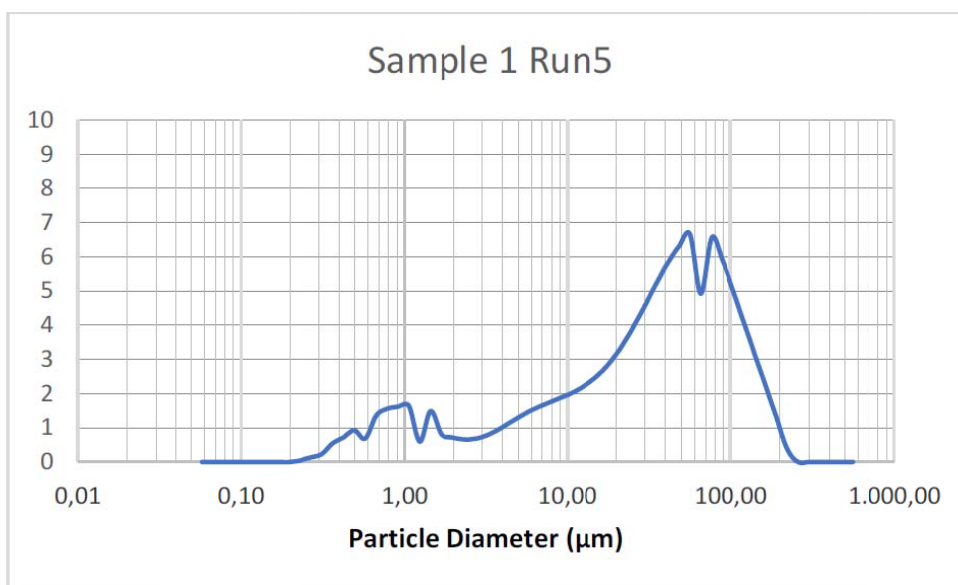


Figure 27. Particle size analysis for Sample 1 (Brick) measurement 5.

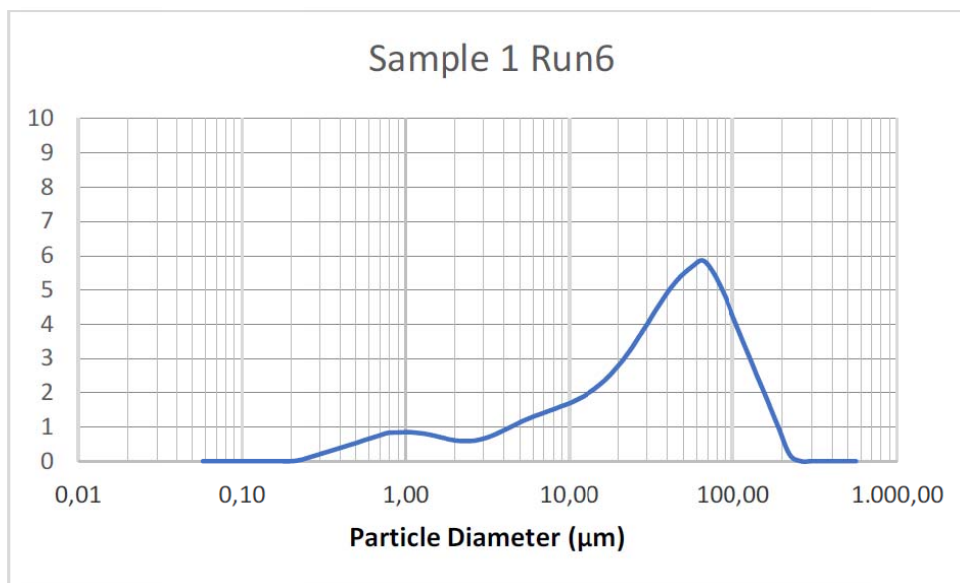


Figure 30. Particle size analysis for Sample 1 (Brick) measurement 6.

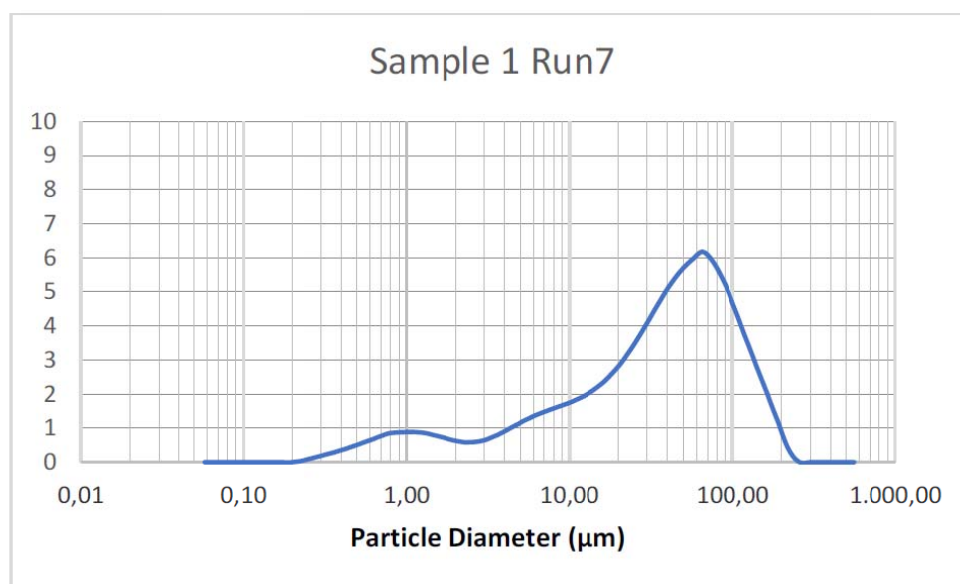


Figure 31. Particle size analysis for Sample 1 (Brick) measurement 7.

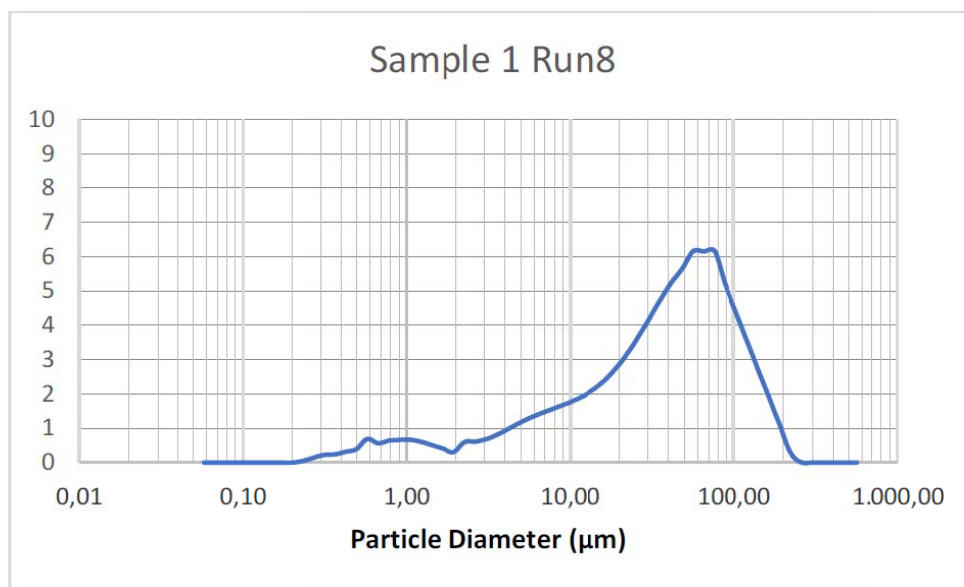


Figure 28. Particle size analysis for Sample 1 (Brick) measurement 8.

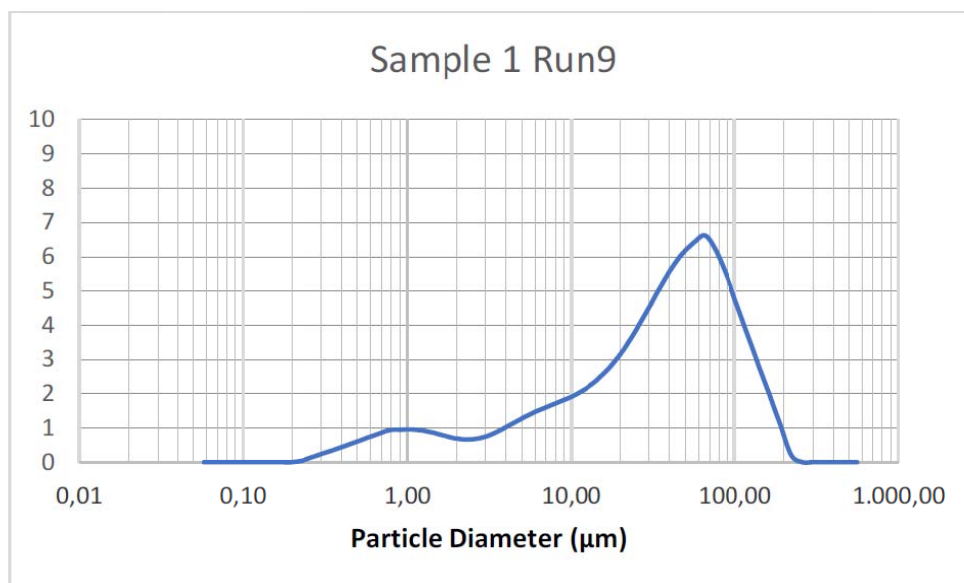


Figure 29. Particle size analysis for Sample 1 (Brick) measurement 9.

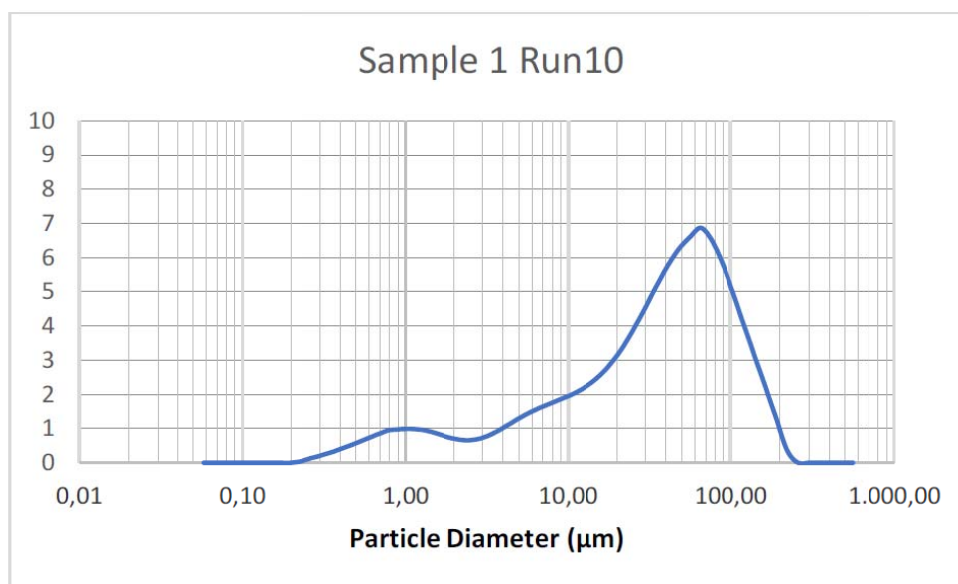


Figure 30. Particle size analysis for Sample 1 (Brick) measurement 10.

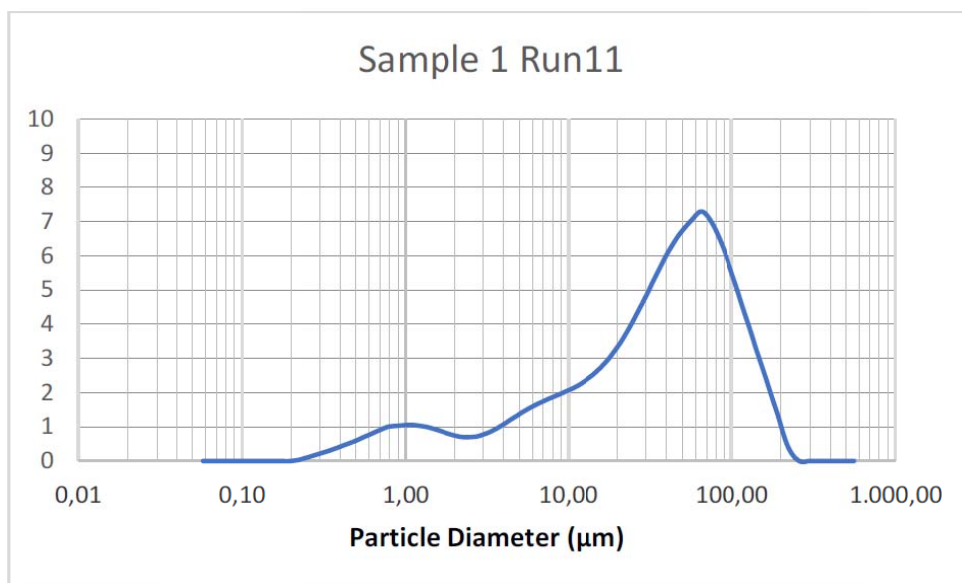


Figure 31. Particle size analysis for Sample 1 (Brick) measurement 11.

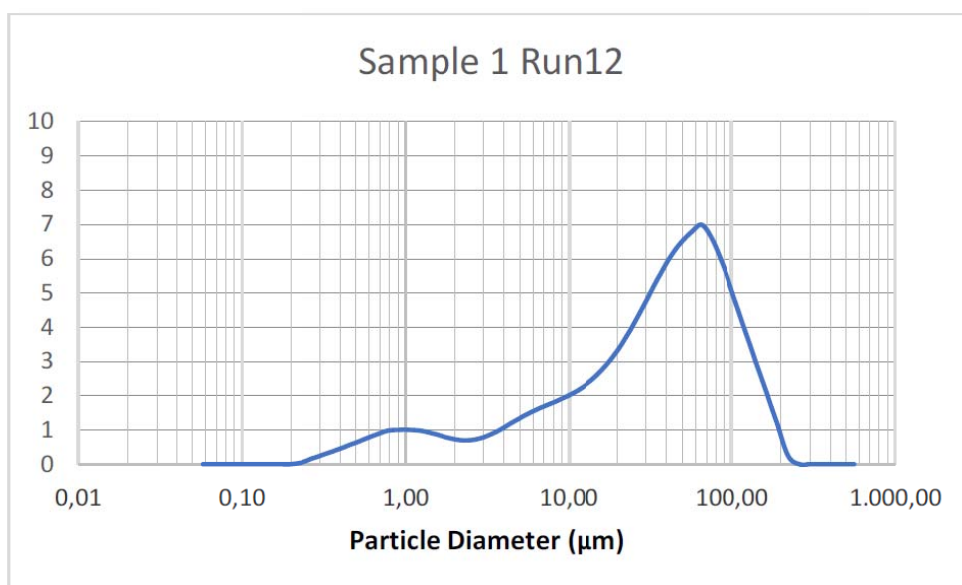


Figure 32. Particle size analysis for Sample 1 (Brick) measurement 12.

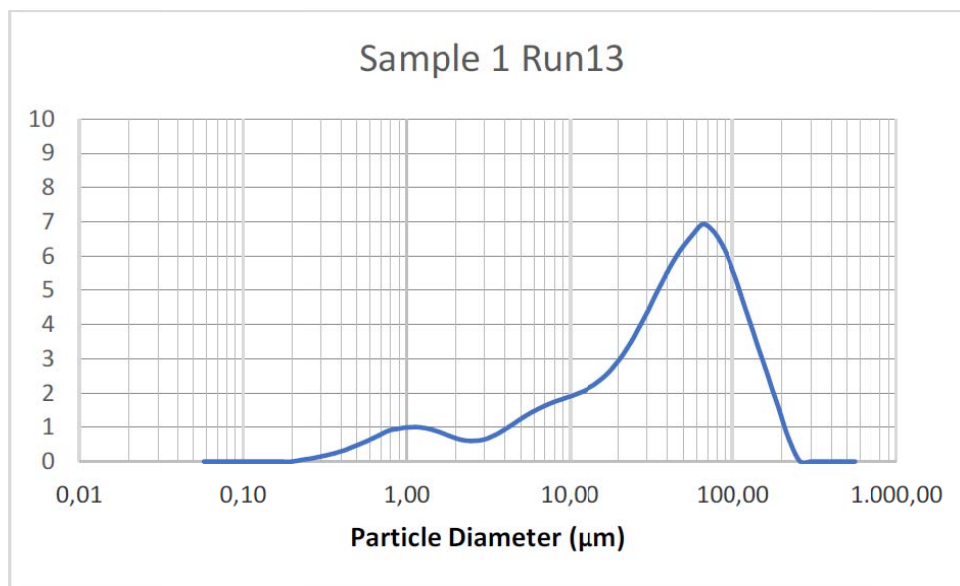


Figure 33. Particle size analysis for Sample 1 (Brick) measurement 13.

SAMPLE 2

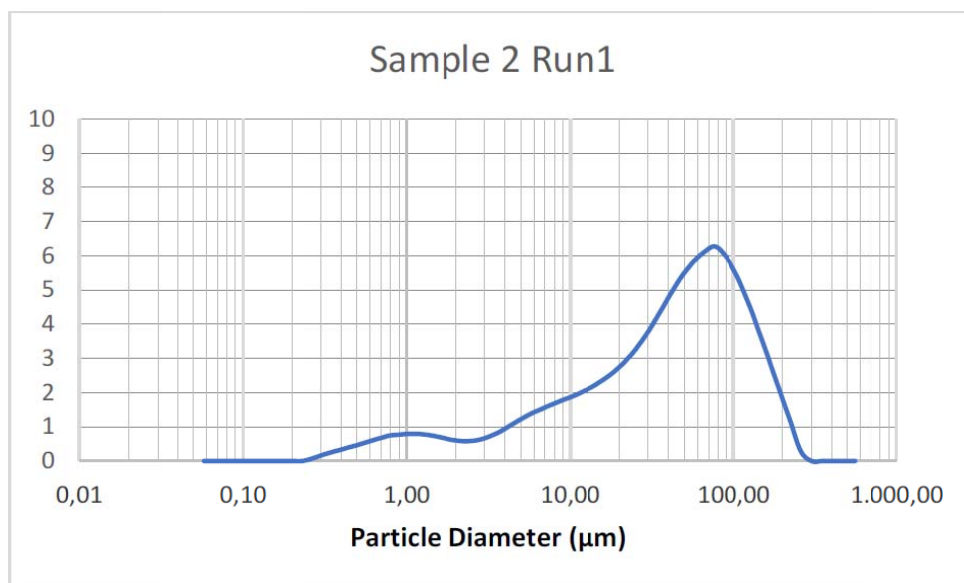


Figure 34. Particle size analysis for Sample 2 (Concrete) measurement 1.

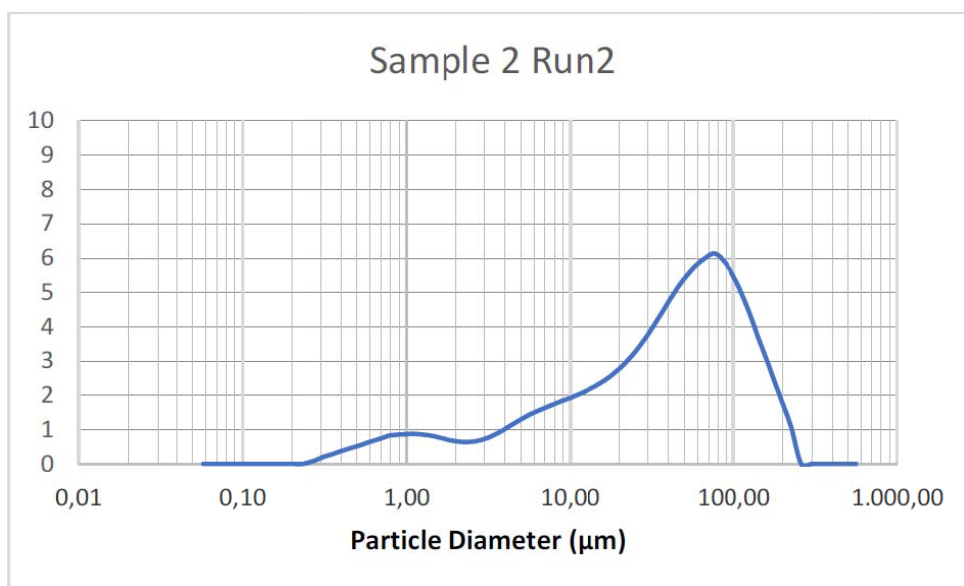


Figure 35. Particle size analysis for Sample 2 (Concrete) measurement 2.

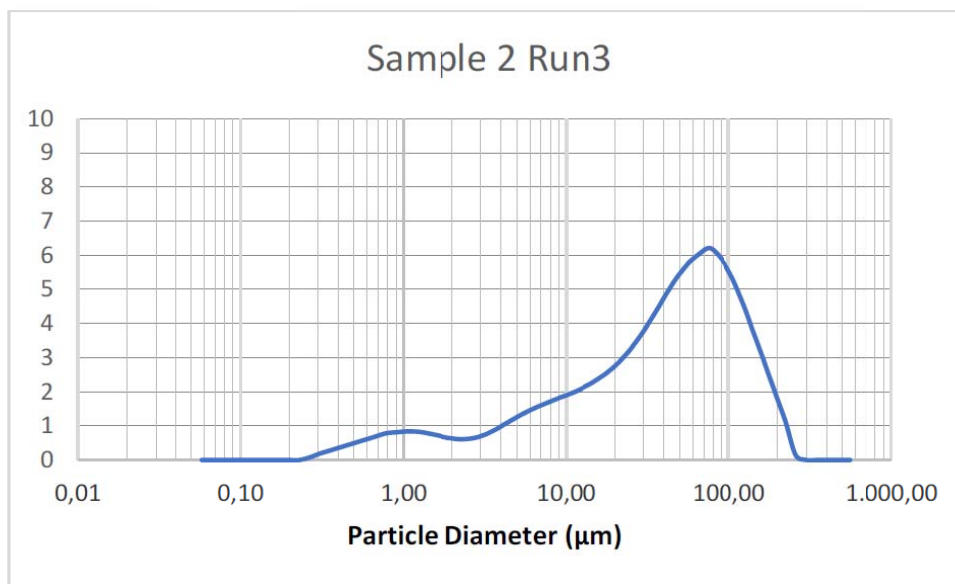


Figure 40. Particle size analysis for Sample 2 (Concrete) measurement 3.

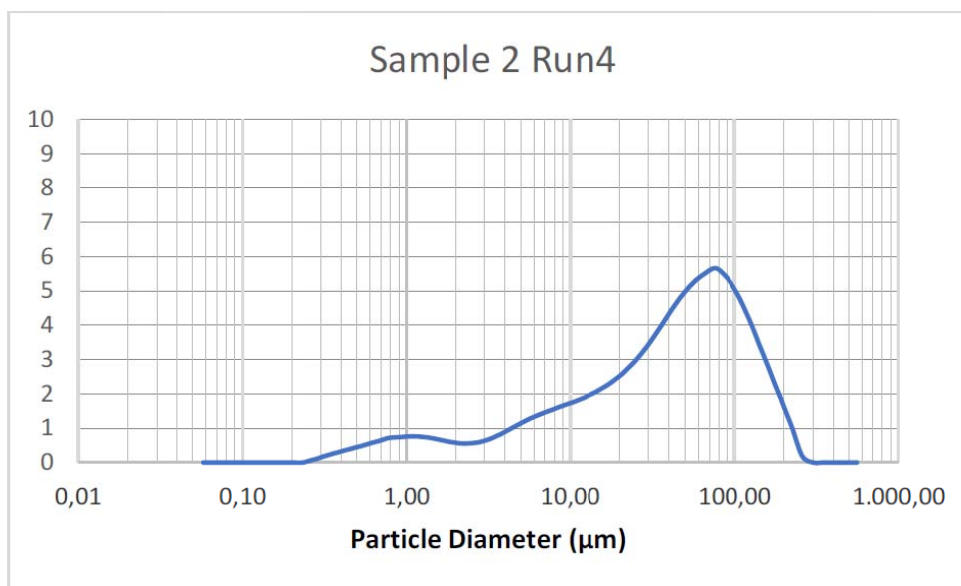


Figure 41. Particle size analysis for Sample 2 (Concrete) measurement 4.

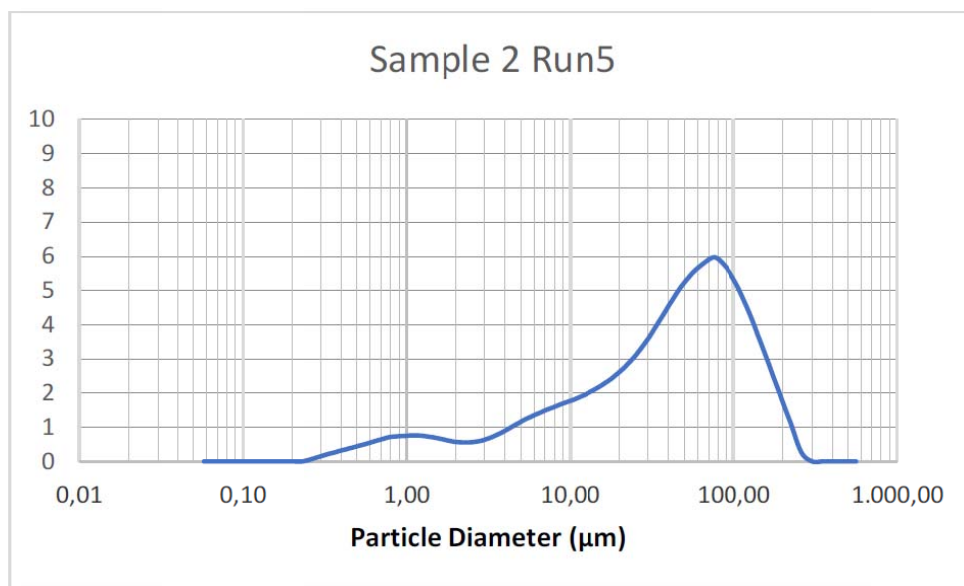


Figure 36. Particle size analysis for Sample 2 (Concrete) measurement 5.

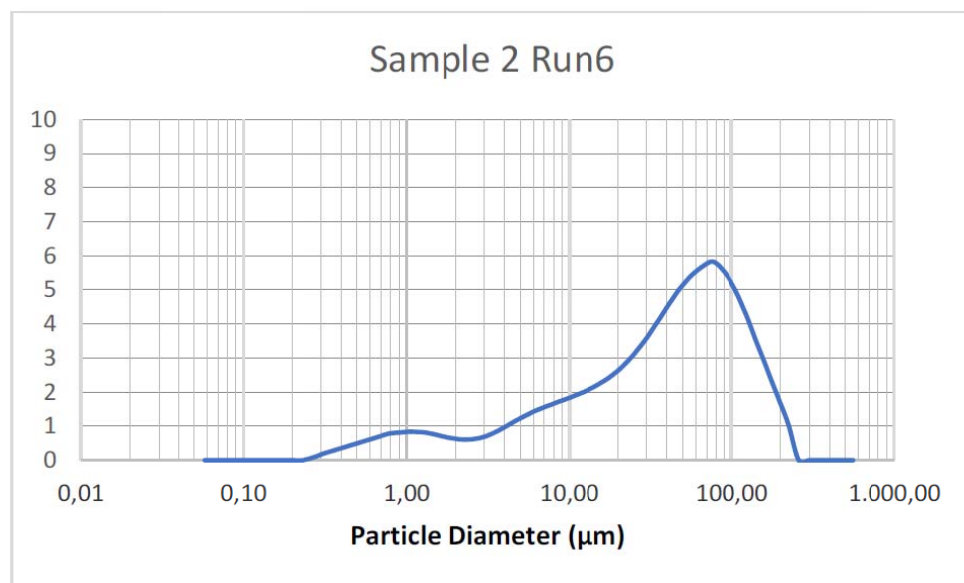


Figure 37. Particle size analysis for Sample 2 (Concrete) measurement 6.

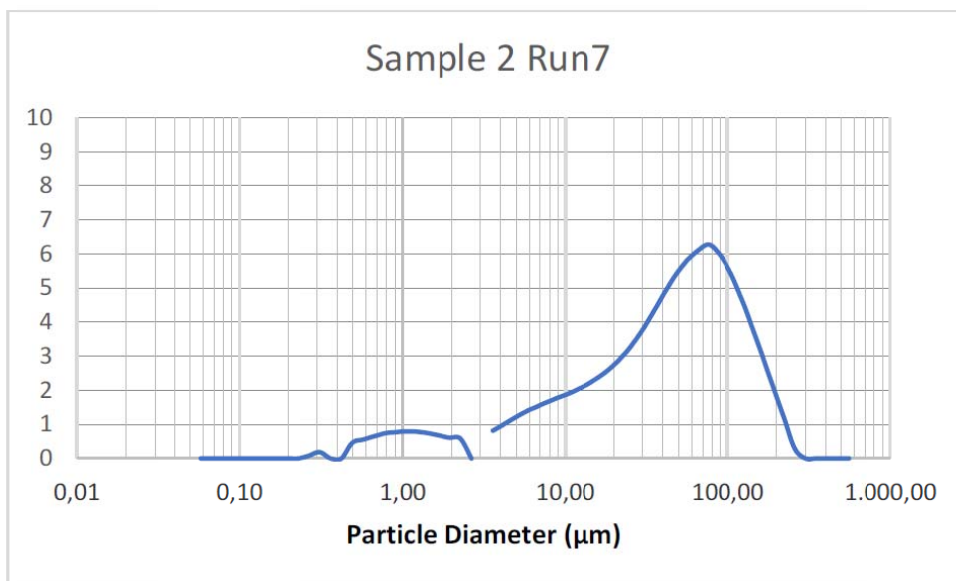


Figure 38. Particle size analysis for Sample 2 (Concrete) measurement 7.

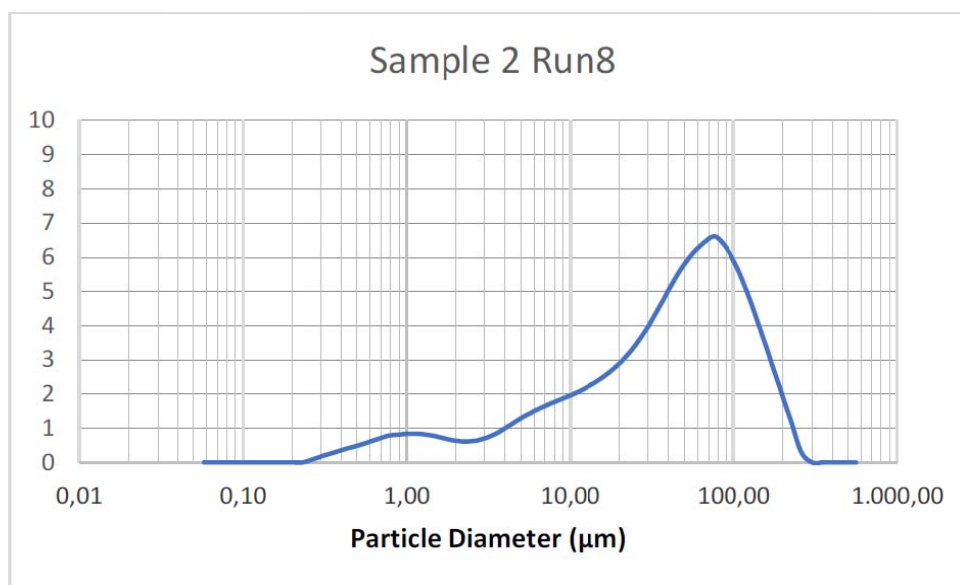


Figure 39. Particle size analysis for Sample 2 (Concrete) measurement 8.

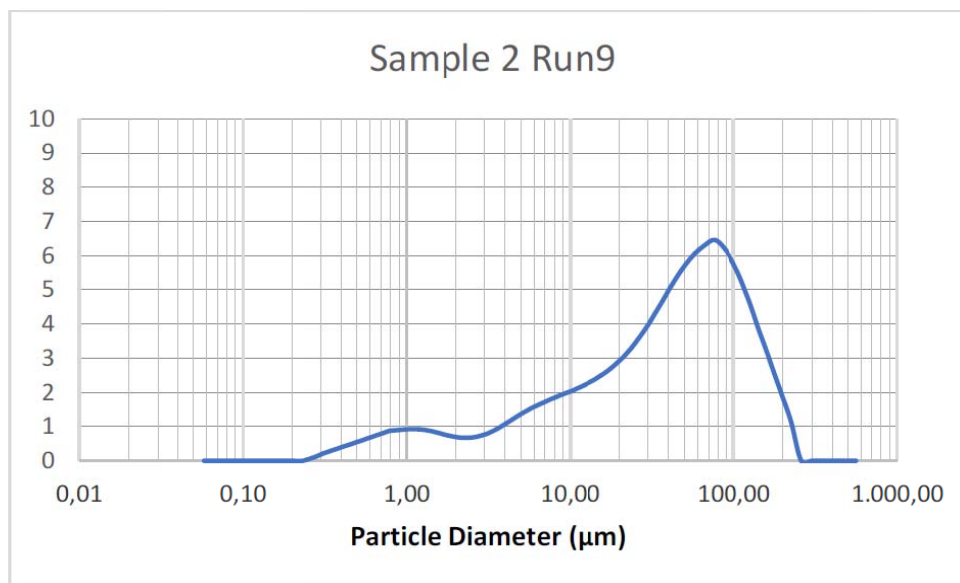


Figure 40. Particle size analysis for Sample 2 (Concrete) measurement 9.

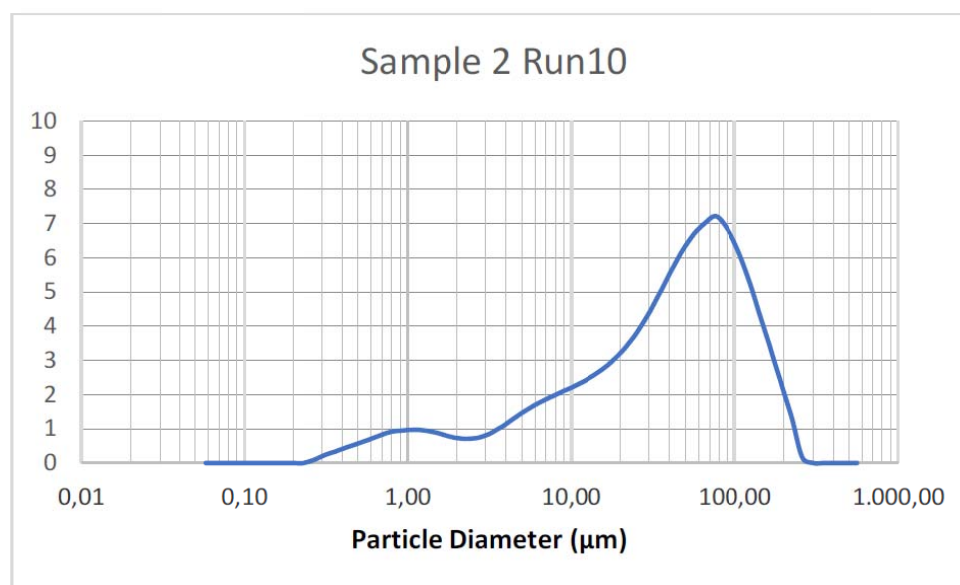


Figure 41. Particle size analysis for Sample 2 (Concrete) measurement 10.

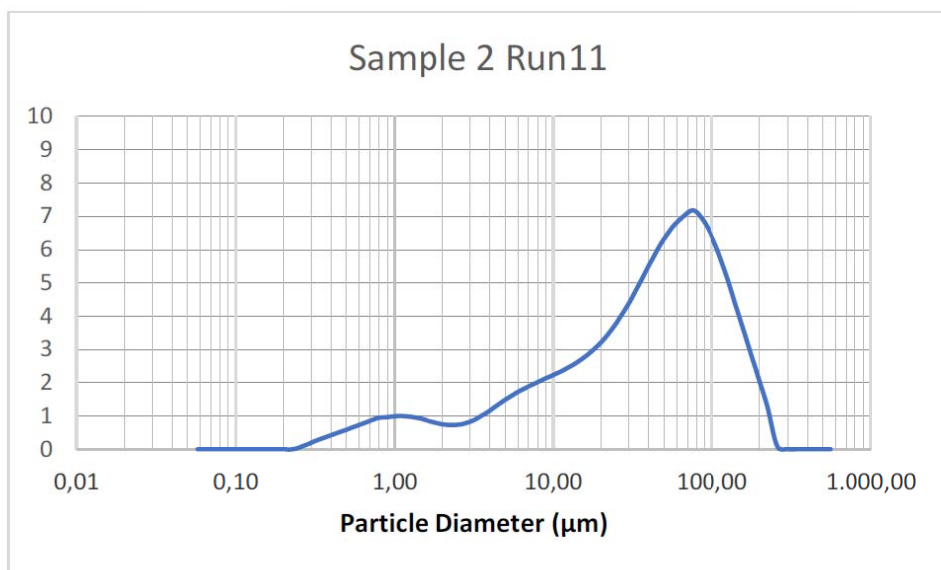


Figure 42. Particle size analysis for Sample 2 (Concrete) measurement 11.

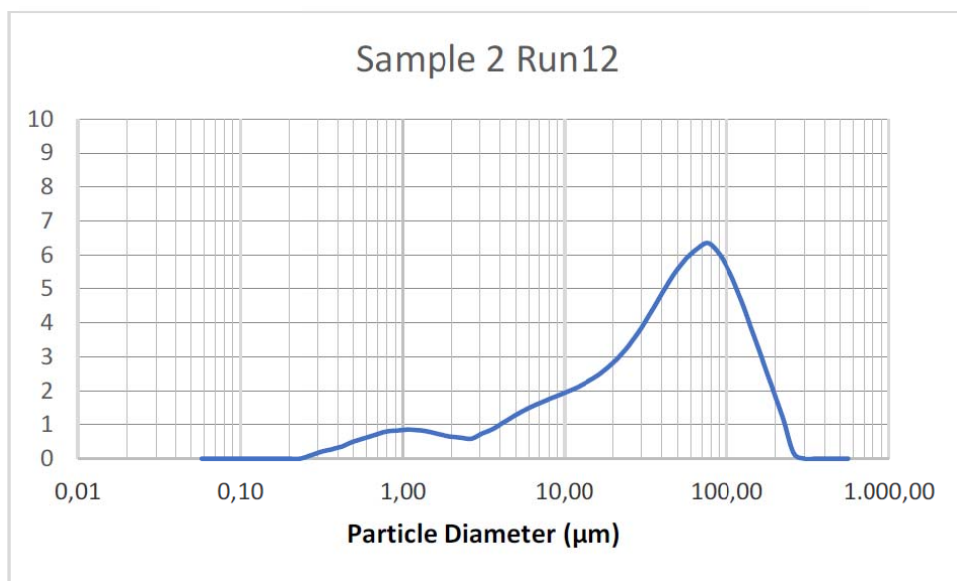


Figure 43. Particle size analysis for Sample 2 (Concrete) measurement 12.

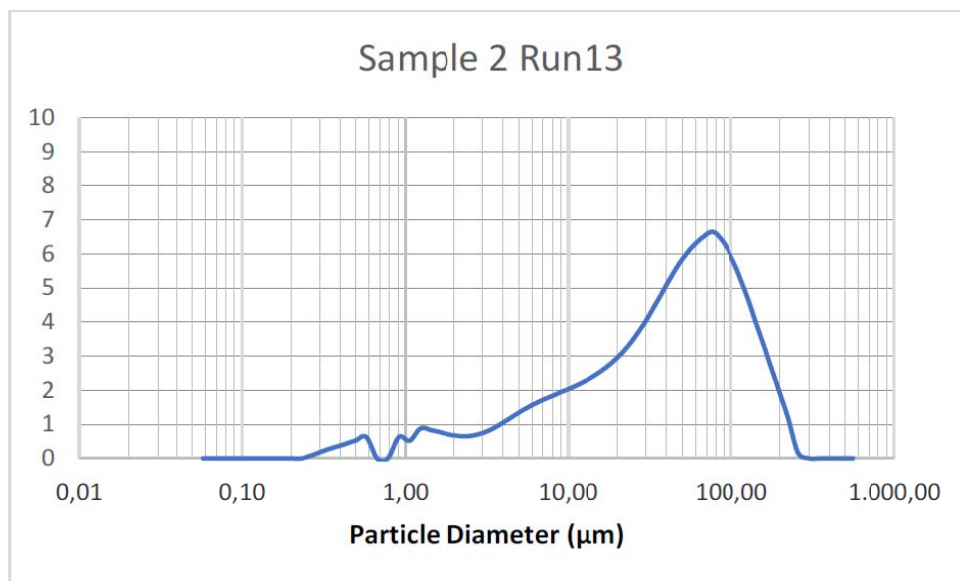


Figure 50. Particle size analysis for Sample 2 (Concrete) measurement 13.

SAMPLE 3

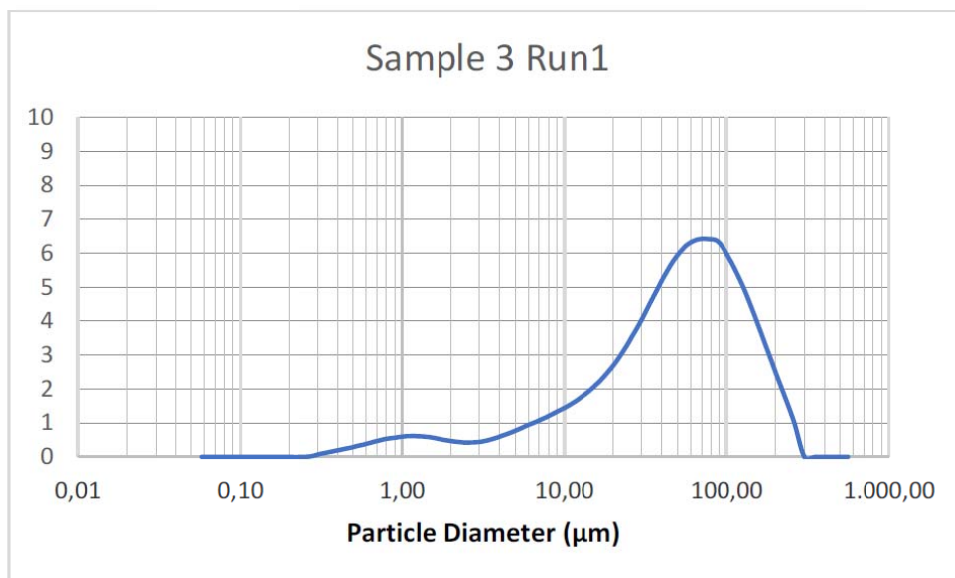


Figure 51. Particle size analysis for Sample 3 (Ceramic tile) measurement 1.

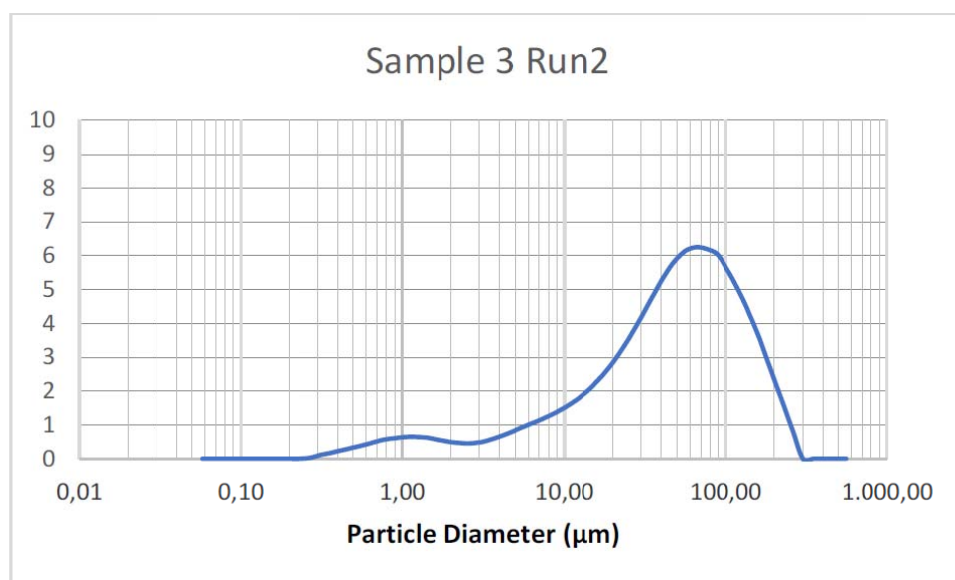


Figure 44. Particle size analysis for Sample 3 (Ceramic tile) measurement 2.

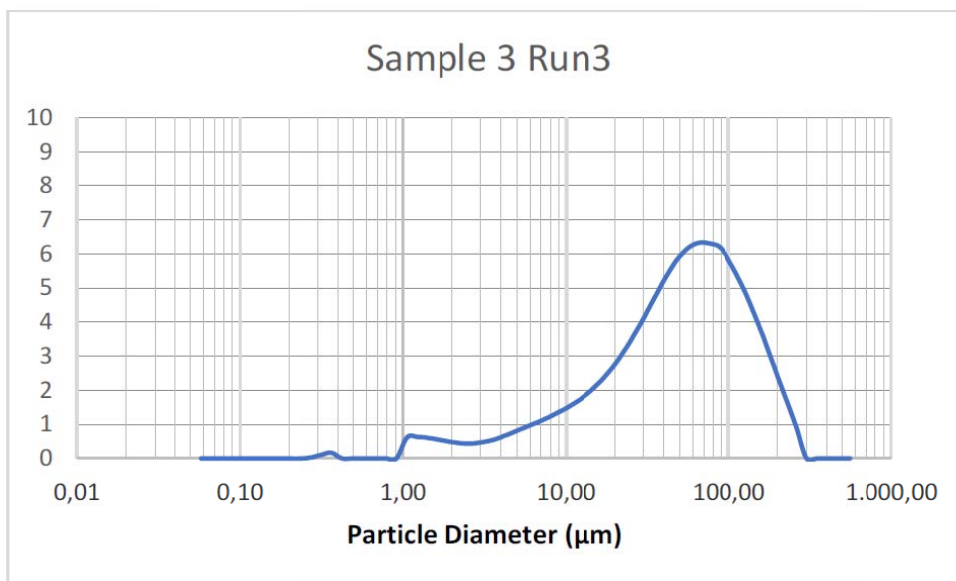


Figure 45. Particle size analysis for Sample 3 (Ceramic tile) measurement 3.

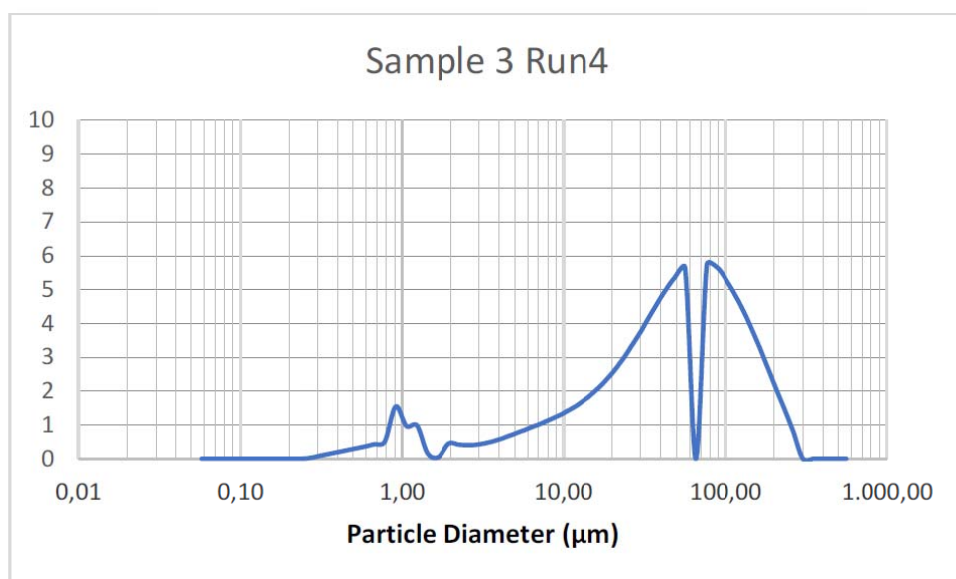


Figure 46. Particle size analysis for Sample 3 (Ceramic tile) measurement 4.

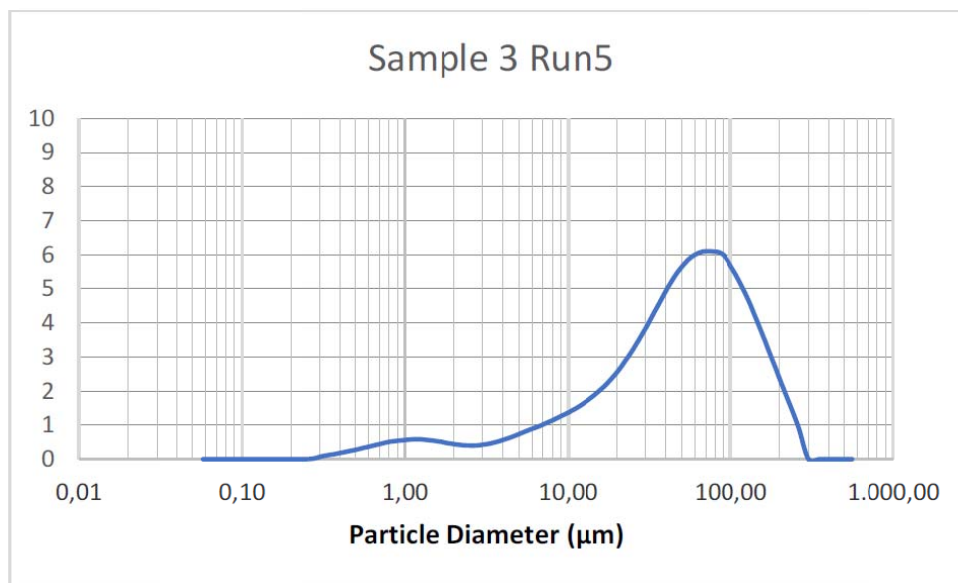


Figure 47. Particle size analysis for Sample 3 (Ceramic tile) measurement 5.

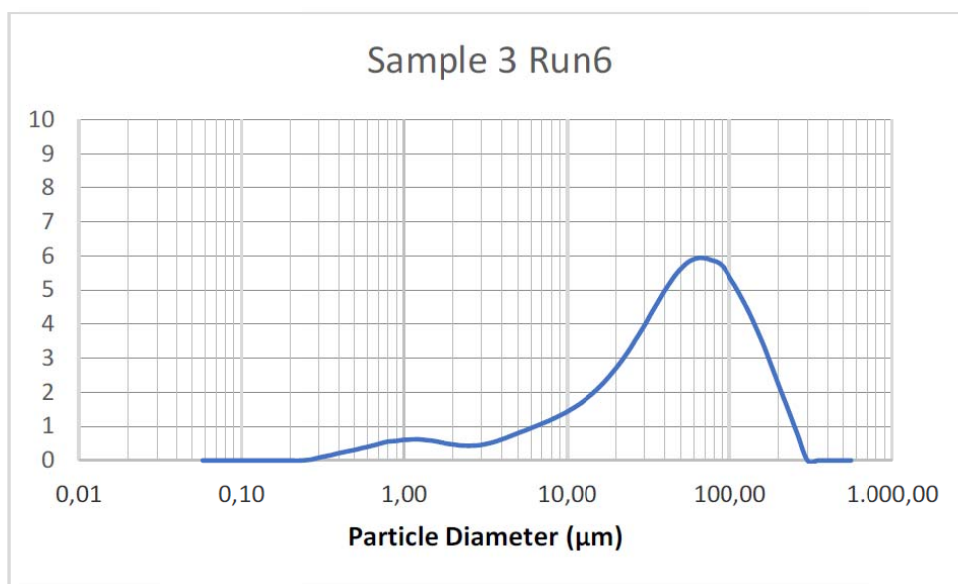


Figure 48. Particle size analysis for Sample 3 (Ceramic tile) measurement 6.

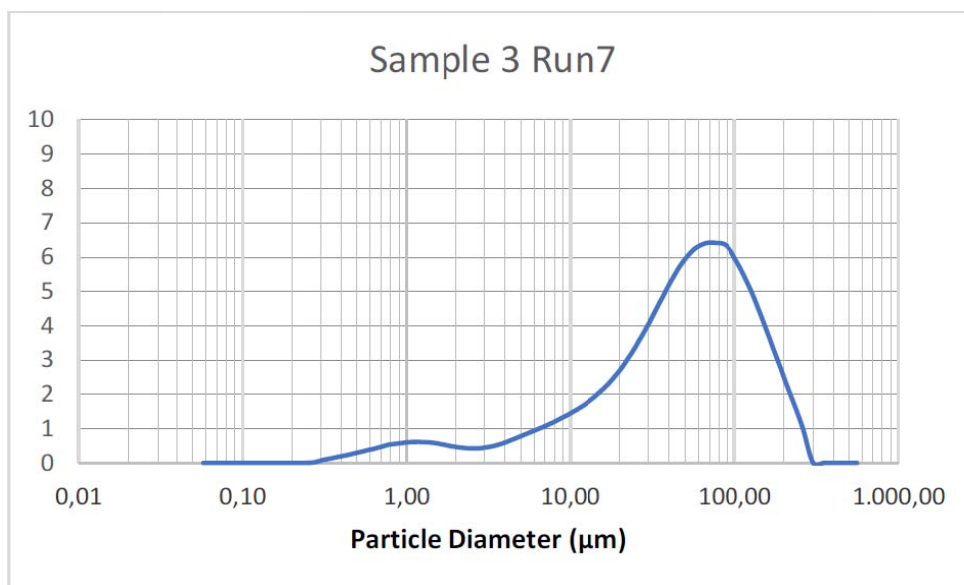


Figure 49. Particle size analysis for Sample 3 (Ceramic tile) measurement 7.

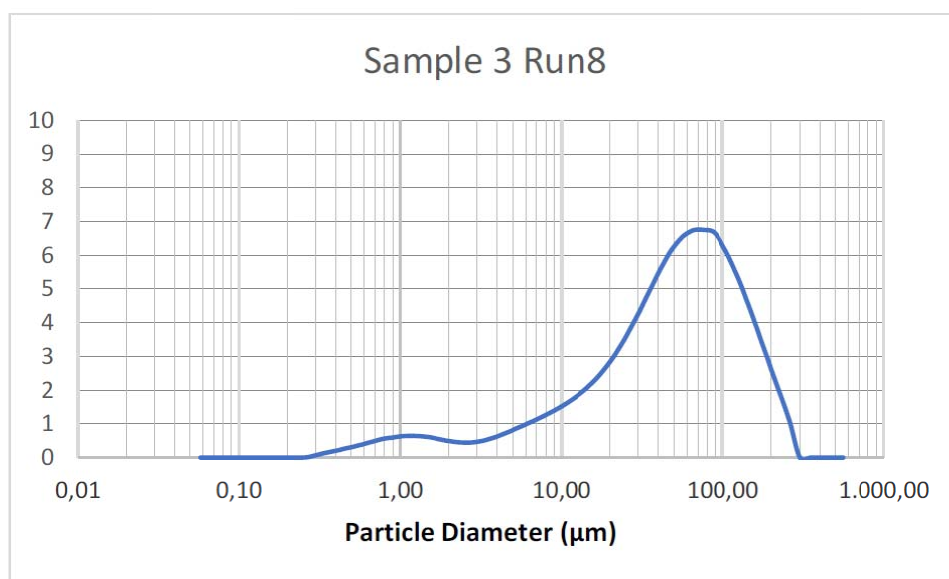


Figure 50. Particle size analysis for Sample 3 (Ceramic tile) measurement 8.

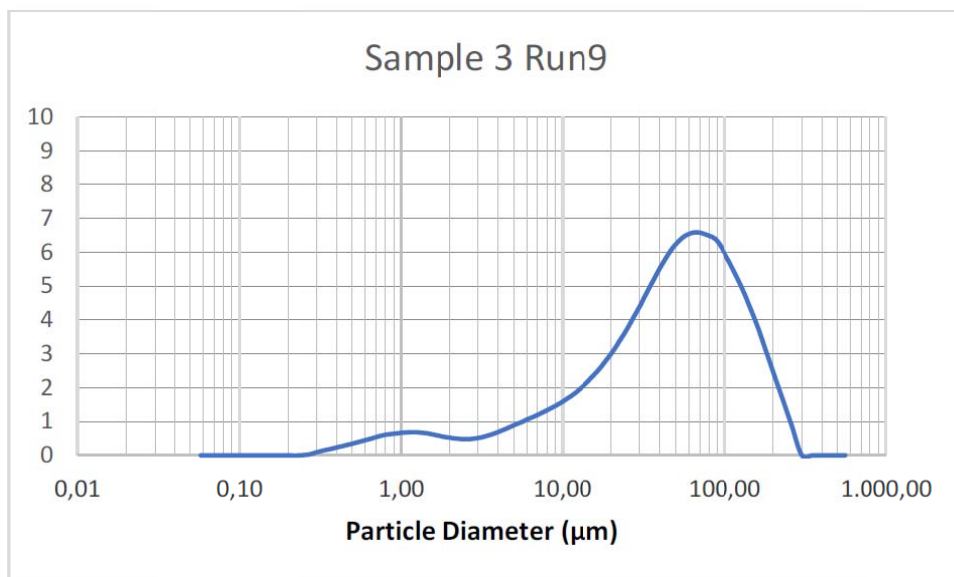


Figure 51. Particle size analysis for Sample 3 (Ceramic tile) measurement 9.

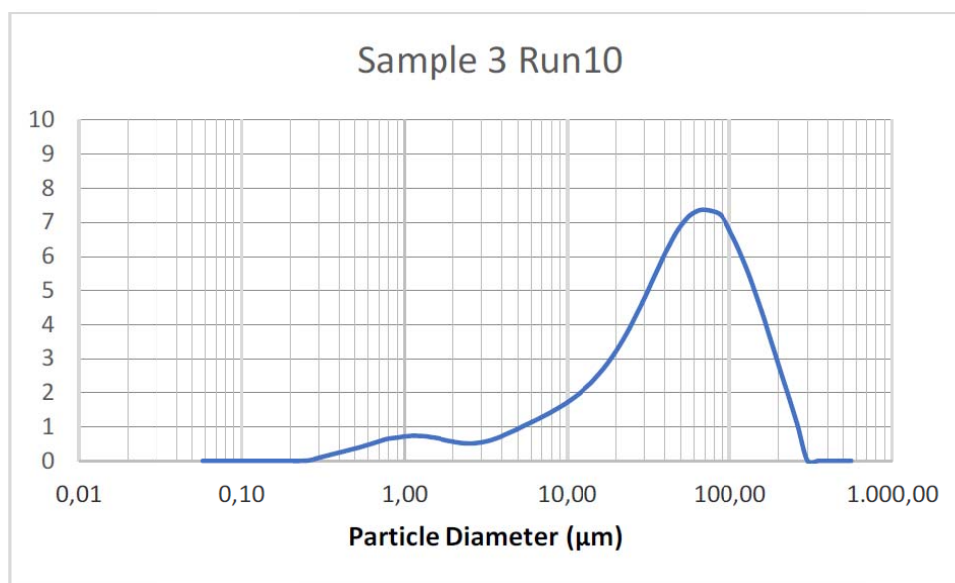


Figure 60. Particle size analysis for Sample 3 (Ceramic tile) measurement 10.

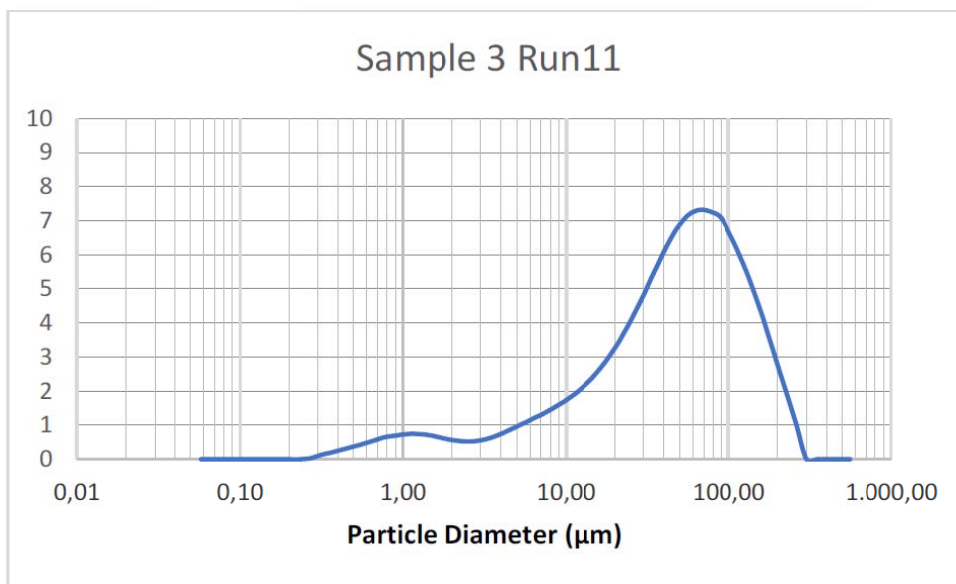


Figure 61. Particle size analysis for Sample 3 (Ceramic tile) measurement 11.

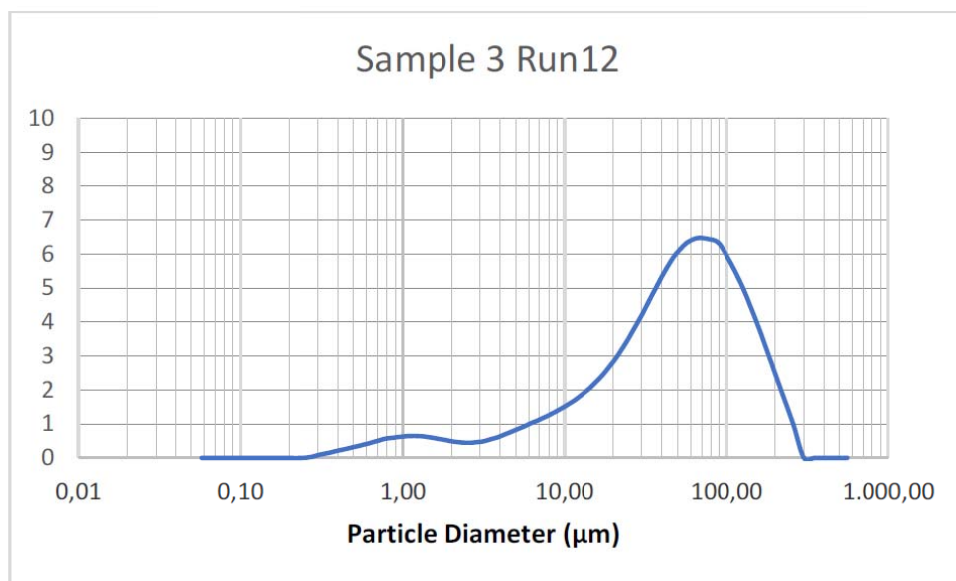


Figure 52. Particle size analysis for Sample 3 (Ceramic tile) measurement 12.

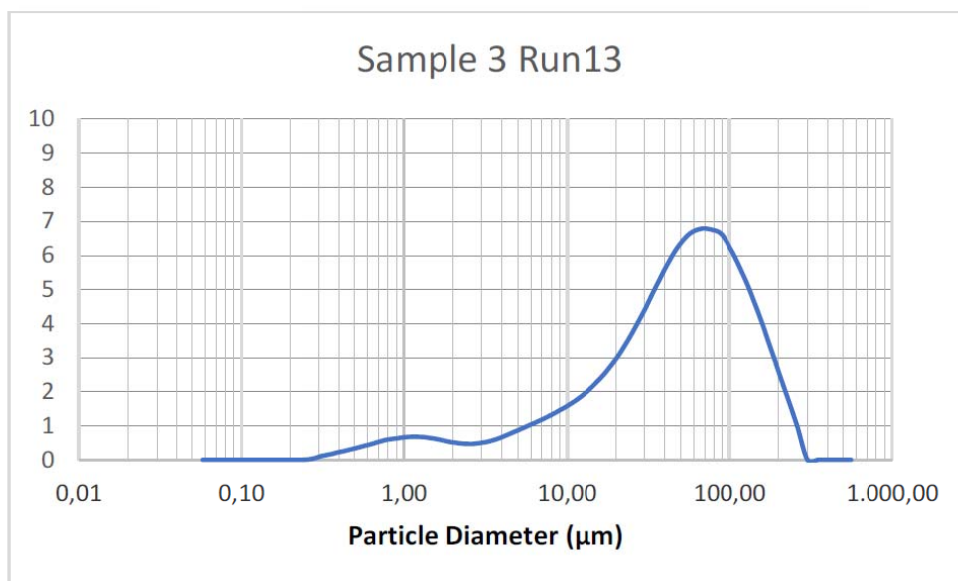


Figure 53. Particle size analysis for Sample 3 (Ceramic tile) measurement 13.

APPENDIX 2

XRF Analysis For All CDW Samples

[SAMPLE 1= BRICK; SAMPLE 2= CONCRETE; SAMPLE 3= CERAMIC TILE]

[each sample was analysed in 13 runs]

SAMPLE 1

Table 4. XRF analysis results for Sample 1 (Brick) Run 1.

Sample1 Run1	Element %	Molar mass	OXIDE	% wt.		
Si	29,43	28,00	SiO ₂	63,06		
Al	5,36	27,00	Al ₂ O ₃	10,12		
Ca	6,60	40,00	CaO	9,25		
Fe	6,91	56,00	FeO	8,88	Fe ₂ O ₃	9,87
K	2,14	39,00	K ₂ O	2,58		
Mg	1,18	24,30	MgO	1,96		
Na	0,47	23,00	Na ₂ O	0,63		
Ti	0,49	47,80	TiO ₂	0,81		
				97,28		98,27

Table 5. XRF analysis results for Sample 1 (Brick) Run 2.

Sample1 Run2	Element %	Molar mass	OXIDE	% wt.		
Si	23,91	28,00	SiO ₂	51,25		
Al	7,75	27,00	Al ₂ O ₃	14,64		
Ca	4,84	40,00	CaO	6,77		
Fe	9,22	56,00	FeO	11,85	Fe ₂ O ₃	13,17
K	4,04	39,00	K ₂ O	4,87		
Mg	3,07	24,30	MgO	5,09		
Na	0,51	23,00	Na ₂ O	0,69		
Ti	0,31	47,80	TiO ₂	0,51		
				95,66		96,98

Table 6. XRF analysis results for Sample 1 (Brick) Run 3.

Sample1 Run3	Element %	Molar mass	OXIDE	% wt.		
Si	24,70	28,00	SiO ₂	52,92		
Al	12,21	27,00	Al ₂ O ₃	23,07		
Ca	4,97	40,00	CaO	6,95		
Fe	8,45	56,00	FeO	10,87	Fe ₂ O ₃	12,07
K	1,19	39,00	K ₂ O	1,43		
Mg	1,04	24,30	MgO	1,72		
Na	0,32	23,00	Na ₂ O	0,43		
Ti	0,65	47,80	TiO ₂	1,08		
				98,48		99,69

Table 7. XRF analysis results for Sample 1 (Brick) Run 4.

Sample1 Run4	Element %	Molar mass	OXIDE	% wt.		
Si	24,51	28,00	SiO ₂	52,51		
Al	8,38	27,00	Al ₂ O ₃	15,84		
Ca	1,32	40,00	CaO	1,85		
Fe	6,68	56,00	FeO	8,59	Fe ₂ O ₃	9,54
K	3,44	39,00	K ₂ O	4,15		
Mg	4,89	24,30	MgO	8,11		
Na	0,41	23,00	Na ₂ O	0,55		
Ti	1,98	47,80	TiO ₂	3,30		
				94,89		95,85

Table 8. XRF analysis results for Sample 1 (Brick) Run 5.

Sample1 Run5	Element %	Molar mass	OXIDE	% wt.		
Si	24,02	28,00	SiO ₂	51,46		
Al	6,16	27,00	Al ₂ O ₃	11,63		
Ca	5,82	40,00	CaO	8,15		
Fe	7,46	56,00	FeO	9,59	Fe ₂ O ₃	10,65
K	4,24	39,00	K ₂ O	5,11		
Mg	3,31	24,30	MgO	5,49		
Na	0,21	23,00	Na ₂ O	0,28		
Ti	0,91	47,80	TiO ₂	1,51		
				93,23		94,29

Table 9. XRF analysis results for Sample 1 (Brick) Run 6.

Sample1 Run6	Element %	Molar mass	OXIDE	% wt.		
Si	25,88	28,00	SiO ₂	55,46		
Al	5,30	27,00	Al ₂ O ₃	10,02		
Ca	3,83	40,00	CaO	5,36		
Fe	8,21	56,00	FeO	10,56	Fe ₂ O ₃	11,73
K	3,40	39,00	K ₂ O	4,10		
Mg	2,90	24,30	MgO	4,81		
Na	0,45	23,00	Na ₂ O	0,61		
Ti	1,19	47,80	TiO ₂	1,98		
				92,90		94,07

Table 10. XRF analysis results for Sample 1 (Brick) Run 7.

Sample1 Run7	Element %	Molar mass	OXIDE	% wt.		
Si	28,41	28,00	SiO ₂	60,88		
Al	8,63	27,00	Al ₂ O ₃	16,30		
Ca	7,76	40,00	CaO	10,86		
Fe	4,23	56,00	FeO	5,44	Fe ₂ O ₃	6,05
K	2,34	39,00	K ₂ O	2,82		
Mg	1,02	24,30	MgO	1,69		
Na	0,32	23,00	Na ₂ O	0,43		
Ti	0,62	47,80	TiO ₂	1,03		
				99,46		100,06

Table 11. XRF analysis results for Sample 1 (Brick) Run 8.

Sample1 Run8	Element %	Molar mass	OXIDE	% wt.		
Si	23,42	28,00	SiO ₂	50,19		
Al	9,15	27,00	Al ₂ O ₃	17,28		
Ca	5,87	40,00	CaO	8,22		
Fe	6,70	56,00	FeO	8,62	Fe ₂ O ₃	9,58
K	3,23	39,00	K ₂ O	3,89		
Mg	2,84	24,30	MgO	4,71		
Na	0,32	23,00	Na ₂ O	0,43		
Ti	1,56	47,80	TiO ₂	2,60		
				95,95		96,91

Table 12. XRF analysis results for Sample 1 (Brick) Run 9.

Sample1 Run9	Element %	Molar mass	OXIDE	% wt.		
Si	22,25	28,00	SiO ₂	47,68		
Al	4,69	27,00	Al ₂ O ₃	8,86		
Ca	3,77	40,00	CaO	5,28		
Fe	9,38	56,00	FeO	12,06	Fe ₂ O ₃	13,40
K	4,34	39,00	K ₂ O	5,23		
Mg	3,34	24,30	MgO	5,54		
Na	1,12	23,00	Na ₂ O	1,51		
Ti	1,49	47,80	TiO ₂	2,49		
				88,65		89,99

Table 13. XRF analysis results for Sample 1 (Brick) Run 10.

Sample1 Run10	Element %	Molar mass	OXIDE	% wt.		
Si	22,18	28,00	SiO ₂	47,53		
Al	8,79	27,00	Al ₂ O ₃	16,59		
Ca	8,29	40,00	CaO	11,60		
Fe	8,79	56,00	FeO	11,30	Fe ₂ O ₃	12,55
K	3,12	39,00	K ₂ O	3,76		
Mg	2,52	24,30	MgO	4,18		
Na	0,44	23,00	Na ₂ O	0,59		
Ti	0,09	47,80	TiO ₂	0,16		
				95,71		96,96

Table 14. XRF analysis results for Sample 1 (Brick) Run 11.

Sample1 Run11	Element %	Molar mass	OXIDE	% wt.		
Si	27,78	28,00	SiO ₂	59,53		
Al	5,07	27,00	Al ₂ O ₃	9,59		
Ca	5,91	40,00	CaO	8,27		
Fe	8,75	56,00	FeO	11,24	Fe ₂ O ₃	12,49
K	3,94	39,00	K ₂ O	4,75		
Mg	1,88	24,30	MgO	3,12		
Na	0,24	23,00	Na ₂ O	0,32		
Ti	0,76	47,80	TiO ₂	1,27		
				98,09		99,34

Table 15. XRF analysis results for Sample 1 (Brick) Run 12.

Sample1 Run12	Element %	Molar mass	OXIDE	% wt.		
Si	25,23	28,00	SiO ₂	54,07		
Al	9,01	27,00	Al ₂ O ₃	17,01		
Ca	7,85	40,00	CaC	10,99		
Fe	9,49	56,00	FeO	12,20	Fe ₂ O ₃	13,55
K	1,94	39,00	K ₂ O	2,34		
Mg	0,89	24,30	MgO	1,48		
Na	0,06	23,00	Na ₂ O	0,08		
Ti	0,24	47,80	TiO ₂	0,41		
				98,57		99,92

Table 16. XRF analysis results for Sample 1 (Brick) Run 13.

Sample1 Run13	Element %	Molar mass	OXIDE	% wt.		
Si	23,27	28,00	SiO ₂	49,86		
Al	8,12	27,00	Al ₂ O ₃	15,33		
Ca	4,79	40,00	CaO	6,70		
Fe	8,74	56,00	FeC	11,24	Fe ₂ O ₃	12,49
K	3,00	39,00	K ₂ O	3,62		
Mg	2,99	24,30	MgO	4,96		
Na	1,55	23,00	Na ₂ O	2,09		
Ti	1,06	47,80	TiO ₂	1,77		
				95,58		96,83

SAMPLE 2

Table 17. XRF analysis results for Sample 2 (Concrete) Run 1.

Sample2 Run1	Element %	Molar mass	OXIDE	% wt.		
Si	15,90	28,00	SiO ₂	34,06		
Al	4,50	27,00	Al ₂ O ₃	8,50		
Ca	10,43	40,00	CaO	14,60		
Fe	1,62	56,00	FeO	2,08	Fe ₂ O ₃	2,31
K	2,14	39,00	K ₂ O	2,58		
Mg	1,18	24,30	MgO	1,96		
Na	0,47	23,00	Na ₂ O	0,63		
				64,41		64,64

Table 18. XRF analysis results for Sample 2 (Concrete) Run 2.

Sample2 Run2	Element %	Molar mass	OXIDE	% wt.		
Si	14,24	28,00	SiO ₂	30,52		
Al	4,10	27,00	Al ₂ O ₃	7,75		
Ca	20,94	40,00	CaO	29,31		
Fe	2,03	56,00	FeO	2,61	Fe ₂ O ₃	2,90
K	4,04	39,00	K ₂ O	4,87		
Mg	3,07	24,30	MgO	5,09		
Na	0,51	23,00	Na ₂ O	0,69		
				80,83		81,13

Table 19. XRF analysis results for Sample 2 (Concrete) Run 3.

Sample2 Run3	Element %	Molar mass	OXIDE	% wt.		
Si	8,97	28,00	SiO ₂	19,22		
Al	2,68	27,00	Al ₂ O ₃	5,06		
Ca	22,73	40,00	CaO	31,82		
Fe	2,04	56,00	FeO	2,63	Fe ₂ O ₃	2,92
K	1,19	39,00	K ₂ O	1,43		
Mg	1,04	24,30	MgO	1,72		
Na	0,32	23,00	Na ₂ O	0,43		
				62,32		62,61

Table 20. XRF analysis results for Sample 2 (Concrete) Run 4.

Sample2 Run4	Element %	Molar mass	OXIDE	% wt.		
Si	18,63	28,00	SiO ₂	39,93		
Al	1,74	27,00	Al ₂ O ₃	3,29		
Ca	15,23	40,00	CaO	21,32		
Fe	2,58	56,00	FeO	3,32	Fe ₂ O ₃	3,69
K	3,44	39,00	K ₂ O	4,15		
Mg	4,89	24,30	MgO	8,11		
Na	0,41	23,00	Na ₂ O	0,55		
				80,66		81,03

Table 21. XRF analysis results for Sample 2 (Concrete) Run 5.

Sample2 Run5	Element %	Molar mass	OXIDE	% wt.		
Si	14,96	28,00	SiO ₂	32,06		
Al	3,97	27,00	Al ₂ O ₃	7,50		
Ca	17,39	40,00	CaO	24,34		
Fe	2,20	56,00	FeO	2,83	Fe ₂ O ₃	3,14
K	4,24	39,00	K ₂ O	5,11		
Mg	3,31	24,30	MgO	5,49		
Na	0,21	23,00	Na ₂ O	0,28		
				77,61		77,92

Table 22. XRF analysis results for Sample 2 (Concrete) Run 6.

Sample2 Run6	Element %	Molar mass	OXIDE	% wt.		
Si	17,56	28,00	SiO ₂	37,63		
Al	3,01	27,00	Al ₂ O ₃	5,68		
Ca	17,55	40,00	CaO	24,57		
Fe	1,70	56,00	FeO	2,18	Fe ₂ O ₃	2,43
K	3,40	39,00	K ₂ O	4,10		
Mg	2,90	24,30	MgO	4,81		
Na	0,45	23,00	Na ₂ O	0,61		
				79,59		79,83

Table 23. XRF analysis results for Sample 2 (Concrete) Run 7.

Sample2 Run7	Element %	Molar mass	OXIDE	% wt.		
Si	15,78	28,00	SiO ₂	33,81		
Al	2,59	27,00	Al ₂ O ₃	4,89		
Ca	16,13	40,00	CaO	22,59		
Fe	2,47	56,00	FeO	3,17	Fe ₂ O ₃	3,53
K	2,34	39,00	K ₂ O	2,82		
Mg	1,02	24,30	MgO	1,69		
Na	0,32	23,00	Na ₂ O	0,43		
				69,40		69,75

Table 24. XRF analysis results for Sample 2 (Concrete) Run 8.

Sample2 Run8	Element %	Molar mass	OXIDE	% wt.		
Si	12,65	28,00	SiO ₂	27,12		
Al	5,03	27,00	Al ₂ O ₃	9,50		
Ca	15,96	40,00	CaO	22,34		
Fe	1,81	56,00	FeO	2,32	Fe ₂ O ₃	2,58
K	3,23	39,00	K ₂ O	3,89		
Mg	2,84	24,30	MgO	4,71		
Na	0,32	23,00	Na ₂ O	0,43		
				70,32		70,57

Table 25. XRF analysis results for Sample 2 (Concrete) Run 9.

Sample2 Run9	Element %	Molar mass	OXIDE	% wt.		
Si	13,35	28,00	SiO ₂	28,62		
Al	3,57	27,00	Al ₂ O ₃	6,74		
Ca	12,86	40,00	CaO	18,00		
Fe	1,83	56,00	FeO	2,35	Fe ₂ O ₃	2,61
K	4,34	39,00	K ₂ O	5,23		
Mg	3,34	24,30	MgO	5,54		
Na	1,12	23,00	Na ₂ O	1,51		
				67,99		68,25

Table 26. XRF analysis results for Sample 2 (Concrete) Run 10.

Sample2 Run10	Element %	Molar mass	OXIDE	% wt.		
Si	14,06	28,00	SiO ₂	30,13		
Al	2,92	27,00	Al ₂ O ₃	5,52		
Ca	22,23	40,00	CaO	31,12		
Fe	2,23	56,00	FeO	2,87	Fe ₂ O ₃	3,19
K	3,12	39,00	K ₂ O	3,76		
Mg	2,52	24,30	MgO	4,18		
Na	0,44	23,00	Na ₂ O	0,59		
				78,17		78,48

Table 27. XRF analysis results for Sample 2 (Concrete) Run 11.

Sample2 Run11	Element %	Molar mass	OXIDE	% wt.		
Si	10,83	28,00	SiO ₂	23,21		
Al	6,84	27,00	Al ₂ O ₃	12,92		
Ca	14,35	40,00	CaO	20,09		
Fe	2,14	56,00	FeO	2,75	Fe ₂ O ₃	3,06
K	3,94	39,00	K ₂ O	4,75		
Mg	1,88	24,30	MgO	3,12		
Na	0,24	23,00	Na ₂ O	0,32		
				67,16		67,46

Table 28. XRF analysis results for Sample 2 (Concrete) Run 12.

Sample2 Run12	Element %	Molar mass	OXIDE	% wt.		
Si	19,30	28,00	SiO ₂	41,36		
Al	4,87	27,00	Al ₂ O ₃	9,20		
Ca	11,11	40,00	CaO	15,56		
Fe	2,77	56,00	FeO	3,56	Fe ₂ O ₃	3,95
K	1,94	39,00	K ₂ O	2,34		
Mg	0,89	24,30	MgO	1,48		
Na	0,06	23,00	Na ₂ O	0,08		
				73,57		73,96

Table 29. XRF analysis results for Sample 2 (Concrete) Run 13.

Sample2 Run13	Element %	Molar mass	OXIDE	% wt.		
Si	10,05	28,00	SiO ₂	21,54		
Al	4,02	27,00	Al ₂ O ₃	7,59		
Ca	16,28	40,00	CaO	22,79		
Fe	1,67	56,00	FeO	2,14	Fe ₂ O ₃	2,38
K	3,00	39,00	K ₂ O	3,62		
Mg	2,99	24,30	MgO	4,96		
Na	1,55	23,00	Na ₂ O	2,09		
				64,73		64,97

SAMPLE 3

Table 30. XRF analysis results for Sample 3 (Ceramic tile) Run 1.

Sample3 Run1	Element %	Molar mass	OXIDE	% wt.		
Si	31,63	28,00	SiO ₂	67,79		
Al	9,45	27,00	Al ₂ O ₃	17,86		
Ca	0,23	40,00	CaO	0,32		
Fe	7,12	56,00	FeO	9,15	Fe ₂ O ₃	10,17
K	1,14	39,00	K ₂ O	1,37		
Mg	0,18	24,30	MgO	0,30		
Na	0,47	23,00	Na ₂ O	0,63		
				97,42		98,44

Table 31. XRF analysis results for Sample 3 (Ceramic tile) Run 2.

Sample3 Run2	Element %	Molar mass	OXIDE	% wt.		
Si	29,59	28,00	SiO ₂	63,40		
Al	9,04	27,00	Al ₂ O ₃	17,08		
Ca	2,08	40,00	CaO	2,92		
Fe	7,43	56,00	FeO	9,55	Fe ₂ O ₃	10,61
K	1,04	39,00	K ₂ O	1,25		
Mg	0,07	24,30	MgO	0,12		
Na	0,51	23,00	Na ₂ O	0,69		
				95,00		96,06

Table 32. XRF analysis results for Sample 3 (Ceramic tile) Run 3.

Sample3 Run3	Element %	Molar mass	OXIDE	% wt.		
Si	27,60	28,00	SiO ₂	59,14		
Al	3,87	27,00	Al ₂ O ₃	7,30		
Ca	0,22	40,00	CaO	0,31		
Fe	6,38	56,00	FeO	8,20	Fe ₂ O ₃	9,12
K	4,89	39,00	K ₂ O	5,89		
Mg	3,44	24,30	MgO	5,71		
Na	0,32	23,00	Na ₂ O	0,43		
				86,99		87,90

Table 33. XRF analysis results for Sample 3 (Ceramic tile) Run 4.

Sample3 Run4	Element %	Molar mass	OXIDE	% wt.		
Si	30,61	28,00	SiO ₂	65,60		
Al	11,95	27,00	Al ₂ O ₃	22,57		
Ca	0,22	40,00	CaO	0,31		
Fe	6,75	56,00	FeO	8,68	Fe ₂ O ₃	9,65
K	0,44	39,00	K ₂ O	0,53		
Mg	0,49	24,30	MgO	0,81		
Na	0,11	23,00	Na ₂ O	0,15		
				98,64		99,61

Table 34. XRF analysis results for Sample 3 (Ceramic tile) Run 5.

Sample3 Run5	Element %	Molar mass	OXIDE	% wt.		
Si	28,60	28,00	SiO ₂	61,29		
Al	7,63	27,00	Al ₂ O ₃	14,42		
Ca	1,39	40,00	CaO	1,95		
Fe	6,60	56,00	FeO	8,48	Fe ₂ O ₃	9,42
K	3,24	39,00	K ₂ O	3,90		
Mg	2,31	24,30	MgO	3,83		
Na	0,21	23,00	Na ₂ O	0,28		
				94,15		95,10

Table 35. XRF analysis results for Sample 3 (Ceramic tile) Run 6.

Sample3 Run6	Element %	Molar mass	OXIDE	% wt.		
Si	29,82	28,00	SiO ₂	63,91		
Al	8,25	27,00	Al ₂ O ₃	15,58		
Ca	0,04	40,00	CaO	0,06		
Fe	7,37	56,00	FeO	9,48	Fe ₂ O ₃	10,53
K	2,40	39,00	K ₂ O	2,89		
Mg	1,90	24,30	MgO	3,15		
Na	0,45	23,00	Na ₂ O	0,61		
				95,67		96,73

Table 36. XRF analysis results for Sample 3 (Ceramic tile) Run 7.

Sample3 Run7	Element %	Molar mass	OXIDE	% wt.		
Si	33,01	28,00	SiO ₂	70,74		
Al	8,64	27,00	Al ₂ O ₃	16,32		
Ca	0,98	40,00	CaO	1,38		
Fe	6,00	56,00	FeO	7,71	Fe ₂ O ₃	8,57
K	1,34	39,00	K ₂ O	1,61		
Mg	0,02	24,30	MgO	0,03		
Na	0,32	23,00	Na ₂ O	0,43		
				98,23		99,08

Table 37. XRF analysis results for Sample 3 (Ceramic tile) Run 8.

Sample3 Run8	Element %	Molar mass	OXIDE	% wt.		
Si	28,29	28,00	SiO ₂	60,62		
Al	5,67	27,00	Al ₂ O ₃	10,71		
Ca	1,03	40,00	CaO	1,44		
Fe	7,21	56,00	FeO	9,27	Fe ₂ O ₃	10,30
K	4,23	39,00	K ₂ O	5,10		
Mg	3,84	24,30	MgO	6,37		
Na	0,32	23,00	Na ₂ O	0,43		
				93,94		94,97

Table 38. XRF analysis results for Sample 3 (Ceramic tile) Run 9.

Sample3 Run9	Element %	Molar mass	OXIDE	% wt.		
Si	25,27	28,00	SiO ₂	54,16		
Al	8,17	27,00	Al ₂ O ₃	15,42		
Ca	3,70	40,00	CaO	5,18		
Fe	7,12	56,00	FeO	9,16	Fe ₂ O ₃	10,18
K	4,34	39,00	K ₂ O	5,23		
Mg	3,34	24,30	MgO	5,54		
Na	0,52	23,00	Na ₂ O	0,70		
				95,39		96,41

Table 39XRF analysis results for Sample 3 (Ceramic tile) Run 10.

Sample3 Run10	Element %	Molar mass	OXIDE	% wt.		
Si	29,10	28,00	SiO ₂	62,35		
Al	6,55	27,00	Al ₂ O ₃	12,37		
Ca	1,12	40,00	CaO	1,57		
Fe	6,59	56,00	FeO	8,47	Fe ₂ O ₃	9,41
K	4,12	39,00	K ₂ O	4,97		
Mg	3,52	24,30	MgO	5,84		
Na	0,44	23,00	Na ₂ O	0,59		
				96,16		97,10

Table 40. XRF analysis results for Sample 3 (Ceramic tile) Run 11.

Sample3 Run11	Element %	Molar mass	OXIDE	% wt.		
Si	27,57	28,00	SiO ₂	59,09		
Al	9,22	27,00	Al ₂ O ₃	17,41		
Ca	1,65	40,00	CaO	2,31		
Fe	5,41	56,00	FeO	6,95	Fe ₂ O ₃	7,73
K	4,94	39,00	K ₂ O	5,95		
Mg	2,88	24,30	MgO	4,78		
Na	0,24	23,00	Na ₂ O	0,32		
				96,82		97,59

Table 41. XRF analysis results for Sample 3 (Ceramic tile) Run 12.

Sample3 Run12	Element %	Molar mass	OXIDE	% wt.		
Si	26,88	28,00	SiO ₂	57,60		
Al	5,48	27,00	Al ₂ O ₃	10,35		
Ca	0,79	40,00	CaO	1,10		
Fe	7,47	56,00	FeO	9,60	Fe ₂ O ₃	10,67
K	4,44	39,00	K ₂ O	5,35		
Mg	3,89	24,30	MgO	6,45		
Na	0,56	23,00	Na ₂ O	0,75		
				91,20		92,27

Table 42. XRF analysis results for Sample 3 (Ceramic tile) Run 13.

Sample3 Run13	Element %	Molar mass	OXIDE	% wt.		
Si	30,58	28,00	SiO ₂	65,52		
Al	7,10	27,00	Al ₂ O ₃	13,41		
Ca	0,24	40,00	CaO	0,33		
Fe	5,37	56,00	FeO	6,90	Fe ₂ O ₃	7,67
K	4,00	39,00	K ₂ O	4,82		
Mg	2,99	24,30	MgO	4,96		
Na	0,55	23,00	Na ₂ O	0,74		
				96,69		97,46

APPENDIX 3

XRD Analysis For All CDW Samples

[SAMPLE 1= BRICK; SAMPLE 2= CONCRETE; SAMPLE 3= CERAMIC TILE]

[each sample was analysed in 13 runs]

SAMPLE 1

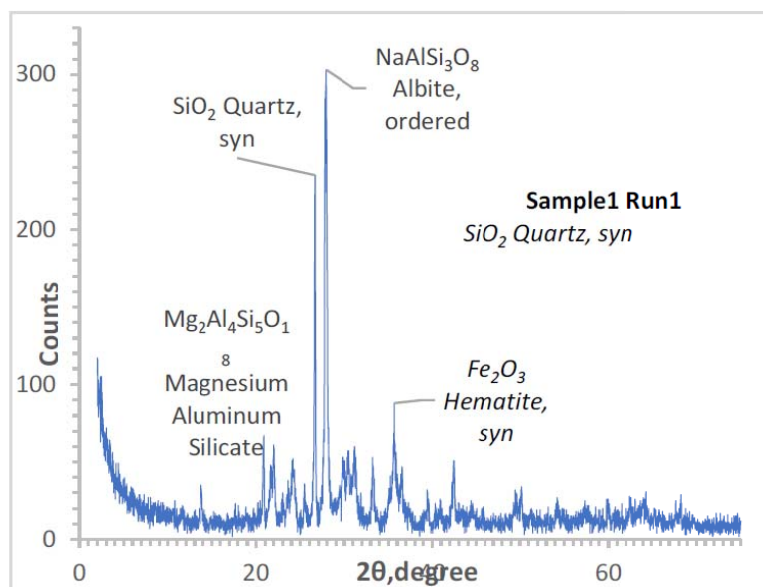


Figure 54. Particle size analysis for Sample 1 (Brick) measurement 1.

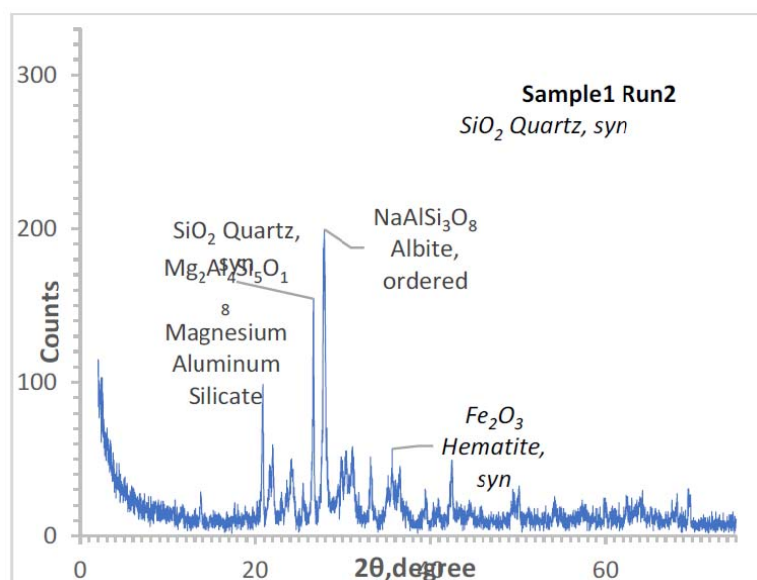


Figure 55. Particle size analysis for Sample 1 (Brick) measurement 2.

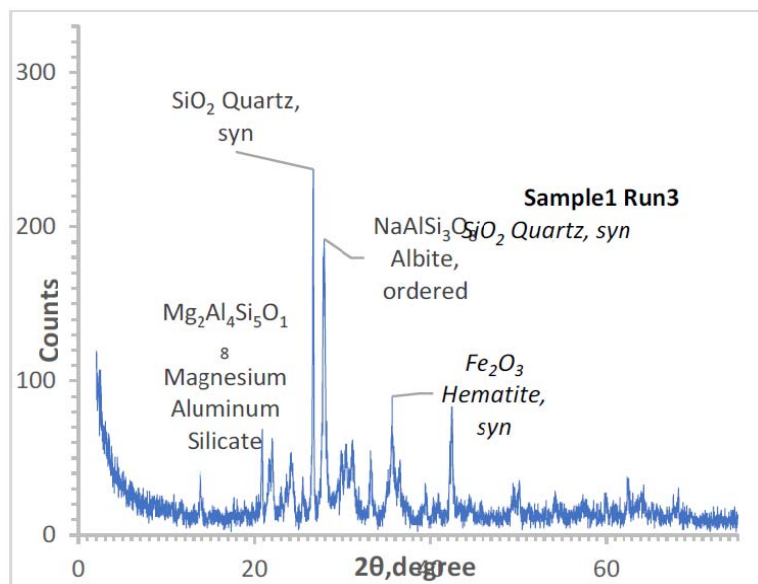


Figure 56. Particle size analysis for Sample 1 (Brick) measurement 3.

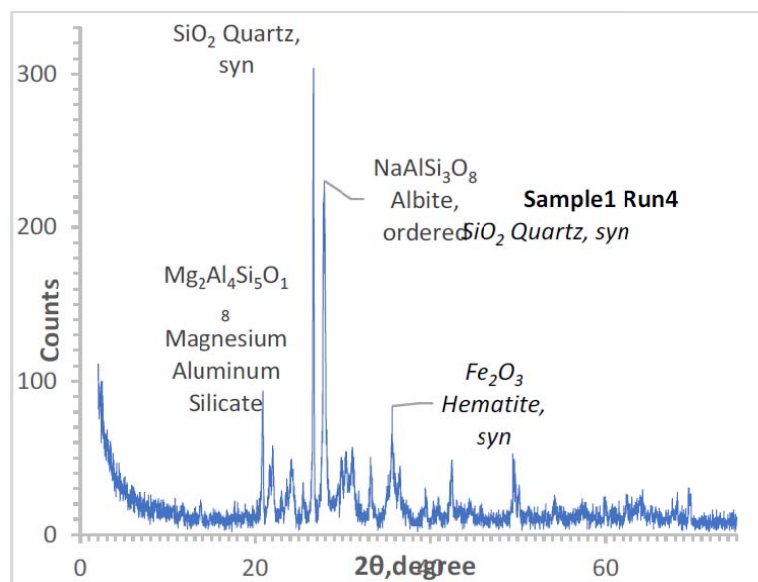


Figure 57. Particle size analysis for Sample 1 (Brick) measurement 4.

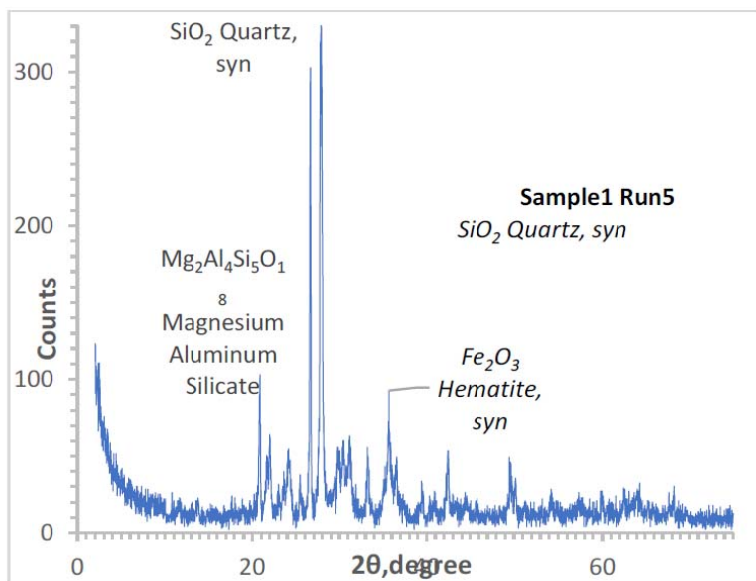


Figure 58. Particle size analysis for Sample 1 (Brick) measurement 5.

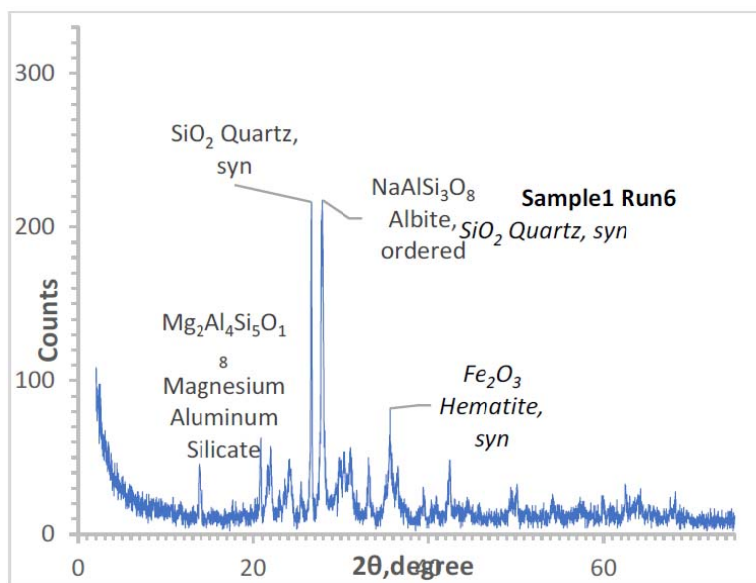


Figure 59. Particle size analysis for Sample 1 (Brick) measurement 6.

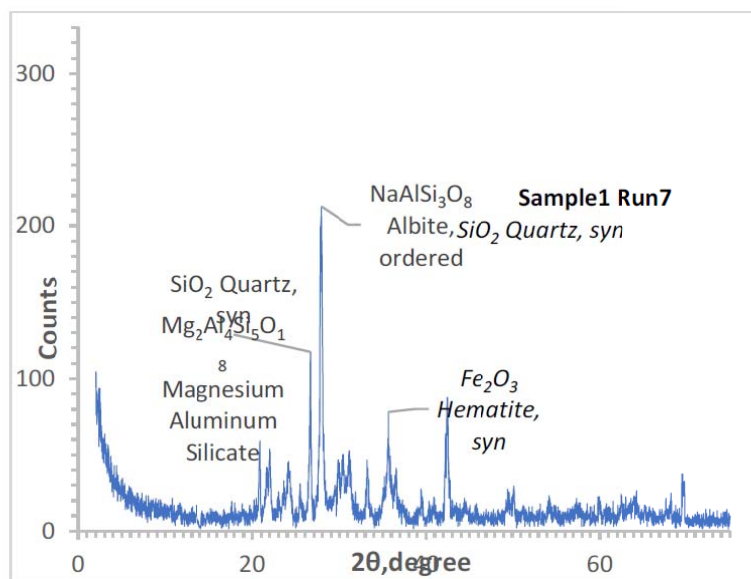


Figure 60. Particle size analysis for Sample 1 (Brick) measurement 7.

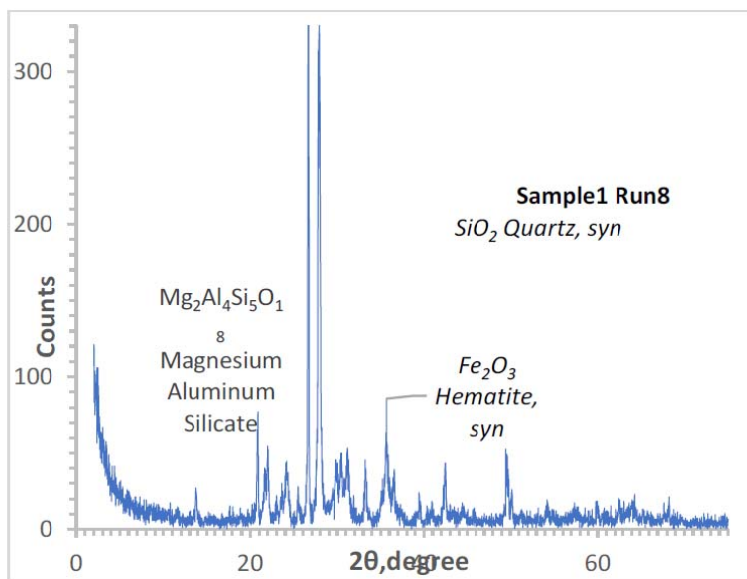


Figure 61. Particle size analysis for Sample 1 (Brick) measurement 8.

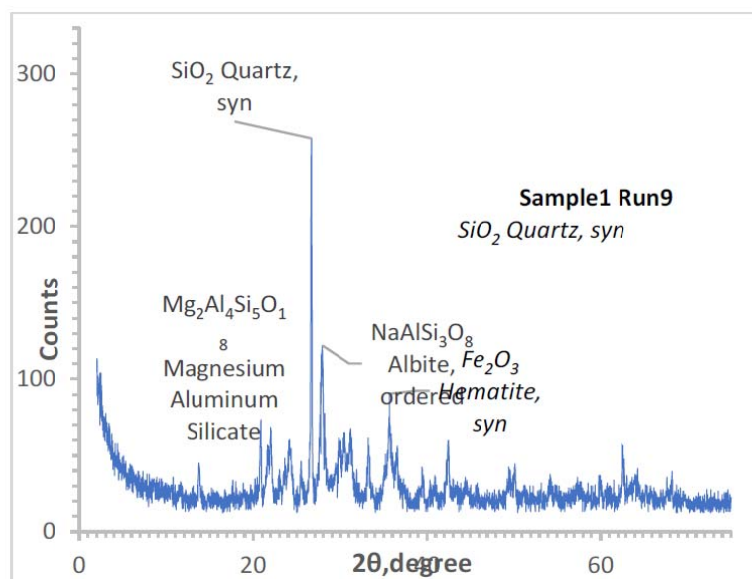


Figure 62. Particle size analysis for Sample 1 (Brick) measurement 9.

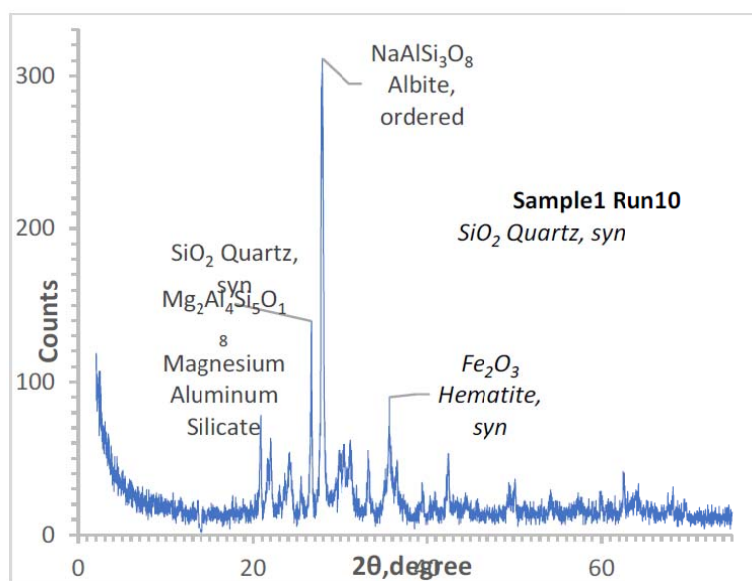


Figure 63. Particle size analysis for Sample 1 (Brick) measurement 10.

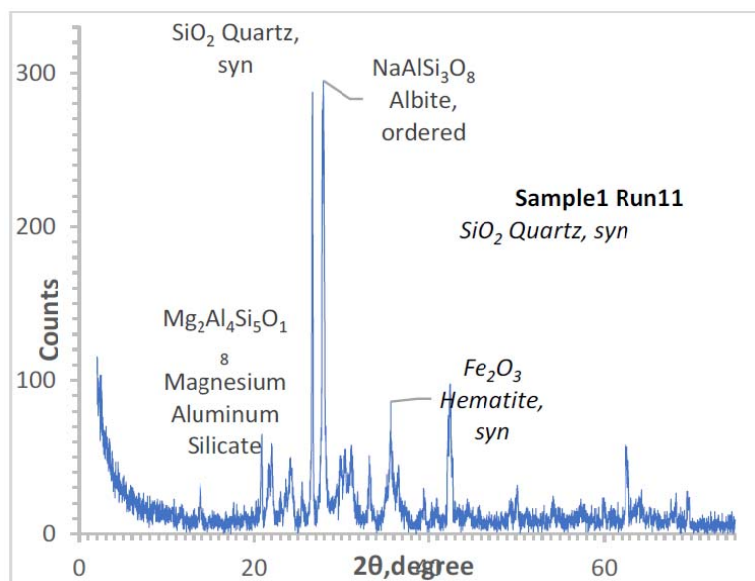


Figure 64. Particle size analysis for Sample 1 (Brick) measurement 11.

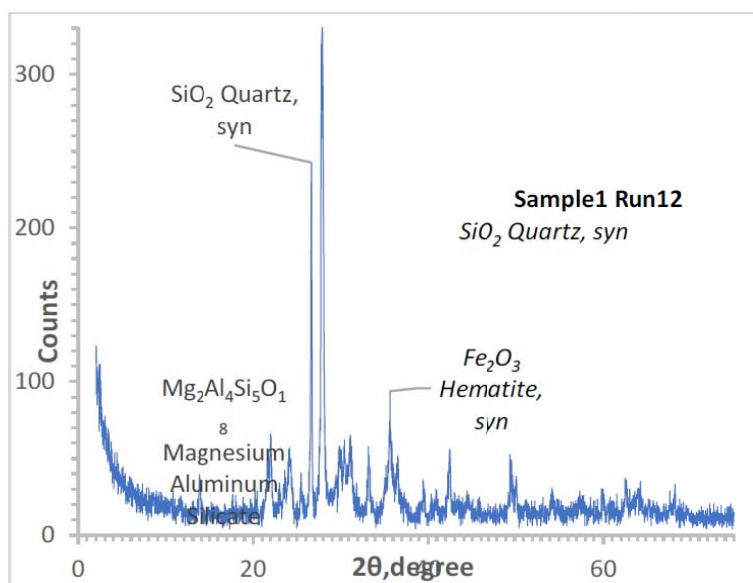


Figure 65. Particle size analysis for Sample 1 (Brick) measurement 12.

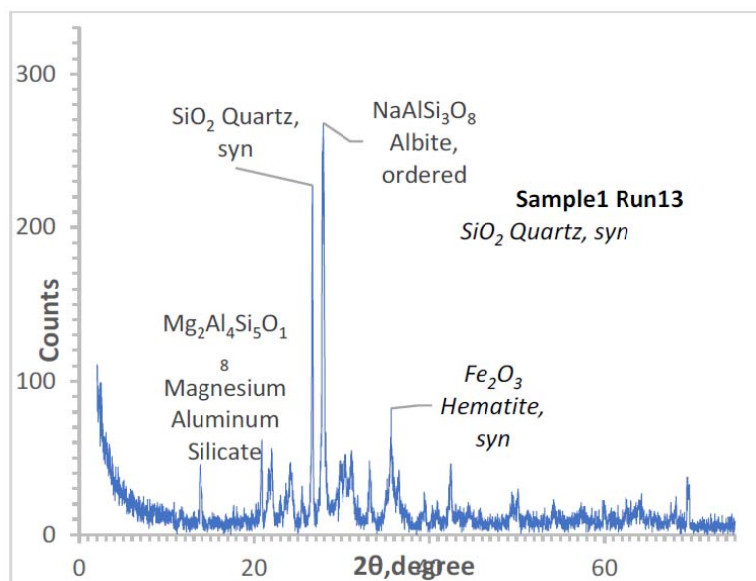


Figure 66. Particle size analysis for Sample 1 (Brick) measurement 13.

SAMPLE 2

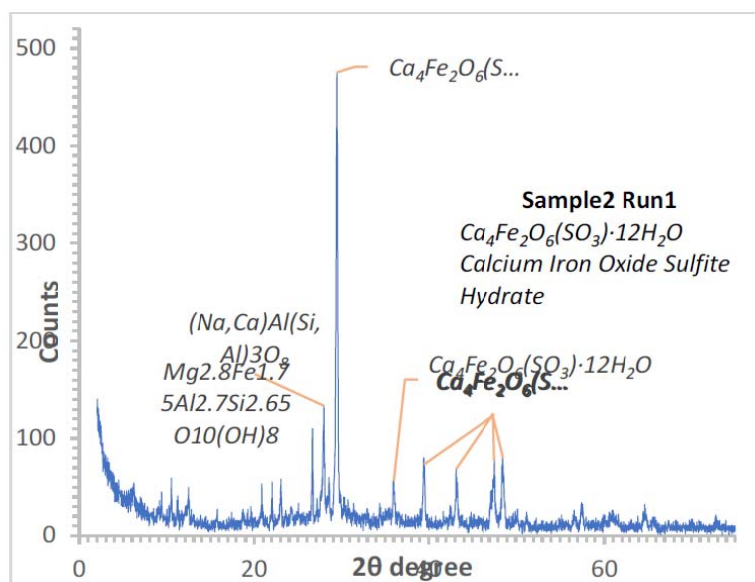


Figure 67. Particle size analysis for Sample 2 (Concrete) measurement 1.

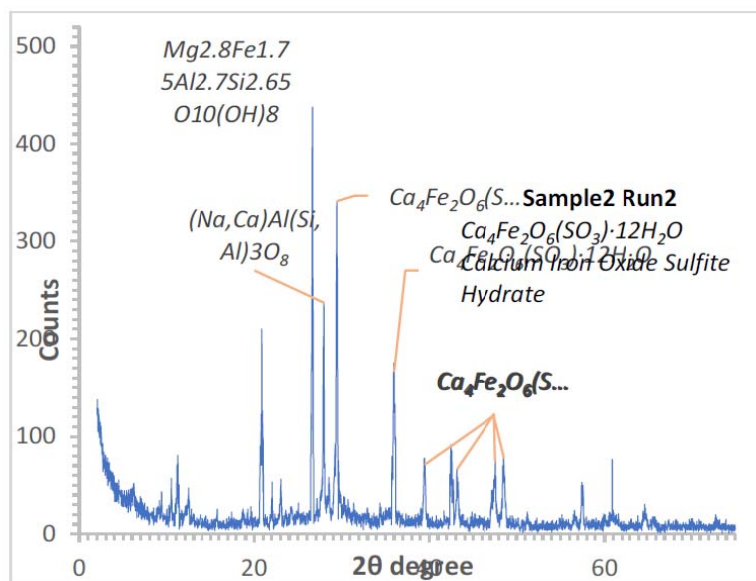


Figure 68. Particle size analysis for Sample 2 (Concrete) measurement 2.

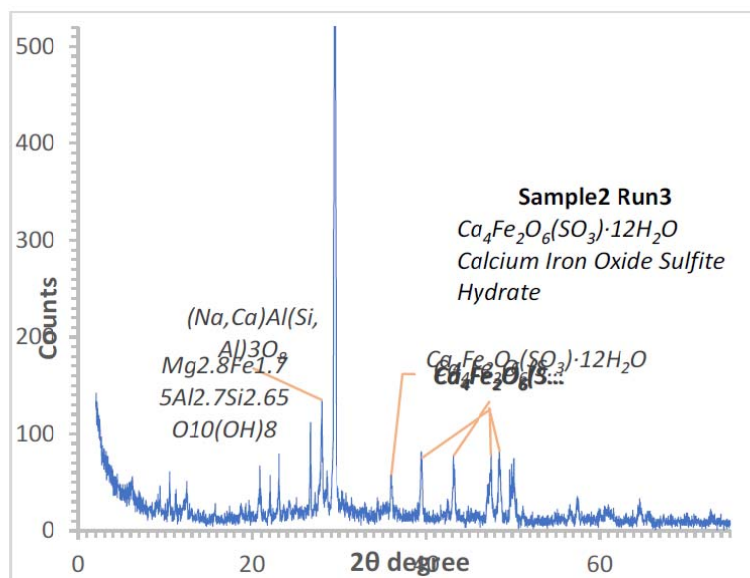


Figure 69. Particle size analysis for Sample 2 (Concrete) measurement 3.

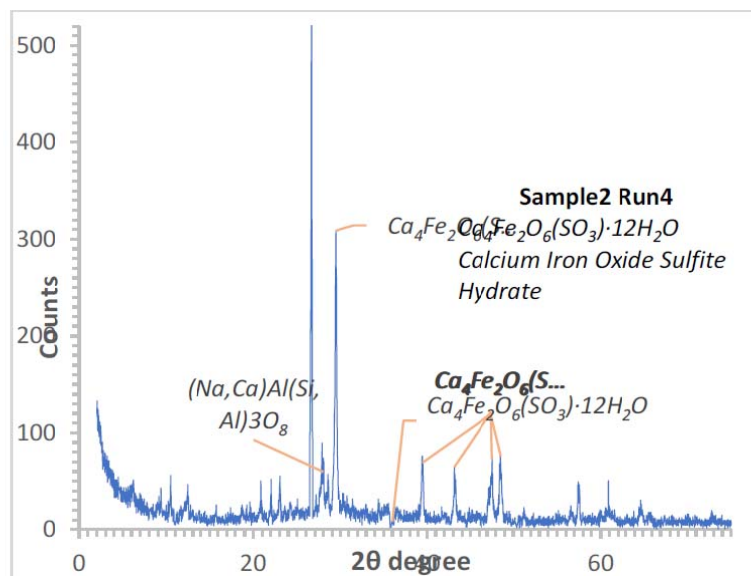


Figure 70. Particle size analysis for Sample 2 (Concrete) measurement 4.

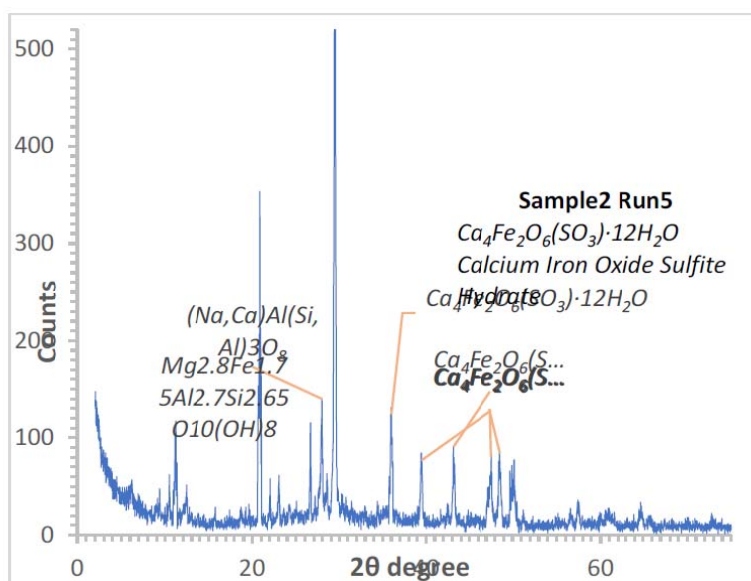


Figure 71. Particle size analysis for Sample 2 (Concrete) measurement 5.

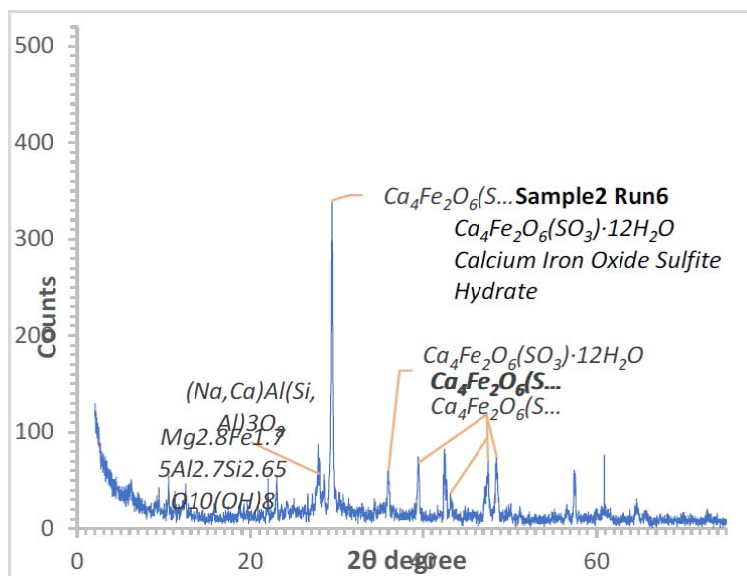


Figure 72. Particle size analysis for Sample 2 (Concrete) measurement 6.

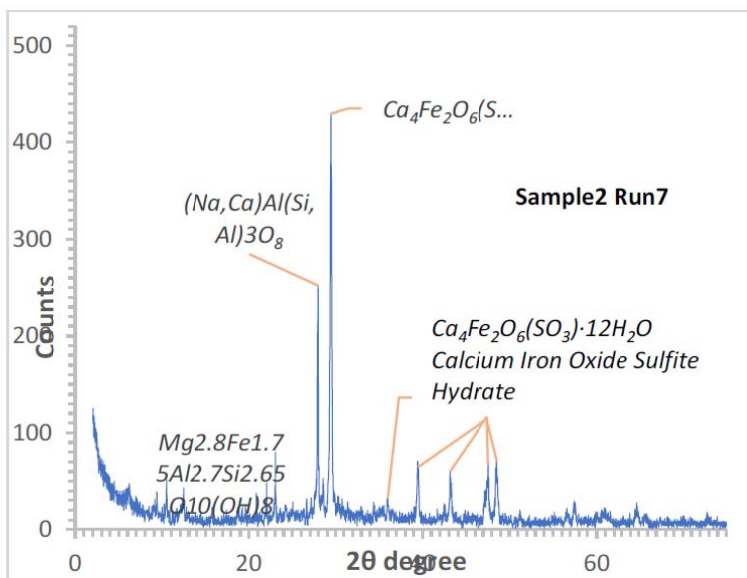


Figure 73. Particle size analysis for Sample 2 (Concrete) measurement 7.

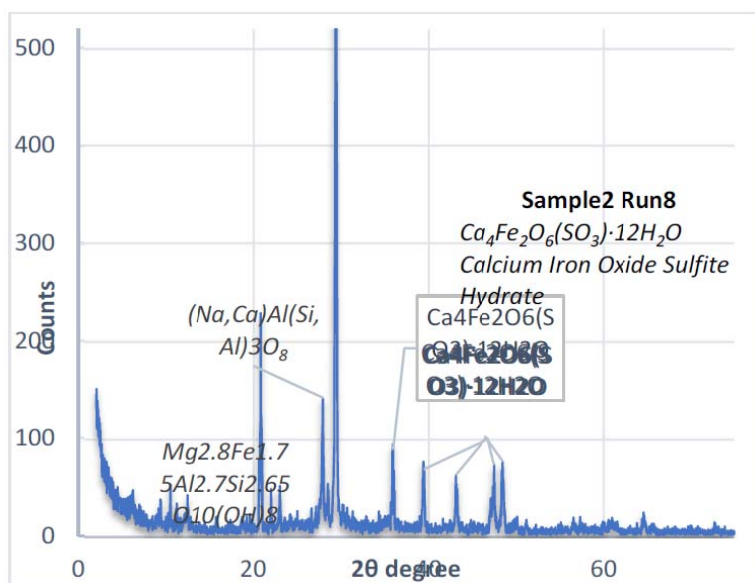


Figure 74. Particle size analysis for Sample 2 (Concrete) measurement 8.

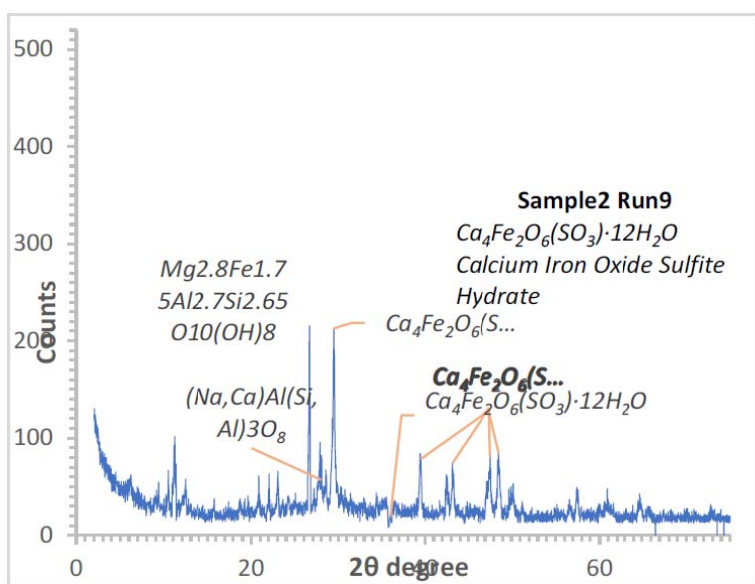


Figure 75. Particle size analysis for Sample 2 (Concrete) measurement 9.

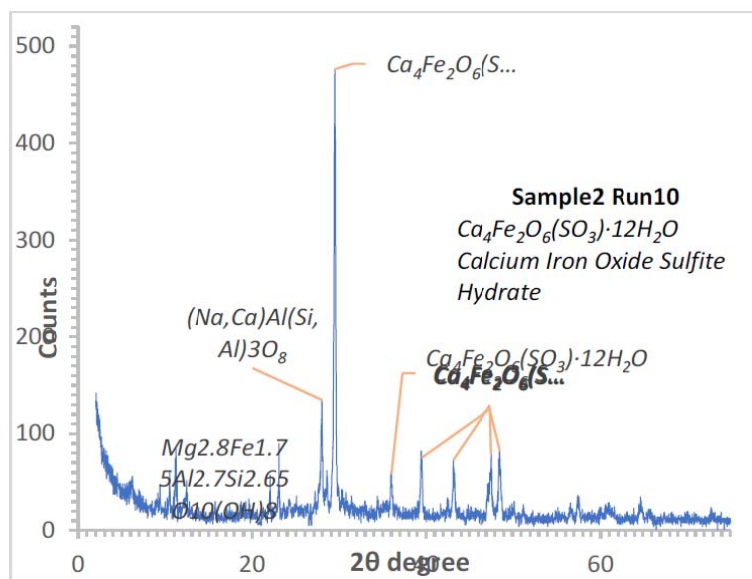


Figure 76. Particle size analysis for Sample 2 (Concrete) measurement 10.

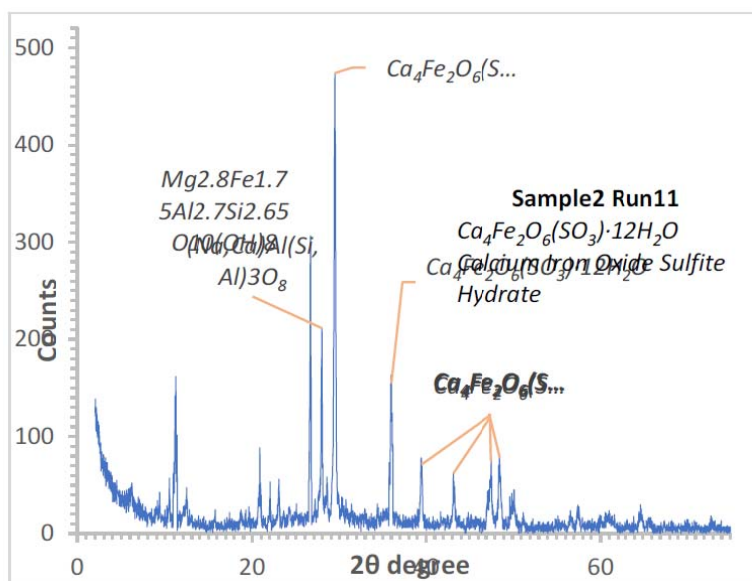


Figure 77. Particle size analysis for Sample 2 (Concrete) measurement 11.

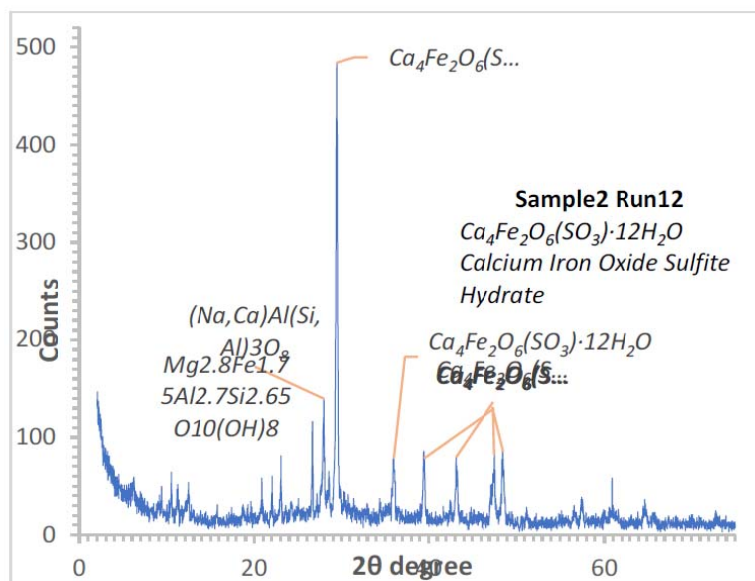


Figure 78. Particle size analysis for Sample 2 (Concrete) measurement 12.

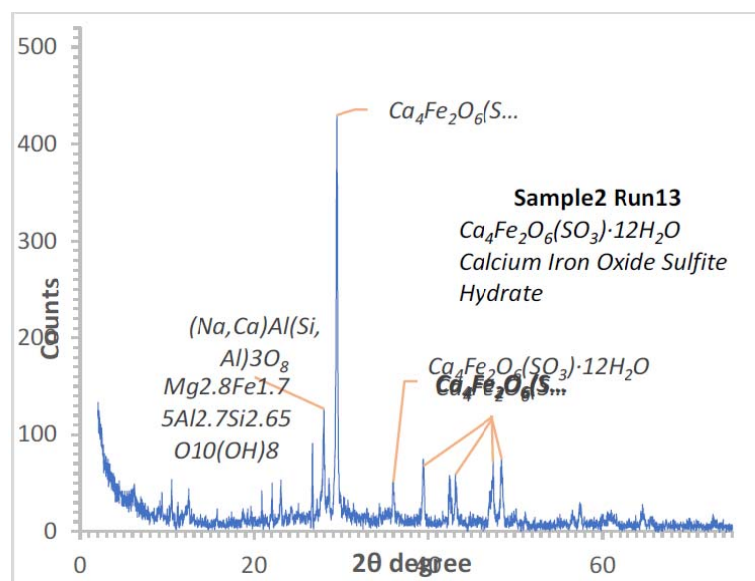


Figure 79. Particle size analysis for Sample 2 (Concrete) measurement 13.

SAMPLE 3

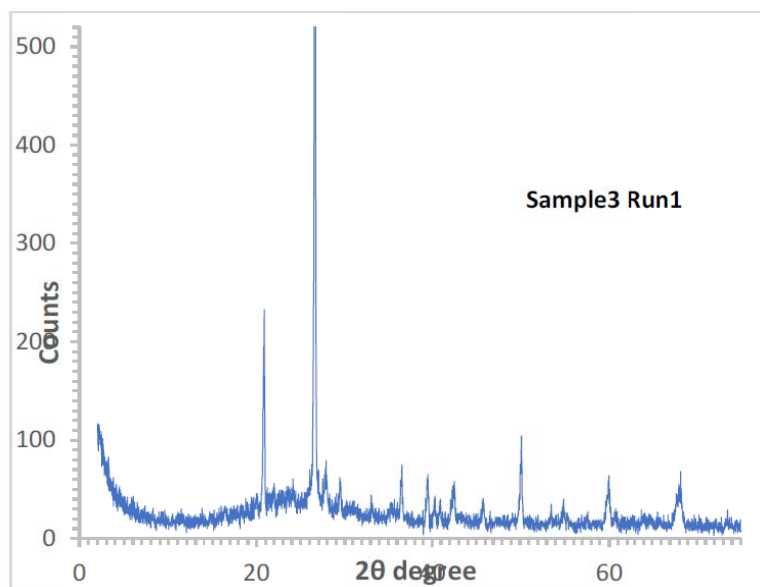


Figure 80. Particle size analysis for Sample 3 (Ceramic tile) measurement 1.

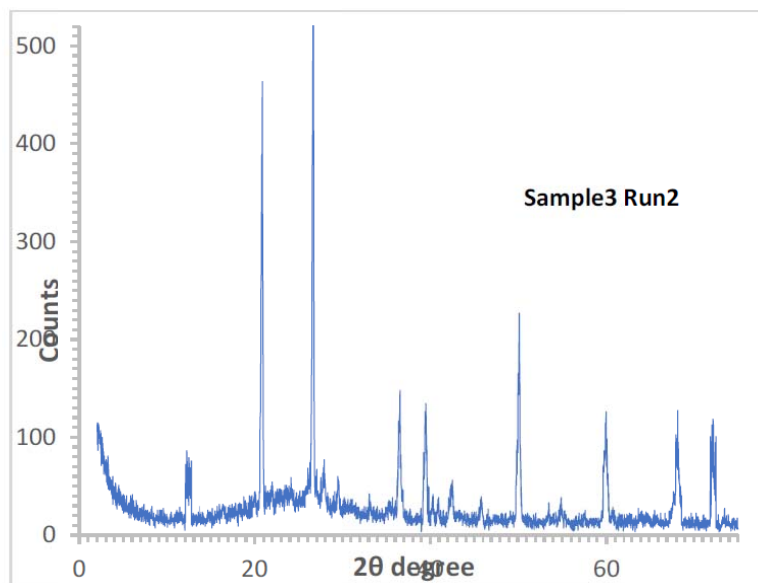


Figure 81. Particle size analysis for Sample 3 (Ceramic tile) measurement 2.

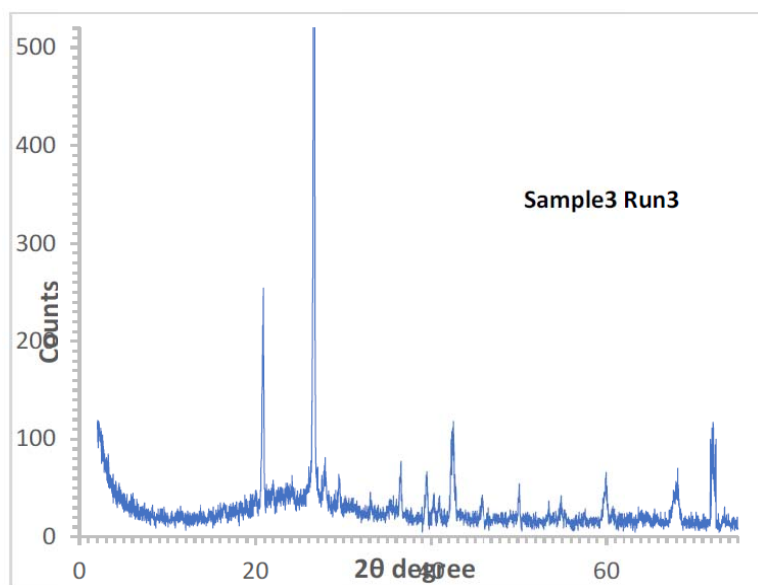


Figure 82. Particle size analysis for Sample 3 (Ceramic tile) measurement 3.

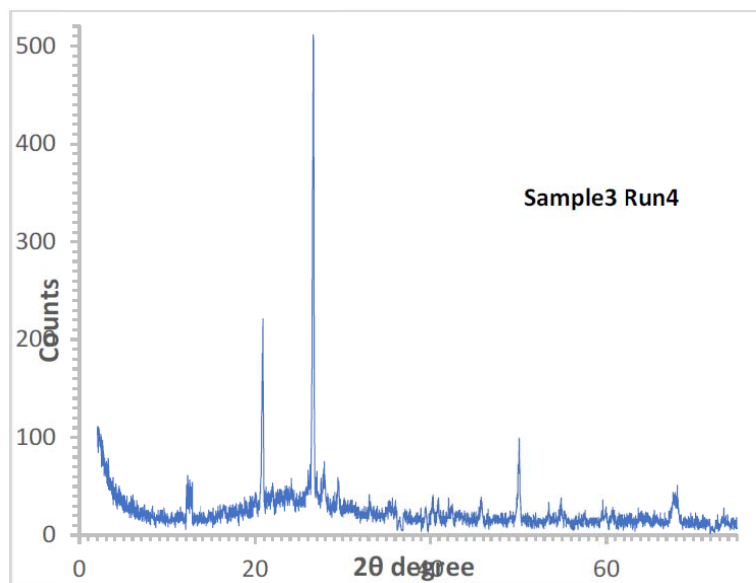


Figure 83. Particle size analysis for Sample 3 (Ceramic tile) measurement 4.

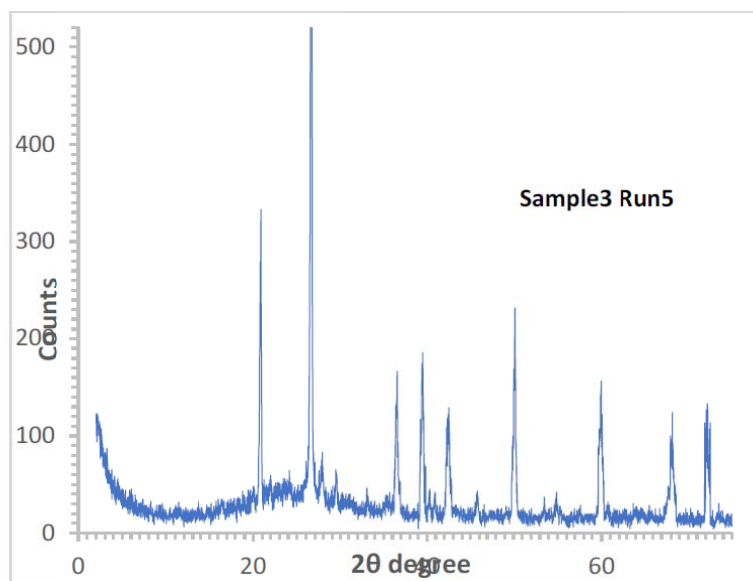


Figure 84. Particle size analysis for Sample 3 (Ceramic tile) measurement 5.

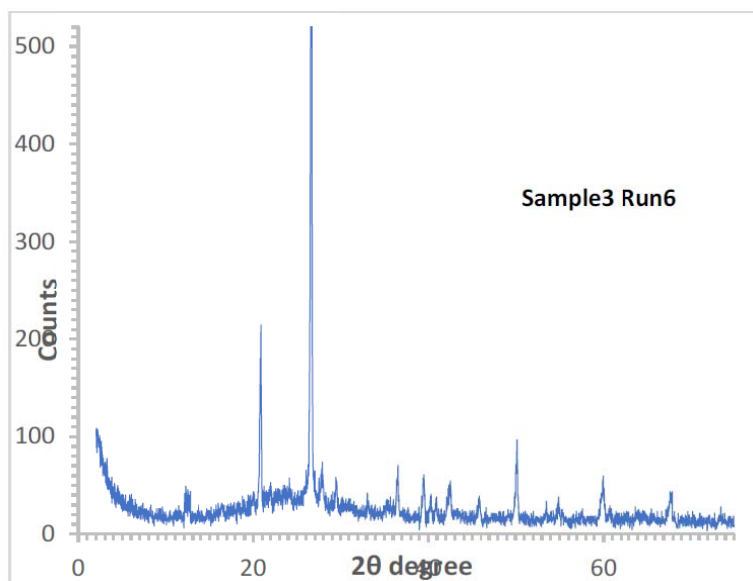


Figure 85. Particle size analysis for Sample 3 (Ceramic tile) measurement 6.

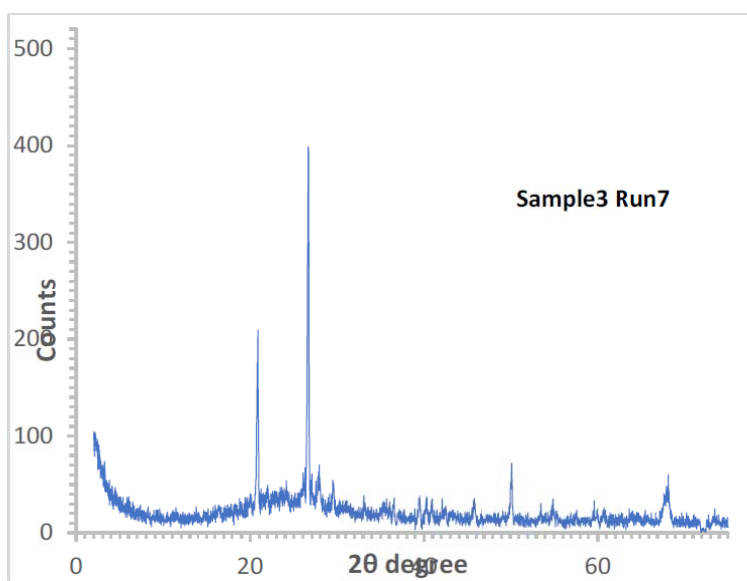


Figure 86. Particle size analysis for Sample 3 (Ceramic tile) measurement 7.

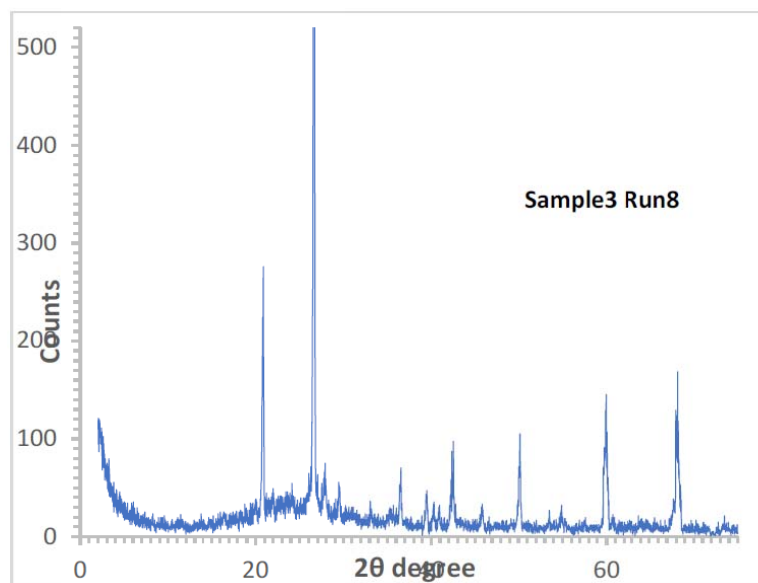


Figure 87. Particle size analysis for Sample 3 (Ceramic tile) measurement 8.

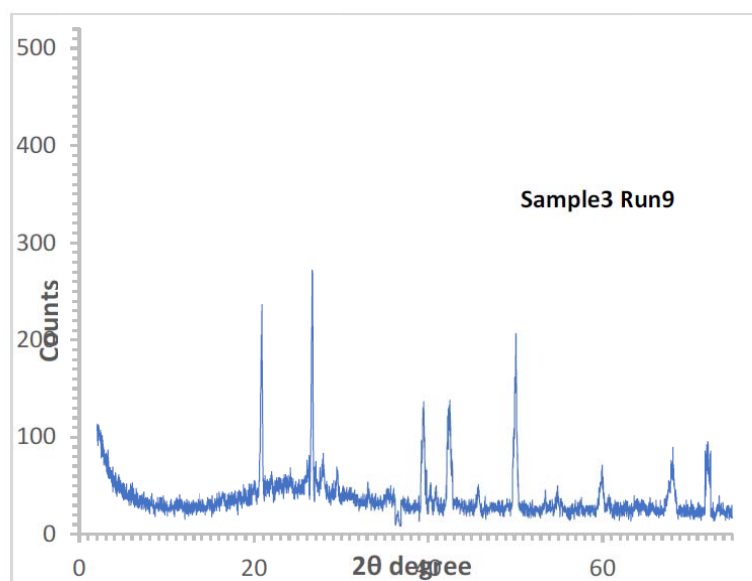


Figure 88. Particle size analysis for Sample 3 (Ceramic tile) measurement 9.

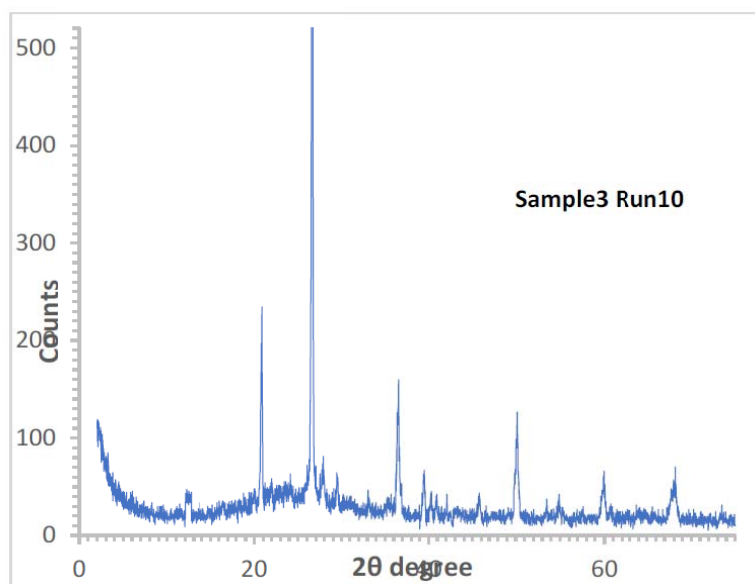


Figure 89. Particle size analysis for Sample 3 (Ceramic tile) measurement 10.

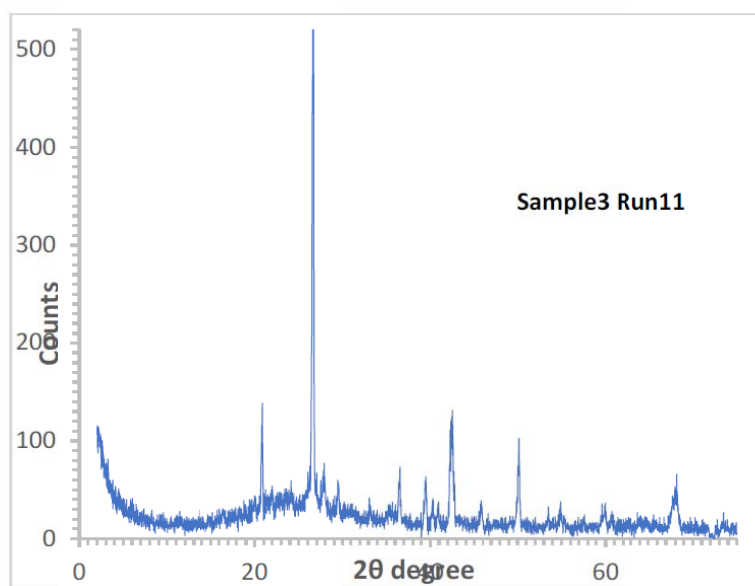


Figure 90. Particle size analysis for Sample 3 (Ceramic tile) measurement 11.

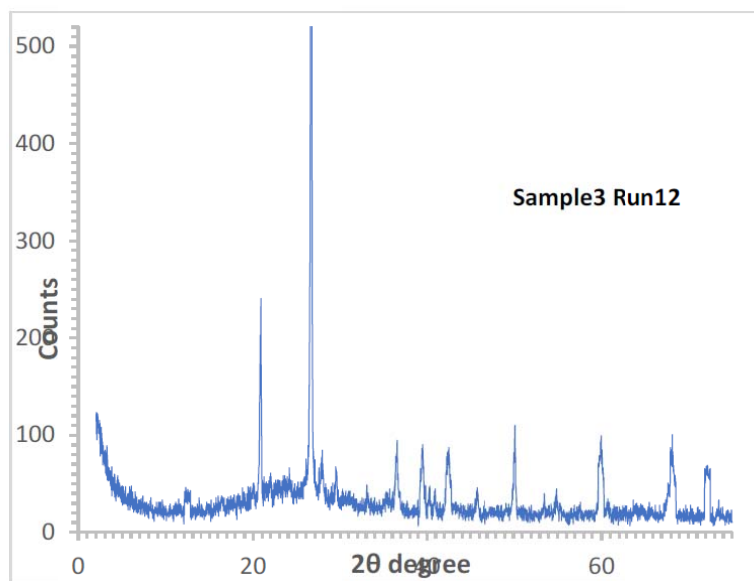


Figure 91. Particle size analysis for Sample 3 (Ceramic tile) measurement 12.

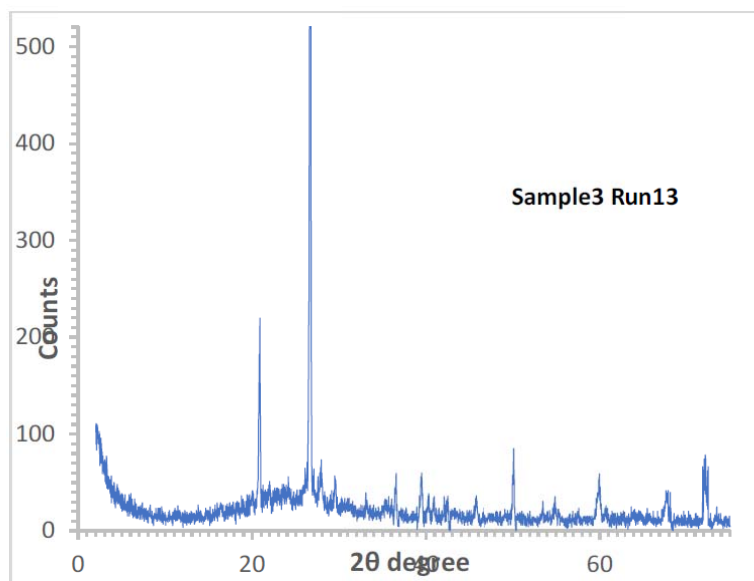


Figure 92. Particle size analysis for Sample 3 (Ceramic tile) measurement 13.